DISSERTATION

A novel AAV9 random peptide library to select for endothelial cell – directed gene transfer vectors

Karl Varadi

DISSERTATION

submitted to the
Combined Faculties for the Natural Sciences and for Mathematics
of the Ruperto-Carola University of Heidelberg, Germany
for the degree of
Doctor of Natural Sciences

A novel AAV9 random peptide library to select for endothelial cell – directed gene transfer vectors

presented by

Diploma-Biologist Karl Varadi
born in: Bucharest
Oral-examination: 28.09.2011

Referees:

Prof. Dr. Jürgen Kleinschmidt

Prof. Dr. Gabriele Petersen

Die vorliegende Arbeit wurde in der Zeit von April 2006 bis August 2011 in der Abteilung für Angewandte Tumorvirologie des Deutschen Krebsforschungszentrums (DKFZ) in Heidelberg unter der wissenschaftlichen Anleitung von Prof. Dr. Jürgen Kleinschmidt verfasst.

Gemäß § 8 (3) der Promotionsordnung erkläre ich hiermit, dass ich die vorliegende Dissertation selbst verfasst und mich dabei keiner anderen als der von mir ausdrücklich bezeichneten Quellen und Hilfen bedient habe.

Heidelberg, im Juli 2011

Parts of the present study have been published:

Varadi K, Michelfelder S, Korff T, Hecker M, Trepel M, Katus HA, Kleinschmidt JA, Müller OJ (2011). **Novel random peptide libraries displayed on AAV serotype 9 for selection of endothelial cell-directed gene transfer vectors.** Gene Ther 2011

Parts of the present study have been presented at international conferences:

Varadi K, Michelfelder S, Hecker M, Trepel M, Katus HA, Kleinschmidt JA, Müller OJ. Generation of a highly diverse random peptide library displayed on Adeno-associated virus 9 for selection of AAV9 vectors targeted to human coronary artery endothelial cells. Annual Meeting of the American Society of Gene Therapy, San Diego, USA, May 27-30, 2009 (**poster presentation**)

Varadi K, Michelfelder S, Hecker M, Trepel M, Katus HA, Kleinschmidt JA, Müller OJ. Generation of a randomized heptapeptide library displayed on AAV9 capsids for selection of AAV9 – vectors targeted to human endothelium. Combined meeting of the European Society of Gene and Cell Therapy (ESGCT), Hannover, Germany, November 20-25, 2009 (**oral presentation**)

INDEX

II. MATERIAL AND METHODS

II.A Material

II.B Molecular biological methods

II.C. Microbiological methods

IV. DISCUSSION

ABBREVIATIONS

(k)V	(kilo) Volt(s), 1E+3 V
%	percent
°C	centigrade Celsius
<	less, lower than
>	more, higher than
1E±y	scientific notation, $10^{\pm y}$
1x	ready-to-use, one-times, single
Å	Ångström (1 Å = 0.1 nm)
ad	up to
bp	base pair(s)
cm	centimetre(s)
CAT	chloramphenicol acetyltransferase
CO_2	carbon dioxide
cpm	counts per min (disintegrations/min)
d	day(s)
DNA	deoxyribonucleic acid
dNTP	deoxyribonucleic triphosphate
ds	double-strand(ed)
e.g.	*exempli gratia*, for instance
EBFP	enhanced blue fluorescent protein
EGFP	enhanced green fluorescent protein
et al.	*et alii*, and others
etc.	*etcetera*, and so on
g	gram(s)
g	Earth's gravity (9.81 m/s^2)
gc	genome copies
h	hour(s)
i.e.	*id est*, that is
kb	kilobase pair(s), 1E+3 bp
kDa	kilo Dalton (1 Da = $^1/_{12}$ mass of ^{12}C)
L	litre(s)
LB	Luria broth
log	logarithmic (10^x)
LN_2	liquid nitrogen
M	molarity (mole/L)
max.	maximum
mg	milligram(s), 1E-3 g
min	minute(s)
ml	millilitre(s), 1E-3 L
n/a	not applied, not assayed
NAB	neutralizing antibody
ng	nanogram(s), 1E-9 g
nm	nanometre(s), 1E-9 m
o/n	over-night (~16 h)
OD_y	optical density at y nm
pg	picogram(s), 1E-12 g
rcf	relative centrifugal force
rel. hum.	relative humidity
RFU	relative fluorescence units
RT	room temperature (20 – 25°C)
s	second(s)
SD	standard deviation
ss	single-strand(ed)
v/v	volume per volume
w/	with
w/o	without
w/v	weight per volume
w/w	weight per weight
µCi	micro Curie (1µCi = 3.7E+4 disintegrations/s)
µF	micro Farad, 1E-6 F
µg	microgram(s), 1E-6 g
µl	microlitre(s), 1E-6 L
Ω	Ohm
x-ray	Röntgen radiation

INDEX OF FIGURES

INDEX OF TABLES

SUMMARIES

English

Endothelial cells play a central role in vascular diseases and represent therefore a clinically relevant cell type for gene therapeutic approaches. However, the endothelium is difficult to transduce with wtAAV vectors at feasible levels. The potential of random peptide libraries displayed on AAV2 to select for AAV2 vectors with improved efficiency of endothelial-directed gene transfer has been demonstrated. AAV9, however, may have advantages over AAV2 because of a lower prevalence of neutralizing antibodies in humans and more efficient gene transfer *in vivo*.

The present study provides evidence that random peptide libraries can be displayed on AAV9 and can be utilized to select for AAV9 capsids redirected to human endothelium, as previously shown for AAV2. An AAV9 peptide display library which ensures that the displayed peptides correspond to the packaged genomes was generated. Four consecutive selection rounds on human coronary artery endothelial cells (HCAEC) performed *in vitro* yielded AAV9 library capsids with distinct peptides that strongly outperformed transduction of wild type AAV9. A central point of this study is posed by the finding that incorporation of sequences selected from AAV2 libraries into AAV9 capsids could not increase transduction as efficient as peptides selected in the AAV9 library context, justifying the generation and selection of an AAV9 library. Furthermore, AAV9 vectors with targeting sequences selected from AAV9 libraries revealed an increased transduction efficiency in presence of neutralising human intravenous immunoglobulins suggesting a reduced immunogenicity and a better suitability of AAV9 as a vector backbone. However, enriched peptides did not restrict AAV9 specificity towards HCAEC. The attempt to restrict transgene expression to this cell type by transcriptional targeting using a murine endothelium-specific promoter may be promising as an additional targeting level. To determine the potential of selected AAV on endothelial cells in the intact natural vascular context, murine mesenteric arteries and human umbilical veins were incubated *in vivo* or *in situ*, respectively, using the most efficient AAV9 vector. Analysis revealed a highly efficient transduction of human umbilical vein endothelial cells (HUVEC) by the vector mutant. Similar to the negligible transduction by wtAAV9 vectors, no transduction of murine mesenteric artery endothelial cell (MMAEC) could be detected. A closer comparative analysis of two selected vectors displaying peptides with divergent sequences revealed a HSPG-independent transduction of and the partial use of a common transduction. The results obtained in the present study permit the conclusion that the novel AAV9 peptide library is functional and can be used to select for vectors for future preclinical and clinical gene transfer applications.

Deutsch

Endothelzellen spielen eine zentrale Rolle in vaskulären Erkrankungen und stellen daher ein klinisch relevantes Ziel für gentherapeutische Ansätze dar. Die Transduktion des Endothels mit Hilfe von Wildtyp AAV (wtAAV)-Vektoren ist jedoch ineffizient. Die Selektion von randomisierten Peptidbanken, die im Kontext der AAV2-Kapsidoberfläche exprimiert wurden, hat das Potential zur Detektion und Herstellung von AAV2-Vektormutanten mit gesteigerter Transduktionseffizienz bezüglich des Endothels gezeigt. Es ist jedoch denkbar, das AAV9 als Serotyp aufgrund des niedrigeren Vorkommens neutralisierender Antikörper im Menschen und einer effizienteren Gewebstransduktion *in vivo* für die Konstruktion und Selektion solcher Peptidbanken besser geeignet ist.

Die vorliegende Studie beweist, dass die Herstellung einer solchen AAV9-Peptidbank möglich ist und eine Selektion auf Endothelzellen ähnlich wie im Falle von AAV2 zur Isolation von Endothel-gerichteten AAV9-Vektormutanten führt. Die nach vier aufeinander folgenden *in vitro*-Selektionsrunden auf humanen koronarartriellen Endothelzellen (HCAEC) angereicherten AAV9 Kapsidvarianten wiesen Transduktionseffizienzen auf, welche die von wtAAV9-Vektoren bei weitem übertrafen. Eine Expression von Peptiden, die im Rahmen einer AAV2-Bibliotheksselektion auf HCAEC isoliert wurden, auf AAV9-Vektoren ergab deutlich niedrigere Transduktionswerte im Vergleich zu Peptiden, die aus AAV9-Bibliotheken selektiert wurden. Weiterhin konnte gezeigt werden, dass die selektierten AAV9-Vektoren eine erhöhte Transduktion in Gegenwart neutralisierender humanen intravenösen Immunoglobuline aufweisen, wodurch eine geringere Immunogenizität angenommen werden kann und AAV9 als den besser geeigneten Serotyp für diesen Zweck erscheinen lässt. Diese Ergebnisse zeigen gemeinsam die Überlegenheit der AAV9 Peptidbibliotheken. Nachfolgende Untersuchungen haben jedoch gezeigt, das die angereicherten Peptide AAV9 keine erhöhte Gewebsspezifität verleihen. Der Einsatz Endothel-spezifischer Promotoren konnte die Spezifität der Transgenexpression jedoch etwas erhöhen. Um das Potential der selektierten AAV-Vektoren zur Transduktion von im Blutgefäßkontext residierenden Endothelzellen zu bestimmen, wurden humane Nabelschnurvenen einer *in situ* und murine Mesenterialarterien einer *in vivo* Behandlung mit dem effizientesten Vektor unterzogen. Im Gegensatz zur hocheffizienten Transduktion der Nabelschnurendothelzellen (HUVEC) durch die Vektormutante, ermöglichte der Wildtyp-Vektor keinen Gentransfer. Überraschenderweise konnte keine Endotheltransduktion der murinen Mesenterialarterien durch die Vektormutante detektiert werden. Eine nähere Charakterisierung zweier Vektormutanten, die Peptide mit divergierender Sequenz exprimierten, ergab eine HSPG-unabhängige Transduktion zweier Zelltypen und wies auf eine partiell gemeinsame Nutzung des Transduktionspfades hin. Die vorliegenden Resultate erlauben den Rückschluss, dass die im Rahmen dieser Studie entwickelte AAV9-Peptidbank funktionell und zur Selektion von Vektoren geeignet ist, welche in künftigen präklinischen und klinischen Gentransferstudien eingesetzt werden könnten.

I. INTRODUCTION

I.A Gene Therapy

I.A.1 Definition

Broadly defined, gene therapy is the concept of directed introduction of foreign genetic material into a cell, tissue or organ for correction of defective genes with the goal to improve the clinical status of a patient. The approach may be differentiated in germ line gene therapy, which would induce heritable changes passed from generation to generation and somatic gene therapy, that restricts the therapeutic effect to the treated individual. Germ line therapy would be highly effective in counteracting genetic disorders and hereditary diseases, however, application in humans is at present unimaginable for several technical and ethical reasons. The broadly accepted somatic therapy can be further discriminated by a fast and easy to perform direct gene transfer to the organism (*in vivo*) or a sophisticated but more specific and controllable transfer to explanted cells or tissues (*ex vivo*), which are re-implanted after treatment.

I.A.2 Methods of gene transfer

Gene transfer to cells can be attempted by the use of either viral or non-viral methods. The latter are based on physical procedures as in the case of micro-injection[1] and electroporation[2] or chemical treatment of naked DNA using transferrin-polycation conjugates[3], polyethyleneimine[4] or liposomes[5]. A more promising alternative may be represented by viruses that in the course of evolution have developed efficient strategies to deliver inherent DNA to the host cells. Partial replacement of viral genetic elements by therapeutic genes and exploitation of the virus' native tropism have yielded viral vectors that reliably and efficiently access the tissue of interest. To date, several human or animal viruses suitable for incorporation of transgenes including Adenovirus (Ad), Adeno-associated virus (AAV) and Retrovirus have been employed in gene transfer attempts with variable success, each of them having advantages and disadvantages in production, application and outcome (reviewed by[6,7,8]).

I.A.3 General problems of gene transfer

Transfer of naked DNA into target cells potentially avoids pronounced host immune response and has a negligible mutagenic capacity since only a low integration rate into the host genome can be assumed. The efficiency and specificity of such approaches, however, is limited. Due to their natural ability to infect a host and to replicate, viruses and derived viral vector systems represent a more efficient gene transfer alternative. Depending on the viral background, the specificity is only moderate, though, leading to off-target effects.

This may be a benefit in case the target cell type is within the host range but will represent a significant drawback when specific transduction is desired. Off-target transduction of healthy tissue lowers the therapeutic impact on targeted tissue and may unfold deleterious effects, such as toxicity, uncontrollable transgene expression or adverse immune reactions. In addition, a high risk of insertional mutagenesis exists due to the native property of latent viruses to integrate into the host genome. These drawbacks have lead to numerous debates on the safety of virus-based gene therapy vectors (reviewed by[9,10,11,12,13]). Despite the negative aspects, improved viral vector systems with an enhanced safety profile have been developed and were approved for clinical trials with promising outcomes.

I.A.4 Gene therapy trials with AAV-derived viral vectors

Some of the most successful gene therapeutic trials have been obtained from AAV-derived vectors. As of 2008, 38 clinical trials were approved by the Recombinant DNA Advisory Committee and the Food and Drug Administration (reviewed by[14,15]). The initial idea of therapy by gene replacement was applied in early phase I or II clinical trials targeting monogenic diseases, such as cystic fibrosis[16] and haemophilia B[17,18]. More recent trials encompassed treatment of heart failure[19], α-1-antitrypsin deficiency[20], Parkinson's neurodegenerative disease[21,22], Leber congenital amaurosis[23] and several others. The spectrum is completed by a plethora of approaches targeting more complex diseases like cancer. Here, several pre-clinical models have been attempted that aim for anti-angiogenesis therapy, immunotherapy, suicide gene therapy and repair of tumour cells (reviewed by[24]). The most advanced clinical phase III trial for AAV as of today has been approved for therapy of prostate cancer (reviewed by[25]).

I.B AAV Biology

I.B.1 AAV in general

AAV was discovered and isolated in 1965 as a contaminant of an Ad production[26,27] and was later assigned to the *Parvoviridae* family[28]. Its inability to complete a replication cycle in absence of a co-infecting helper virus has earned AAV its own genus of *Dependovirus*. The name-giving helper virus Adenovirus reconstitutes the replication-deficiency of AAV by providing the early adenoviral proteins E1A, E1B, E4 and E2A involved in activation of S-phase and DNA replication of the host cell[29]. Besides Ad, several other unrelated DNA viruses, such as herpes simplex virus type 1 and 2[30], human Cytomegalovirus[31], Vaccinia virus[32] or human Papilloma virus type 16[33] are able to support the replicative cycle of AAV. In absence of a helper virus, AAV establishes a latent infection in which the genome persists episomally or integrates preferentially at site AAVS1 located on chromosome 19 of the host genome [34,35,36,37]. Super-infection with a helper virus mediates the rescue of integrated genomes and reactivates the productive replication cycle[29].

I.B.2 AAV serotypes

The term serotype refers to distinct variations of antigenic properties within a virus (or bacterial) species. A new serotype is defined when no cross-reaction with antibodies directed against all known serotypes of the same genus can be detected. As of today, 12 different AAV serotypes are known, AAV1 to AAV12, which have been isolated from human (serotypes 2[38], 3[39], 5[40], 6[41] and 9[42]) and non-human primate samples (serotypes 1[43], 4[44], 7[45], 8[45], 10[46], 11[46], 12[47]). The serotypes have been classified into six different phylogenetic clades A-F on the basis of their genetic sequence and antigenic reactivities, with AAV4 and AAV5 considered to be clonal isolates[42] and AAV6 the only natural recombinant of AAV1 and AAV2 differing by only 6 amino acids[41]. All serotypes are capable of infecting cultured human cells, independent of their natural host and display upon *in vivo* application a distinct tropism. AAV2 has been subject to the most extensive studies so far, but recently also other serotypes gained importance in the field of gene therapy. Especially AAV9 has attracted much interest due to its strong transduction of rodent muscle, liver and lung with an about 100-fold enhanced efficiency over AAV2. A central reason for the emerging popularity of AAV9 is its remarkable ability to cross the blood brain barrier (BBB, reviewed by[48]) and a strong and efficient *in vivo* cardiac transduction in mice[49,50,51].

I.B.3 AAV genomic organisation

AAV packages a ~4.7 kb single stranded DNA genome of either polarity[38,52]. Due to the limited space for packaging of genetic material viruses have developed the ability to increase their coding capacity of short DNA fragments. Three mRNA transcripts from only two open reading frames (ORFs) are sufficient to synthesize a total of eight proteins. This is only possible by efficient combination of alternative promoter usage, transcript splicing and depositing of genetic information in alternative ORFs. The primary ORF contains the slightly overlapping *rep* and *cap* genes encoding four non-structural proteins (Rep, regulatory proteins[53]) and three structural proteins (VP, capsid proteins[54,55]), respectively. Recently, the presence of another non-structural protein was discovered in the AAV2 secondary ORF of *cap* (AAP, assembly-activating protein[56]). The *rep* and *cap* ORFs are under helper virus-dependent transcriptional control of three promoters, p5, p19 and p40, with the numbering related to their relative position on the AAV genome map divided in 100 units. The transcription of the two major *rep*-encoded proteins Rep78 and its splice variant Rep68 is controlled by p5, Rep52 and its splice variant Rep40 by p19 and the structural proteins VP1, VP2 and VP3 (90, 72 and 62 kDa, respectively) as well as AAP (23 kDa) by p40. All transcripts can be subject to splicing, since the *rep* and *cap* overlapping region contains a small intron flanked by a single splice donor (SD) and two alternative splice acceptors (SA), a major (SAmaj) and a minor one (SAmin). *Rep* and *cap* are flanked by inverted terminal repeats (ITRs) that complete the AAV genome.

I.B.3.1 The ITRs

The ITRs consist of 145 complementary nucleotides (nt) that self-anneal and form t-shaped hair-pin structures[57]. Each hairpin comprises three palindromic sequences of in total 125 nt that form stem and arms of the t-shaped structure. The ITRs function as *cis*-acting elements for viral genome replication, packaging, rescue from integrated state[57,58,59] and were shown to regulate viral gene expression and host genome integration (reviewed by[60,61]). The palindromic sequences harbour two Rep-binding elements (RBE)[62,63,64] and a terminal resolution site (trs). The ITR structure is completed by the remaining non-palindromic 20 nt that form the single-stranded D-sequence required for AAV DNA replication and genome packaging[65,66,67].

I.B.3.2 The rep ORF

Synthesis of Rep proteins occurs from two transcripts initiated from p5 and p19. The SAmin mediates the splicing of Rep78 and Rep52 mRNA to Rep68 and Rep40, respectively. Spliced and unspliced Rep proteins therefore have distinct C-terminal zinc-finger domains that interact with cellular kinases PKA[68] and PRKX[69] in case of Rep78/68 or with members of the 14-3-3 protein family in case of Rep52/40[70]. The N-termini of Rep78/68 contain additionally a DNA endonuclease function which is missing in Rep52/40 due to transcription from p19. Both unspliced Rep are able to contact the RBE of the ITRs and to cleave the DNA strand at the trs, a process required for the replication of viral DNA. All Rep share a nuclear localisation signal (NLS) close to the C-terminus required for nuclear import and the Helicase/ATPase function of the core protein domain. Additionally, the Rep proteins were reported to function as effectors of viral replication, genome packaging and integration into host genome[71,72,73,74,75,76], as well as to interact with cellular proteins involved in DNA replication, RNA processing, membrane transport, chromatin dynamics and ubiquitination[77]. Rep78/68 additionally function as negative regulators of AAV gene expression during latency[78,79].

I.B.3.3 The cap ORF

The structural VP proteins and AAP are translated from one mRNA transcript initiated from the p40 promoter. Depending on which SA is involved in mRNA splicing, a 2.6 kb (SAmin) or a 2.3 kb transcript (SAmaj) are formed. The longer transcript retains the first AUG start codon and enables translation of the entire *cap* ORF to produce VP1. Since SAmin has a lower efficiency than SAmaj, the shorter transcript predominates, excluding the first AUG start codon and preventing VP1 translation. From this major transcript, capsid proteins VP2 and VP3 are created by accession of the non-canonical (weaker) start codon ACG which is surrounded by an optimal Kozak motif and the conventional AUG start codon, respectively[55,80,81,82]. The translation of the smallest AAV2 protein AAP is mediated by non-canonical promoter bearing a CUG start codon located in the secondary ORF of the p40 transcript.

Due to the use of different start codons the VP proteins share C-terminal domains while the N-termini remain unique to VP1 or VP2. VP1, the largest protein, harbours at its N-terminus a phospholipase A_2 (PLA_2) domain known to be involved in endosomal release and nuclear entry during viral infection[83,84,85,86]. The VP N-termini contain in total four conserved motives of positively charged amino acids (KKR) termed basic regions (BR), whereas BR1 is uniquely present on the VP1 N-terminus, BR 2 and 3 are shared by VP1/2 and BR 4 is common to all three VPs[87]. The BRs constitute putative NLS and may be involved in nuclear transfer of VP proteins for capsid assembly[86,88,89]. The C-terminus present in all VP contains five basic amino acids (R484, R487, K532, R585 and R588) responsible for the binding of AAV2 to its primary attachment receptor heparan sulphate proteoglycan (HSPG)[90,91,92]. Another motive shared between VPs from all AAV but 4, 5 and 11 is NGR (residues 511-513, VP1 numbering) that promotes binding to one of the AAV2 secondary internalization receptors α5ß1[19]. The assembly-activating protein AAP targets capsid proteins to the nucleoli and fulfils a direct function in the capsid assembly process itself.

I.B.4 AAV structure

The icosahedral AAV capsid is formed by 60 VP1-3 subunits[55] that assemble at a molar ratio of ~1:1:10 (VP1:VP2:VP3). The 10-fold higher abundance of VP3 can be explained by the predominating major p40 transcript and the use of the conventional AUG start codon (Chapter I.B.3.3). The icosahedron has ~25 nm in diameter and may be divided in 20 triangular faces formed by any of the three VP proteins that share identical interaction sites and spatial arrangement. This geometrical set up results in 2-fold, 3-fold and 5-fold symmetry axes with a triangulation number of T=1 defining size and complexity[93]. The atomic structure of several serotypes has been resolved by x-ray crystallography to a resolution of 2-3 Å (AAV2[94], 3b[95], 4[96], 6[97] and 8[98]) or by cryoelectron microscopy and image reconstruction to 10-16 Å (AAV2[99], 4[100], 5[101]). Currently, the crystal structures of AAV1[102], 7[103] and 9[104] are being investigated.

The VPs of all serotypes analysed so far share a common structure comprising of a conserved eight-stranded antiparallel ß-barrel (ßB-ßI) buried within the assembled capsid. This motif is common in virus capsids and has also been described for other parvoviruses like canine parvovirus (CPV)[105] feline Panleukopenia virus (FPV)[106], minute virus of mice (MVM)[107] or the human parvovirus B19[108]. Each ß-sheet is connected to its neighbour by interstrand loops that define the landscape of the assembled capsid surface: a depression at the 2-fold axis (“dimple”), finger-like projections at the 3-fold axes (“spikes”), another depression surrounding the pore/cylinder at the 5-fold axis (canyon)[94], and a flat region located between two spikes (“plateau”)[109]. The interstrand loops are grouped by convention into 5 groups (I-V)[110] and comprise a total of 9 variable regions between the AAV serotypes (VR I-IX)[100]. Loop 4, the largest loop, is further divided in 4 subloops (1-4) and connects the ß-strands G and H (GH-loop).

According to the known structure of AAV2, the GH-loop of two adjacent VP subunits form a spike. Subloops 1 (VR IV) and 4 (VR VIII) of one VP are located on the opposing sides of the spike while subloop 2 (VR V) of the other VP resides in between them[111]. The majority of the 2-fold symmetry interactions are provided by a conserved loop located after ßI and loop HI promotes interaction of 5 adjacent VP monomers at the 5-fold symmetry axis[112]. X-ray crystallography allowed the detection of all but 14 N-terminal residues from AAV2[94]. Consequently, the VP1/2 N termini buried within assembled capsids were not visible. However, cryoelectron microscopy and image reconstruction of AAV capsid cross-sections revealed globular structures located at the 2-fold axis inside the capsid, which may represent the VP1/2 N-termini that become externalized through the 5-fold cylinder during AAV infection[83,86].

I.B.5 AAV receptors

The first step in AAV cell transduction is represented by binding of the capsid to cellular receptors. At the same time, this step determines the broadness of viral tropism which is enlarged in case the target receptor is commonly expressed on many cell types. Several glycans with different biochemical termini serve as attachment or primary receptors for different AAV serotypes. The attachment receptor of AAV2 and 3 is cellular HSPG[92,113] while AAV1, 5 and 6 employ N-linked (α-2,3 in case of AAV1 and 5 and α-2,6 in case of AAV6) and AAV4 O-linked sialic acid containing glycans[114,115,116]. Recently, AAV9 has been shown to use O-linked galactose containing glycans as a primary receptor[117]. However, evidence was given that AAV may use more than one receptor for efficient transduction of cells: in absence of HSPG, persistent transduction has been demonstrated for AAV2[118] and 3[119] and mutant AAV2 vectors with abrogated HSPG binding showed increased transduction of heart *in vivo*[90]. Subsequently, integrins αVß5[120] and α5ß1[19], hepatocyte growth factor receptor (c-Met)[121] and CD9[122] were revealed to function as co-receptors for AAV2 and are believed by convention to mediate cellular uptake. AAV2 and AAV3 both utilize fibroblast growth factor receptor 1 (FGFR-1)[123,124] and the 37/67 kDa laminin receptor (LamR) serves as a co-receptor for AAV2, 3, 8 and 9[125]. In contrast, AAV5 transduction is mediated by the platelet derived growth factor receptor (PDGFR)[126].

I.B.6 Infection and replicative cycle

The infection and replication process has been most intensively studied in case of AAV2. Upon binding to HSPG, structural rearrangements that render the capsid compatible to interaction with α5ß1 were proposed[19] but could not be proven in a structural analysis of an AAV-2 heparin complex[127]. Interaction of AAV2 to cellular co-receptors mediates the dynamin-dependent endocytosis process via clathrin-coated pits into endosomes[128 129]. For AAV5, internalization has also been shown to take place in caveosomes via the caveolar pathway[130].

Endocytosis of particles is a rapid process lasting only milliseconds[131] and is promoted by the posphatidylinositol-3-kinase (PI3K) pathway via Rac1 that controls the intracellular trafficking of AAV to the nucleus along microfilaments and microtubules[132].

The vesicular trafficking is slow and represents a rate limiting step in many cell types[133,134,135,136]. To date, several potential intracellular trafficking pathways have been described for AAV2 and AAV5. Following internalization, the viruses residing in early endosomes may (I) be released into cytoplasm and travel in a vesicle-independent manner to the nucleus[128,137], may (II) be directed to late endosomal compartments and alternatively be released into cytoplasm from there, or (III) may accumulate in perinuclear recycling endosomes (PNRE)[138,139,140]. From PNRE or late endosomes, virions could also be rerouted to the *trans*-Golgi network before nuclear translocation takes place[141]. The use of alternative trafficking routes is not only cell type specific but also dose dependent, since a high multiplicity of infection (MOI) relocated AAV2 capsid accumulation from late endosomes to PNRE[142]. All pathways assume a final escape of particles into the cytoplasm before lysosomal degradation can occur.

The endosomal release of virions into the cytoplasm depends on externalization of the VP1/2 N-terminal domains containing the PLA_2 activity through the cylinders located at the 5-fold axis. The PLA_2 domain is shared by all serotypes[85] and essential for viral release[143,144]. A necessary but not sufficient trigger for the externalization seems to be the acidification of the endosomal compartment, and involvement of other unknown factors is probable[86,99]. Such factors could be posed by the endosomal proteases cathepsin B an L that are involved in uncoating of AAV2 and 8 *in vitro*[145] and may induce capsid modifications needed during externalization.

Upon accomplished release into cytoplasm, AAV is subject to ubiquitination and ubiquitin-dependent degradation by proteasomes. Employment of proteasome inhibitors[133,146] or mutation of surface exposed tyrosines prone to phosphorylation and ubiquitination[147] increased transduction efficiencies by preventing proteasomal degradation. Perinuclear accumulation of free AAV particles is probably mediated by Brownian diffusion or ATP-dependent cytoskeletal motor proteins[132,131,148]. The nuclear import is regarded as another inefficient and rate-limiting step and only little knowledge is existent about the process. One possibility involves the basic regions present within exposed VP1/2 N-termini (BR1-3) that would mediate the import via the nuclear pore complex (NPC)[88] but also alternative NPC-independent entry pathways have been postulated[135,137]. Since assembled viral capsids were detected within nucleoli, import of intact viral shells into the nucleus is expected, revealing the uncoating of viral DNA as an intranuclear process[128,86].

Another rate limiting step is posed by the conversion of the single-stranded viral DNA into the double-stranded state necessary for genome stability and gene expression[149,150]. Relocation of viral particles from nucleoli into nucleoplasm allows uncoating and may determine the efficiency of single-strand conversion[151]. The helper virus dependent DNA replication process is mediated at distinct nuclear foci and is antagonized by the host cell DNA repair complex MRN[152]. Here, the ITRs act as an origin of replication (reviewed by[60]) and contact domain of Rep78/68 proteins which interact with the RBE and trs sequences and unwind the double-stranded DNA. Rep52/40 are involved in the accumulation of single-stranded AAV genomes from double-stranded replicative intermediates. When latent, the Rep proteins mediate site-specific integration of AAV2 into the q-arm of the host chromosome 19 (AAVS1) or, as observed mainly *in vivo*, extrachromosomal persistence as circular episomes[153].

Besides uncoating and DNA replication, also assembly of capsids and packaging of newly replicated DNA in to pre-formed capsid occurs in the nucleus, more specifically in nucleoli[154]. Nucleophosmin and nucleolin on the one hand[155,156] and virus-own AAP[56] on the other, represent proteins that co-localize with VP proteins and support capsid formation. Initiation of viral genome encapsidation into pre-formed capsids is at least partially controlled by Rep78/68 proteins, probably by establishing contact between DNA and capsid[157,158,159]. The progression of DNA insertion is mediated by the helicase activity of Rep proteins in a 3' to 5' direction[76] through the 5-fold pore complex of the capsid[160]. Finally, the release of newly produced AAV virions is aided by the helper virus mediated cell lysis.

I.B.7 AAV Immunology

Due to its apparent lack of pathogenicity and low immunogenicity, AAV poses an interesting candidate for gene therapy trials in humans. However, about 50–80% of the human population has neutralizing antibodies (NABs) against AAV2, the template of most vectors currently used in gene-therapy trials, with the highest antibody prevalence shown for AAV2 and AAV1[161,162]. Antibodies against serotypes 5, 6, 8 and 9 were found less frequently but still remain a threat to satisfactory therapeutic returns. Despite the low general immunogenicity, interactions with the host immune system can be found at the level of innate, humoral and cell-mediated responses (reviewed by[163,164]). The innate responses to AAV investigated in animal models displayed a weak transient production of pro-inflammatory cytokines and chemokines and some infiltration of neutrophils and other leukocytes into the liver[165,166]. Triggering of Toll-like receptor (TLR) signalling was shown in mice[167] to lead to an increased uptake of AAV into macrophages and activation of the humoral immune response[163]. In seropositive humans, circulating IgG antibodies for AAV2 are primarily composed of the IgG1 and IgG2 subclasses, with negligible levels of IgG3 or IgG4[168]. Comparable to persistent AAV specific antibody levels, prime-boost studies in animals and clinical trials revealed that the B-cell memory is also strong[169,170].

But AAV-mediated immune response is not only restricted to B-cell activation, also the cell-mediated response involving T-cell activation is involved. Mingozzi *et al.*[171] reported the activation of AAV2 capsid-specific $CD8^+$ memory T-cells in humans but not in mice, leading to a lack of hepatic transgene expression by rejection of transduced hepatocytes. Investigation of exposed AAV2 capsid domains revealed several sites prone to recognition by the cellular and humoral immune system. Moskalenko *et al.*[172] identified seven regions of the capsid as epitopes for human polyclonal NABs. Especially the „spike“ and „plateau“ regions seem to play a crucial role in epitope formation. Point mutations of R471A or N587A as well as peptide insertion behind residue 587 prevented binding and neutralization by antibodies[173,174,109], suggesting that exposed capsid domains are more easily accessible to the immune system and may be preferred for epitope formation. As well, a number of candidate T-cell stimulating epitopes have been identified within the AAV capsid protein VP1, which may be attractive targets for modification of the capsid to avoid cell-mediated immune responses[168,175].

I.C AAV as a gene therapy vector

I.C.1 AAV-derived gene vectors

Recombinant AAV (rAAV) vectors are constructed by replacement of *rep* and *cap* ORFs with an expression cassette containing a transgene under the transcriptional control of a suitable promoter. Their synthesis occurs in a suitable producer cell line by transfection of three plasmids: one harbours the expression cassette flanked by ITRs (the only element required in *cis*), another provides the *rep* and *cap* helper sequences *in trans* and the third encodes adenoviral helper genes E2A, E4 and VA[176,177]. Alternatively, vectors can be produced from transfection of only two plasmids, since AAV and Ad helper genes can be combined in one plasmid[178]. These cotransfection approaches enable the generation of replication-deficient, wild type-free and adenovirus-free rAAV vector stocks at suitable titres. Since transduction by AAV vectors is characterized by a delayed onset of transgene expression derived from the rate-limiting process of double-strand conversion[149], self-complementary AAV (scAAV) vectors have been created by deletion of the D sequence[179] or by mutation of the trs sequence[180] present in the ITRs. This vector type packages dimeric inverted repeat DNA molecules, circumventing double-strand conversion and providing pseudo-first order kinetics upon uncoating (reviewed by[181]) albeit with a 50% reduced packaging capacity. Such AAV vectors lead to a sustained and efficient transgene expression in a wide variety of non-dividing cells *in vitro* and *in vivo* and provide a low integration rate into the host cell genome. Drawbacks are represened by a broad tissue tropism, a low transduction of a set of cell types and the prevalence of pre-existing humoral immunity, especially against AAV2.

To overcome these limitations, modern vectorology has turned towards the molecular engineering of AAV capsids in order to improve transduction efficiency, target specificity and escape from neutralization by capsid antibodies, which may be regarded as the three main support structures sustaining a viral gene transfer vector (reviewed by[6,182]).

I.C.2 Rational design of AAV vectors – the first steps

Significant improvement of AAV-derived vectors with respect to efficiency, specificity and immune evasion will most likely occur mainly by modification of the capsid, which represents the interface to receptors and antibodies. During the last decade, designer gene delivery vectors using more and more sophisticated approaches were developed that addressed and partially improved performance of AAV. This chapter (and reviews by[183,182,184]) gives a brief overview over applied technologies and their impact on the three pillars of vectorology.

I.C.2.1 Isolation of new serotypes and pseudotyping of vectors

Vectors based on AAV2 have been the most studied and have been shown to deliver genes to a broad range of cells in muscle, brain, retina, liver, and lung *in vivo*. However, the broad tropism, inefficient transduction of a set of clinically relevant tissues as well as a high prevalence of NABs soon rendered AAV2 insufficient for targeted gene delivery. First efforts focused on exploitation of alternative serotypes and provided a first opportunity to improve gene transfer to tissues. Over 100 serotypes from different animal species were isolated[42,183] and many *in vitro* and *in vivo* studies proved that these various natural variants displayed distinct tropisms and transduction patterns. Pseudotyping, *i.e.* the cross-packaging of a genome of one serotype into the capsid of another serotype, created infectious vectors with the tropism of the new capsid. For instance, a pseudotyped vector harbouring an AAV2 genome and AAV4 capsid (AAV2/4) exhibited ependymal cell-specific transduction, whereas AAV2/2 showed transduction biased to neurons in the central nervous system[185]. Pseudotyping is not only a convenient technique to isolate and characterize the capsid properties of newly identified serotypes but may also tackle the issue of prevalent NABs that differ between serotypes in humans. Antibodies generated against AAV2 did not cross-neutralize AAV1 vectors in mice[43] and pseudotyped AAV2/7 and AAV2/8 vectors exhibited negligible neutralization following pre-administration of AAV2 vector[45]. Despite the improvements in tropism and immune evasion achieved by pseudotyping, an increase of specificity to a single cell type by this method remains improbable.

I.C.2.2 Mosaic and chimerical capsids

A logical evolution in vector engineering was the combination of VPs from different serotypes, *i.e.* transcapsidation, thereby creating mosaic capsids that would combine the properties of the serotypes applied. By mixing the *rep* and *cap* helper plasmids during vector production, AAV1 and AAV2 VPs were combined in a vector that efficiently transduced both muscle (AAV1) and liver (AAV2)[186]. Rabinowitz *et al*.[187] extended the approach by producing mosaic capsids made from pair wise combinations of AAV serotype 1 to 5 plasmids employed at different ratios. Combination of AAV3 and AAV5 at the 3:1 ratio yielded vectors with dual binding properties to heparin and mucin agarose, which mimic the primary binding receptors for AAV3 and AAV5, respectively. Shortcomings of the transcapsidation attempt may represent the potential neutralization by NABs directed against either serotype and the combination of tropism from employed serotypes which may furthermore broaden the host cell spectrum.

I.C.2.3 Chemical and genetic engineering of capsids

The first attempt to restrict AAV tropism was posed by chemical or genetic modification of capsids which enabled attachment of conjugates to the capsid. The conjugates bridge interactions between vector and specific receptors, thereby allowing AAV transduction of non-permissive cells. In a pioneer study, indirect labelling of AAV by a bi-specific F(ab')2 antibody[188] or by avidin-biotin coupling to a fusion protein[189] mediated interaction between AAV and specific surface receptors from cells, which were non-permissive for normal AAV infection. However, the potentially transient and immunogenic nature of these protein complexes may be a limiting factor for transduction *in vivo*. To provide a more stable ligand interaction, AAV capsids were genetically engineered to express ligands at the N-terminal region of VP2 proteins, such as single-chain antibodies, serpin or ApoE receptor ligands, which significantly improved transduction of AAV-refractory cells[190,191,192]. In a pioneer study[193], insertion of a 14 amino acid peptide containing an RGD motif known to bind several cellular integrin receptors at capsid position 587 redirected AAV2 to αVß5 expressing cells. This approach was later employed on a regular basis for display of foreign peptides on the capsid surface. Position 587 was chosen via homology mapping to the known crystal structure of canine parvovirus[110] since the AAV2 structure was solved several years later[94] and has several implications. First, mutation of this essential HSPG-binding site at position 587[194] or 588[195,196] leads to a detargeting of AAV2 from liver after systemic application. Second, vectors modified at position 587 have the potential to escape immune neutralization without losing the ability to transduce tissue via targeted receptors[174]. Third, structural modelling of AAV2 allocated R585/588 at an exposed position on the shoulder of the 3-fold spikes that are present 60 times on the capsid. Peptide display at this site may therefore be feasible for receptor-ligand interaction and does not hamper capsid assembly.

I.C.3 High-through put library systems

Despite the success of AAV vectors based on serotypes other than AAV2, mosaic vectors, or rationally modified capsids, these approaches have only a limited potential for generating AAV tropism beyond those already present in natural serotypes. Ligand conjugation to AAV capsids improved targeting to non-permissive cells but modification of VP N-termini resulted in deficiencies of packaging and intracellular trafficking (reviewed by[197]). Encouraged by the results obtained from peptide insertion into the capsid, several groups have developed library-based systems that theoretically can be screened on any cell type of interest to detect variants that would maximize transduction efficiency, specificity and immune evasion. The selection process is performed by incubating target cells with virus library particles which will bind to cell surface receptors and enter the cell. Super-infection with Ad leads to selective amplification of internalized particles that can be purified and subjected to a new selection round for further enrichment of the most suitable mutants. The selection process not only leads to an enrichment of variants efficient in binding of receptors but also in intracellular processing, replication and progeny virus production. Peptide library-display on phage/AAV capsids, directed evolution and DNA family shuffling represent the basic techniques and individual or combined applications have yielded novel AAV vector variants with promising features for future clinical application.

I.C.3.1 Peptide library-display on AAV capsids

The display of randomized peptide libraries on phages represented the initial attempt to select for suitable ligands that retargeted vectors to previously inaccessible tissue[198]. Such phage-display selected ligands were later successfully incorporated into the AAV2 capsid and lead to selective targeting of AAV non-permissive cells[199,200]. Transfer of phage-derived peptides to the AAV capsid may however impose limitations. The peptide conformation may be altered when displayed in the AAV capsid context resulting in reduced or lost affinity to the receptor. Furthermore, selection of phage libraries occur only in favour of efficient receptor-ligand binding, while subsequent steps involved in efficient AAV transduction such as cell entry, intracellular trafficking and nuclear translocation remain unaffected. To overcome these limitations, two different peptide screening system have been developed independently Perabo *et al*.[194] and Müller *et al.*[195]. Both systems shared the generation of a plasmid library encoding random peptide heptamers that are displayed behind AAV2 capsid residues 587 or 588, respectively. The differences between the two approaches arose during subsequent production steps. In their two-step protocol, Perabo *et al*. transfected library and helper plasmid containing Ad genes alone into producer cells, potentially producing mosaic library capsids assembled from several VP library variants. Thus, packaged genomes and capsid variants did not correspond and presence of several library peptides on the same capsid could potentially lead to inconsistent selection and mislead evaluation.

The three step protocol of Müller *et al*. solved the problem by transfecting a second helper plasmid encoding wtAAV2 *rep* and *cap* sequences, intentionally creating a mosaic capsid library assembled from library and wtAAV2 VP subunits that was termed transfer shuttle library (TSL). In the third step, the intermediate TSL was used to re-infect the HEK 293T producer cell line at a multiplicity of infection (MOI) of one, thus theoretically limiting the virus DNA transfer to one library genome/cell. Upon super-infection with Ad, the internalized genome was packaged in capsids assembled from only one subunit library variant, maximizing the likelihood of genome packaging into corresponding capsids. It was assumed that the presence of wtAAV2 subunits within the TSL capsids would ensure equal infection efficiency of each TSL particle, preventing a biased production process. A serious drawback of this approach is represented by the generation of wild type viruses from homologous recombination of wild type and library *cap* sequences during TSL production. The use of a synthetic wtAAV2 *cap* fragment generated by alternative codon usage prevented recombination events and lead to the production of a wild type-free AAV2 random peptide library[201]. *In vitro* and *in vivo* selection of combinatorial AAV2 libraries have lead to identification of distinct peptide sequences that improved but did not completely restrict transduction of targeted tissues[201,202,196,203]. The low cell specificity of selected mutants may arise from ubiquitous expression of targeted receptors or the fact that AAV requires more than one receptor for transduction which probably binds to different capsid domains. Insertion of peptides may therefore retarget AAV to a new primary receptor leaving secondary receptor affiliations unattended. These receptors might be able to mediate vector uptake into cells in absence of an adequate primary receptor[119,118,90]. As well, some improvement of escape from antibody neutralization could be reported by disruption of epitopes via insertion of peptides[174,109,173].

I.C.3.2 Directed evolution

Directed evolution has been applied for creation of proteins with improved biological activities, antibodies with enhanced binding affinity or retroviral vectors with improved properties[204,205,206]. This powerful approach was independently adapted by Perabo *et al*.[207] and Maheshri *et al*.[208] primarily to create AAV2 capsids devoid of HSPG-binding with an antibody-evading phenotype. Basically, a plasmid library was prepared by error-prone PCR amplification of the AAV2 *cap* gene followed by the staggered extension process[209]. Subsequent cotransfection with sequences containing Ad helper genes resulted in the final virus library with distributed random point mutations throughout the capsid protein. Heparin affinity fractionation and/or *in vitro* selection in presence of NABs yielded AAV2 mutants with low HSPG affinities, high immune evasion properties *in vivo* and differential tropism compared to parent serotypes. However, a maximum of six (two) mutations prior (post) selection was the upper limit for this library type, rendering respective lead candidates nearly identical to wtAAV2. This low level of mutagenesis in fact may have improved immune escape but a specific retargeting and efficient transduction of tissue strongly differing from parental serotypes can not be expected.

I.C.3.3 DNA family shuffling

DNA shuffling is a process for directed evolution, which generates diversity by recombination[210], combining useful mutations from individual genes of a family. Thus, libraries of chimerical genes can be generated by random fragmentation of a pool of genes, followed by reassembly of the fragments in a self-priming polymerase chain reaction (PCR). The molecular breeding was first applied for murine leukaemia virus (MLV)[211] and conveyed to AAV by Koerber *et al*.[212] and Grimm *et al*.[213]. Several AAV *cap* genes from different serotypes were fragmented by DNase I digestion using various incubation times and fragments various in length and origin were reassembled by PCR to obtain full-length shuffled *cap* genes. The shuffled capsid libraries were then produced by cotransfecting the library plasmid containing the shuffled *cap* genes and a helper plasmid containing Ad genes. Selection of such libraries *in vitro* lead to an enrichment of distinct capsid chimeras composed of *cap* fragments from different serotypes. Consequently, another group prioritized the selection of the shuffled capsid library *in vivo* to select for myocardium-tropic mutants[214]. The approach was extended by Grimm *et al*.[213] who additionally inserted a peptide heptamer library (see Chapter I.C.3.1) into the AAV backbone capsid they previously selected from the shuffled capsid library *in vitro* to redirect and enhance transduction of lowly permissive tissue by subsequent *in vivo* selection. A subsequent study performed by Gray *et al*.[215] combined the initial shuffling technique with the directed evolution method (I.C.3.2) to select for variants that would cross the blood brain barrier (BBB) and transduce tissue from the central nervous system. Finally, Jang *et al*.[216] combined all three methods by first applying the shuffling technique, then inserting a peptide library and subsequently creating point mutations in the *cap* gene by error-prone PCR (Chapter I.C.3.2) to select for neural stem cell-specific “designer” vectors. Together, the selection of shuffled AAV capsid libraries on the cell/tissue type of interest generated mutants that outperformed transduction of wtAAV vectors of different serotype origin *in vitro* and *in vivo*. The chimerical character of the vector shells reduced neutralization by capsid antibodies, especially when library selection occurred in presence of neutralizing antibodies *in vitro*. However, shuffled capsids still harbour wtAAV sequences which could represent epitopes for pre-existing antibodies that were not abundant during *in vitro* exposure. In addition, the serotypes employed in the shuffling process limit vector retargeting to the respective serotype tropisms, except the shuffling technique is combined with other library approaches as in case of Grimm *et al*.[213], Gray *et al*.[215] or Jang *et al*.[216].

I.C.4 The endothelium as a target for AAV-mediated gene transfer

The endothelium is composed of a thin monolayer of endothelial cells (ECs) that line the interior surface of blood vessels, forming an interface between circulating blood and mural cells (smooth muscle cells, pericytes).

Endothelial tissue is a specialized type of mesenchymal tissue involved in many aspects of vascular biology, including atherosclerosis, blood clotting, inflammation, angiogenesis and vasoconstriction/vasodilatation. In some organs, highly differentiated and specialized endothelial cells perform filtering functions, as in case of the blood brain barrier. The endothelium acts as a selective barrier controlling the passage of molecular cargo and the transit of white blood cells into and out of the bloodstream. Endothelial dysfunction entails vascular diseases and may represent a key early event in the development of atherosclerosis. Impaired endothelial function is often seen in patients with coronary artery disease, diabetes mellitus, hypertension or hypercholesterolemia. A main mechanism of endothelial dysfunction is the decreased production of nitric oxide by increase in reactive oxygen species[217]. Thus, endothelium represents an interesting target tissue for therapeutic approaches and specific and efficient drug delivery or therapeutic gene transfer is in great demand. Since AAV has been discovered as a promising gene transfer vector, transduction of a multitude of cells and tissues has been attempted and depending on the permissiveness of cells for wtAAV, targeting occurred with more or less success. A less permissive cell is represented by the ECs and transduction efficiency with wtAAV was found to be very low *in vivo*[218,219] and *in vitro* [218,220,141]. Selection of a phage display peptide library on ECs *in vitro*[221] yielded peptides that upon insertion into the AAV2 capsid behind residue 587 improved transduction of endothelium over wtAAV2 *in vitro*[200] and *in vivo*[222]. In a subsequent *in vivo* selection attempt of the phage display library, peptides were isolated that redirected AAV2 successfully to the vascular bed *in vivo*[223]. These previous approaches used AAV2 serotype vectors which might not be ideal for future clinical approaches since there is a high prevalence of IgG against AAV2 in human serum[161,162]. In contrast, AAV9 serotype vectors are less affected by neutralizing factors in human serum[161] and allow a highly efficient gene transfer after intravenous vector administration to rodents[224,50,49,225]. Thus, combinatorial approaches displaying a library of randomized peptides on the AAV surface or capsid modification by shuffled or error-prone PCR may represent reasonable alternatives.

I.C.5 Goal of the present study

Efficiency of endothelial gene transfer using wtAAV vectors is low. The potential of random peptide libraries displayed on AAV2 to select for AAV2 vectors with improved efficiency for endothelium-directed gene transfer has been demonstrated. Transduction efficiency of endothelial cells could be increased *in vitro* and *in vivo* by introduction of an endothelial targeting peptide identified by phage display within the AAV capsids or selection of random AAV display peptide libraries on endothelial cells. However, these previous approaches used AAV2 serotype vectors which might not be ideal for future clinical approaches since there is a high prevalence of IgG against AAV2 in human serum.

In contrast, AAV9 serotype vectors are less affected by neutralizing factors in human serum peptide and allow a highly efficient gene transfer after intravenous vector administration. Thus, AAV9 vectors might be a more suitable basis for developing an endothelial gene transfer vector using endothelial targeting peptides. Therefore, the aim of the study was (I) to identify a suitable insertion site for targeting peptides within the AAV9 capsid surface, (II) to generate a random AAV9 peptide display library for selection of an AAV9-based targeting vector on endothelial cells, and (III) to compare vectors selected from AAV9 libraries with those from previous AAV2 libraries and to closer characterize them in terms of transduction efficiency *in vitro* and *in vivo*, target cell specificity and ability to evade neutralisation by NABs.

II. MATERIAL AND METHODS

II.A Material

II.A.1 Eukaryotic and prokaryotic cells

Primary eukaryotic cells

Denotation	*Description*	*Source, ordering number*
HCAEC	Human coronary artery endothelial cells	Promocell, C-12221
HCASMC	Human coronary artery smooth muscle cells	Promocell, C-12511
HUVEC	Human umbilical vein endothelial cells	Isolated from umbilical veins (Chapter II.F.7)

Immortalized eukaryotic cells

Denotation	*Description*	*Source, ordering number*
911	Adenoviral E1A/B transformed human embryonic retinoblastoma cells	Fallaux *et al*.[226]
HEK 293T	Adenoviral E1A/B and SV40 large T-antigen transformed human embryonic kidney epithelial cells	DuBridge *et al*.[227]
HeLa	Human cervical adenocarcinoma epithelial cells, positive for HPV-18 sequences	ATCC-No. CCL-2
HepG2	Human hepatocellular carcinoma epithelial cells	ATCC-No. HB-8065
H5V	Murine malignant hemangiosarcoma endothelial cells derived from heart capillaries	Garlanda *et al*.[228]

Prokaryotic cells (*E. coli*)

Denotation	*Source, ordering number*
ElektroMAX^{TM} DH5α-E Competent Cells	Invitrogen, 11319-019
Subcloning Efficiency DH5α Competent Cells	Invitrogen, 18265-017
One Shot DH5α-T1^{R} Chemically Competent Cells	Invitrogen, K4595-01

II.A.2 Cell culture media, supplements and associated solutions

Basal media, solutions and supplements for eukaryotic cell culture

Denotation	*Description*	*Source, ordering number*
Cell dissociation solution (1x)	Non-enzymatic	Sigma-Aldrich, C5789
CryoSFM	Solution for cryo-preserving of cells	Promocell, C-29910
DetachKit	Kit containing HepesBSS, Trypsin/EDTA and TNS	Promocell, C-41210
DMEM	Dulbecco's modified Eagle's medium	Sigma-Aldrich, D5796
ECGM	Endothelial cell growth medium kit	Promocell, C-22110
ECGM-MV	Endothelial cell growth medium MV kit	Promocell, C-22020
FBS	Fetal bovine serum	PAA, A15-100
Gelatine solution (2%)	2% w/v gelatine from bovine skin, 100 mM HCl in 1x PBS (dissolve at 37°C)	
HANKS (1x)	w/o Mg^{2+} and Ca^{2+}	PAA, H15-009
L-glutamine (100x)	200 mM	Invitrogen, 25030

PBS (1x)	8 g NaCl, 0.2 g KCl, 0.2 g KH_2PO_4, 1.15 g Na_2HPO_4•$2H_2O$, *ad* 1 L ddH_2O	
PSF (100x)	Penicillin (10.000 IU/ml), streptomycin sulphate (10 mg/ml), fungizone (25 µg/ml)	Promocell, C-42020
RPMI	RPMI-1640 medium	Sigma-Aldrich, R8758
SMCGM 2	Smooth muscle cell growth medium 2 kit	Promocell, C-22162
Trypan blue	0.4%	Sigma-Aldrich, T8154
Trypsin (1x)	0.05% trypsin, 0.02% EDTA	Invitrogen, 25300-062

Ready-to-use media for eukaryotic cell culture

Cell type	*Medium*
HCAEC	Provided supplements, 1x PSF in ECGM-MV
HCASMC	Provided supplements, 1x PSF in SMCGM 2
HUVEC	Provided supplements w/o hydrocortisone, 1x PSF in ECGM
HeLa, HEK 293T, 911, Hep G2, H5V	1x L-glutamate, 10% FBS, 1x PSF in DMEM

Media, solutions and supplements for prokaryotic cell culture

Denotation	*Description*	*Source, ordering number*
Amp	100 mg/ml ampicillin in ddH_2O, sterile-filtered	See also II.A.11
Kana	50 mg/ml kanamycin sulphate in ddH_2O, sterile-filtered	
LB medium	10 g Bacto Tryptone, 5 g yeast-extract, 10 g NaCl *ad* 1 L ddH2O, autoclave	
LB-amp/kana medium	10 g Bacto Tryptone, 5 g yeast-extract, 10 g NaCl *ad* 1 L ddH2O, autoclave, add 1 ml Amp/Kana at < 50°C	
LB-amp/kana agar plates	See LB-amp/kana, with additional 7.5 g Bacto agar, pour into 56.7 cm^2 cell culture dishes	
SOC	Ready-to-use bacterial broth w/o amp/kana	Invitrogen, 15544-034

II.A.3 Plasmids

Denotation	*Size (kb)*	*Description**	*References*
pBLCAT3	6.8	CAT-vector containing the entire murine VE-cadherin promoter (-2486 to +24, EMBL databank accession no. Y10887)	Prof. Dr. H. Augustin, DKFZ
pDGΔVP	20.7	Ad5 genes E4, E2A, VA essential for AAV packaging, *cap*2 partially deleted, used for serotype-independent AAV vector production	Dubielzig *et al*.[159]
pDP2(9)rs	23.6 (23.8)	Based on pDG, *rep*2/wt*cap*2(9), RSV-promoter controlled RFP gene for transfection control, used for production of wtAAV2(9) vectors	Grimm *et al*.[178] (Dr. R. Sprengel, MPI)
pMT-187-XX2 (pXX2-187)	8.3	*Rep*2/*cap*2mut, no ITRs, mutated HSPG binding site (R484E), used for production of AAV2 vectors with peptide display behind VP1 residue 588	Michelfelder *et al*.[202]
p5E18-VD2/9	7.3	*Rep*2/wt*cap*9, no ITRs, used for creation of p5E18-VD2/9-*SfiI*1759	Gao *et al*.[45]
p5E18-VD2/9-*SfiI*1759	7.3	Based on p5E18-VD2/9, *rep*2/*cap*9mut, used for production of AAV9 vectors with peptide display behind VP1-3 residue 589	This study

dsAAV-CMV-EGFP	5.8	ITRs, CMV-promoter controlled EGFP, used for serotype-independent production of scAAV vectors	Wu *et al*.[179]
dsAAV-CMV_{enh}-MLC_{260}-EGFP	6.0	Based on dsAAV-CMV-EGFP, CMV core element replaced by the myosin light chain promoter 260 bp fragment (MLC_{260})	Boecker *et al*.[229]
dsAAV-CMV-EGFPΔG67	5.8	Based on dsAAV-CMV-EGFP, non-fluorescent EGFP due to G67-deletion within ORF	This study
dsAAV-CMV_{enh}-163-EGFP	5.9	Based on dsAAV-CMV_{enh}-MLC_{260}-EGFP, MLC_{260} promoter replaced with the 163/313 bp fragment from murine VE-cadherin promoter	This study
dsAAV-CMV_{enh}-313-EGFP	6.1		This study
pRSV-VP3co	5.3	RSV-promoter controlled codon-optimized *cap*2 (VP3), used for production of serotype-independent transfer shuttle library particles	Waterkamp *et al*.[201]
pGA4	3.8	Contains a 975bp *cap*9mut-fragment harbouring 2 *SfiI* sites, used for creation of p5E18-VD2/9-*SfiI*1759	Geneart
pSSV9 (pSub201)	8.3	pEMBL(+) containing the entire AAV2 genome, 2 flanking *XbaI* sites for *rep*2/*cap*2 excision, used for creation of pKV-AAV9Lib	Samulski *et al*.[230]
pKV-AAV9Lib	8.3	Based on pSSV9, *rep*2/*cap*2 exchanged for *rep*2/*cap*9mut, used for creation of AAV9 library plasmid	This study
pEBFP-C1	4.6	CMV-promoter controlled EBFP reporter gene	Clontech, 6070-1

*All plasmids contain the *bla*-ORF providing ampicillin resistance to transformed *E.coli*, except pEBFP, which features the *npt*-ORF providing kanamycin resistance.

II.A.4 Single nucleotides and oligonucleotides

Single nucleotides

Denotation	*Description*	*Source, ordering number*
dNTPs	dATP, dTTP, dGTP and dCTP mix, PCR grade (10 mM each)	Invitrogen, 18427-013
α-^{32}P dCTP	Deoxycytidine 5'' triphosphate, [α-^{32}P] in 10 mM tricine (pH 7.6)	Perkin Elmer, NEG013H250UC

Primer for regular PCR

Denotation	*Sequence (5' to 3')*
AAV9cap-F	CCA TAC CCG GAA GAA TTC CTT GGT TTT G
AAV9cap-F2	GGA GGA TCC GCA GGT ACA GGT GTG T
AAV9cap-R	GCT TGA TGA ATT CTG GAC CTG CTA TGG C
VE-Cad-R	AAA **AAG CCT** AGT CTG TCC AGG GCC GAG
VE-Cad-F1	AAA **AGG ACC C**CT GCA GGC AGC TCA CAA A
VE-Cad-F2	AAA **AGG ACC C**AG CTT AGA GCC CCC ACA G

Primer for plasmid library generation

Denotation	*Sequence (5' to 3')*
NNK-Oligo	CAG TCG GCC AAG CAG GC $(NNK)_7$ GCC CAG GCG GCT GAC GAG
NNK-Oligo-2nd	CTC GTC AGC CGC CTG G

Primer for qRT-PCR

Denotation	*Sequence (5' to 3')*
CMV-F	TGC CCA GTA CAT GAC CTT ATT G
CMV-R	GAA ATC CCC GTG AGT CAA ACC
CMV-P (probe)	6-FAM – AGT CAT GCG TAT TAC CAT GG – MGB
Rep-F	AAG TCC TCG GCC CAG ATA GAC
Rep-R	CAA TCA CGG CGC ACA TGT
Rep-P (probe)	6-FAM – TGA TCG TCA CCT CCA ACA – MGB

Primer for sequencing

Denotation	*Sequence (5' to 3')*
AAV2cap-588ins	GTG TTT AAG TCC GAA TCC AC
AAV9cap-589ins	CAA ACA AGG AAC TGG AAG AG
EGFP-N	Clontech, 6479-1

Primer for PCR-mutagenesis

Denotation	*Sequence (5' to 3')*
EGFPΔG67-F	GAC CAC CCT GAC CTA CGT GCA GTG CTT CAG GGC G
EGFPΔG67-R	GCG GCT GAA GCA CTG CAC GTA GGT CAG GGT GGT C
IVM-F	CAA TTA CAG ATT ACG AGT CAG ATA TCG TGC CAA TGG GGC GAG
IVM-R	CTC GCC CCA TTG GCA CGA TAT CTG ACT CGT AAT CTG TAA TTG

Oligonucleotides for AAV2 peptide insertion

Orientation	*Linker 5'*	*Sequence (5' to 3')*							*Linker 3'*
Forward	AGGC	AAT	GAT	GTT	AGG	GCG	GTG	AGT	GCCCAGG
Reverse	GGGC	ACT	CAC	CGC	CCT	AAC	ATC	ATT	GCCTCTC
Peptide		**N**	**D**	**V**	**R**	**A**	**V**	**S**	
Forward	AGGC	TCT	CTG	AGG	TCG	CCT	CCG	TCA	GCCCAGG
Reverse	GGGC	CGA	CGG	AGG	CGA	CCT	CAG	AGA	GCCTCTC
Peptide		**S**	**L**	**R**	**S**	**P**	**P**	**S**	
Forward	AGGC	CGT	GGT	GAT	TTG	CGT	GTG	TCT	GCCCAGG
Reverse	GGGC	AGA	CAC	ACG	CAA	ATC	ACC	ACG	GCCTCTC
Peptide		**R**	**G**	**D**	**L**	**R**	**V**	**S**	
Forward	AGGC	AAT	TTG	CAT	TCT	CCT	CCG	GCT	GCCCAGG
Reverse	GGGC	AGC	CGG	AGG	AGA	ATG	CAA	ATT	GCCTCTC
Peptide		**N**	**L**	**H**	**S**	**P**	**P**	**A**	
Forward	AGGC	AAT	TCC	GTC	TCC	TCC	GCC	TCC	GCCCAGG
Reverse	GGGC	GGA	GGC	GGA	GGA	GAC	GGA	ATT	GCCTCTC
Peptide		**N**	**S**	**V**	**S**	**S**	**A**	**S**	
Forward	AGGC	AAT	TCC	TCC	AGA	GAT	CTG	GGG	GCCCAGG
Reverse	GGGC	CCC	CAG	ATC	TCT	GGA	GGA	ATT	GCCTCTC
Peptide		**N**	**S**	**S**	**R**	**D**	**L**	**G**	

Oligonucleotides for AAV9 peptide insertion

Orientation	*Linker 5'*	*Sequence (5' to 3')*							*Linker 3'*
Forward	AGGC	AAT	GAT	GTT	AGG	GCG	GTG	AGT	GCCCAGG
Reverse	GGGC	ACT	CAC	CGC	CCT	AAC	ATC	ATT	GCCTGCT
Peptide		**N**	**D**	**V**	**R**	**A**	**V**	**S**	
Forward	AGGC	TGG	CTC	ACC	CTG	GTC	GGG	AAG	GCCCAGG
Reverse	GGGC	CTT	CCC	GAC	CAG	GGT	GAG	CCA	GCCTGCT
Peptide		**T**	**E**	**W**	**D**	**Q**	**P**	**F**	
Forward	AGGC	CGT	GGT	GAT	TTG	CGT	GTG	TCT	GCCCAGG
Reverse	GGGC	AGA	CAC	ACG	CAA	ATC	ACC	ACG	GCCTGCT
Peptide		**R**	**G**	**D**	**L**	**R**	**V**	**S**	
Forward	AGGC	AAT	AAT	GTT	CGG	GGG	TTT	GTG	GCCCAGG
Reverse	GGGC	CAC	AAA	CCC	CCG	AAC	AAT	AAT	GCCTGCT
Peptide		**N**	**N**	**V**	**R**	**G**	**F**	**V**	
Forward	AGGC	TCT	CTG	AGG	TCG	CCT	CCG	TCA	GCCCAGG
Reverse	GGGC	CGA	CGG	AGG	CGA	CCT	CAG	AGA	GCCTGCT
Peptide		**S**	**L**	**R**	**S**	**P**	**P**	**S**	
Forward	AGGC	TCT	ATT	AGG	TCT	CCT	CCT	TCT	GCCCAGG
Reverse	GGGC	AGA	AGG	AGG	AGA	CCT	AAT	AGA	GCCTGCT
Peptide		**S**	**I**	**R**	**S**	**P**	**P**	**S**	
Forward	AGGC	AAT	TTT	ACT	CGG	TTG	TCG	GCG	GCCCAGG
Reverse	GGGC	CGC	CGA	CAA	CCG	AGT	AAA	ATT	GCCTGCT
Peptide		**N**	**F**	**T**	**R**	**L**	**S**	**A**	
Forward	AGGC	CGT	GGG	GAT	TTT	AGG	GTT	GGT	GCCCAGG
Reverse	GGGC	ACC	AAC	CCT	AAA	ATC	CCC	ACG	GCCTGCT
Peptide		**R**	**G**	**D**	**F**	**R**	**V**	**G**	
Forward	AGGC	AAT	TTG	CAT	TCT	CCT	CCG	GCT	GCCCAGG
Reverse	GGGC	AGC	CGG	AGG	AGA	ATG	CAA	ATT	GCCTGCT
Peptide		**N**	**L**	**H**	**S**	**P**	**P**	**A**	
Forward	AGGC	CCT	TCT	CTG	CCT	TCT	AGG	TCT	GCCCAGG
Reverse	GGGC	AGA	CCT	AGA	AGG	CAG	AGA	AGG	GCCTGCT
Peptide		**P**	**S**	**L**	**P**	**S**	**R**	**S**	
Forward	AGGC	TCT	GAT	TTG	CGT	CGT	GGT	GTG	GCCCAGG
Reverse	GGGC	CAC	ACC	ACG	ACG	CAA	ATC	AGA	GCCTGCT
Peptide		**S**	**D**	**L**	**R**	**R**	**G**	**V**	
Forward	AGGC	AAT	TCC	GTC	TCC	TCC	GCC	TCC	GCCCAGG
Reverse	GGGC	GGA	GGC	GGA	GGA	GAC	GGA	ATT	GCCTGCT
Peptide		**N**	**S**	**V**	**S**	**S**	**A**	**S**	
Forward	AGGC	AAT	TCC	TCC	AGA	GAT	CTG	GGG	GCCCAGG
Reverse	GGGC	CCC	CAG	ATC	TCT	GGA	GGA	ATT	GCCTGCT
Peptide		**N**	**S**	**S**	**R**	**D**	**L**	**G**	

II.A.5 Enzymes

Denotation	*Source, ordering number*
Antarctic phosphatase (supplied w/ 10x Antarctic phosphatase reaction buffer)	NEB, M0289S
Benzonase	Sigma-Aldrich, E1014-25KU
Dispase	Invitrogen, 17105041
Restriction enzymes	Roche, NEB, Fermentas
T4 DNA ligase (supplied w/ 10x T4 DNA ligase reaction buffer)	NEB, M0202S
T4 DNA polymerase (supplied w/ 10x NEBuffer 2 and 100x BSA)	NEB, M0203S
Taq DNA polymerase (supplied w/ 10x TaqBuffer)	NEB, M0273G
TaqMan Universal PCR Master Mix	Applied Biosystems, 4304437

II.A.6 DNA standards and loading buffers

Denotation	*Source, ordering number*
Gel Loading Dye Blue (6x)	NEB, B7021S
O'RangeRuler 50 bp DNA Ladder	Fermentas, SM0613
O'RangeRuler 1 kb DNA Ladder Plus	Fermentas, SM1343

II.A.7 Antibodies

Denotation	*Description*	*Source, ordering number*
ADK9	WtAAV9 capsid binding murine monoclonal antibody	Prof. Dr. J. A. Kleinschmidt, DKFZ
IVIG	Human pooled intravenous immunoglobulin, 10%, Gamunex R	Talecrid Biotherapeutics, 80A4895
PECAM-1	FITC-conjugated mouse anti-human monoclonal antibody	Lifespan Biosciences, LS-C43861

II.A.8 Viruses

Denotation	*Description*	*Source, ordering number*
Ad5	Human wild type Adenovirus 5	Laboratoire de Thérapie Génique (II.A.15)

II.A.9 Kits

Denotation	*Source, ordering number*
DNeasy Blood & Tissue Kit	Qiagen, 69504
Mini Quick Spin Oligo Columns	Roche, 11814397001
PeqGOLD Plasmid Miniprep Kit I	Peqlab, 12-6942-02
QIAamp MinElute Virus Spin Kit	Qiagen, 57704
QIAGEN HiSpeed Plasmid Maxi Kit	Qiagen, 12663
QIAGEN Plasmid Giga Kit	Qiagen, 12191
QIAGEN Plasmid Mega Kit	Qiagen, 12183
QIAquick Gel Extraction Kit	Qiagen, 28704
QIAquick Nucleotide Removal Kit	Qiagen, 28304
QIAquick PCR Purification Kit	Qiagen, 28104
QuickChange II Site-Directed Mutagenesis Kit	Stratagene, 200523-5

Random Primed DNA Labelling Kit	Roche, 11004760001
Rapid DNA Ligation Kit	Fermentas, K1421
Sequenase DNA Sequencing Kit 2.0	GE Healthcare, E70775Y
TOPO TA Cloning Kit for Sequencing	Invitrogen, K4595-01

II.A.10 Buffers and solutions

*Denotation**	*Description*	*Source, ordering number*
Annealing buffer	10 mM TRIS, 150 mM NaCl in ddH_2O (pH not adjusted)	
$CaCl_2$ (0.1M)	14.7 g $CaCl_2$ *ad* 1 L ddH_2O	
$CaCl_2$/glycerol	14.7 g $CaCl_2$, 16.1 ml 87% glycerol, *ad* 1 L ddH_2O	
Denaturation buffer	1.5 M NaCl, 0.5 M NaOH in ddH_2O	
Elution buffer	10 mM TRIS in ddH_2O (adjust to pH 9 with 1 N HCl)	
EDTA (0.2 M)	58.45 g EDTA *ad* 1 L ddH_2O	
EtOH (70%)	70% v/v ethanol in ddH2O	
HCl (40 mM)	40 ml 1 N HCl *ad* 1 L ddH2O	
HBSS	Hank's buffered salt solution, w/o Ca^{2+} and Mg^{2+}	Invitrogen, 14175
HBSS	Hank's buffered salt solution, w/ Ca^{2+} and Mg^{2+}	Invitrogen, 14065
HSNH	10 mM HEPES, 10 mM NaN_3, 2% v/v NCS in 1x HBSS	
Hybridisation buffer	7% SDS, 125 mM Na_2HPO_4•$2H_2O$, 125 mM NaH_2PO_4, 250 mM NaCl, 1 mM EDTA, 45% formamide in ddH_2O (dissolve under stirring at 37°C)	
$MgCl_2$ (0.1 M)	20.33 g $MgCl_2$ *ad* 1 L ddH_2O	
MNT	50 mM TRIS, 150 mM NaCl, 5 mM $MgCl_2$ in ddH_2O (adjust to pH 8.5 with 1 M HCl, add 1x Protease Inhibitor Mix HP prior to use)	
NaCl (0.3M)	17.53 g NaCl *ad* 1 L ddH_2O	
NaOAc (3 M)	408.24 g NaOAc *ad* 1 L ddH_2O	
NaOH (2 M)	80 g NaOH pellets *ad* 1 L ddH_2O	
NCS	Newborn calf serum	Sigma-Aldrich, N4762
Neutralization buffer	0.5 M TRIS, 0.3 M $Na_3C_6H_5O_7$•$2H_2O$, 3 M NaCl in ddH_2O (adjust pH to 7 with 1 N HCl)	
Iodixanol (60%)	OptiPrep	Axis Shield, 1114542
PBS-MK	1 mM $MgCl_2$, 2.5 mM KCl in 1x PBS	
PBS-MKN	1 M NaCl in 1x PBS-MK	
PEI (7.5 mM)	0.323 g polyethyleneimine *ad* 1 L ddH_2O	See also II.E.1
Phenol red (0.07%)	0.07 g phenol red *ad* 100 ml ddH_2O	
SSC (20x)	3 M NaCl, 0.3 M $Na_3C_6H_5O_7$•$2H_2O$ in ddH2O (adjust pH to 7 with 1M NaOH)	
Sodium heparin solution	280 mg/ml sodium heparin in ddH_2O (42.000 IU/ml)	
Staining solution	1 µg/ml propidium iodide in 1x HSNH	
TAE	4.84 g TRIS, 0.37 g EDTA, 1.14 ml acetic acid, *ad* 1 L ddH_2O (pH not adjusted)	
TE	1 mM TRIS, 0.01 mM EDTA, in ddH_2O (adjust pH to 8 with 1 N HCl)	
TRITC-lectin solution	20 µg/ml TRITC-lectin in 1x HBSS w/ Ca^{2+} and Mg^{2+}	
Washing solution	1x SSC, 0.1% SDS in ddH2O	
X-gal	40 mg/ml BCIG in DMF	

*All buffers and solutions are ready-to-use (1x) except when otherwise indicated.

II.A.11 Chemicals

Denotation	*Description*	*Source, ordering number*
Acetic acid	Glacial	Merck, 1.00063.1011
Agar		Gerbu, 1340
Agarose		Sigma-Aldrich, A9539
Ampicillin		Sigma-Aldrich, A0166
Bacto Tryptone		BD Biosciences, 0123-17-3
BCIG (X-gal)	5-bromo-4-chloro-3-indolyl-β-D-galactopyranoside	Roche, 10651745001
$CaCl_2$•$2H_2O$	Calcium chloride dihydrate	Sigma, C7902
Cryo-embedding compound	Tissue-Tek O.C.T	Sakura Finetek
ddH_2O	Double-demineralised water (ultrapure water system)	
DMF	N,N-dimethylformamide	Sigma-Aldrich, 40250
EDTA	Disodium ethylenediamine tetraacetate	Gerbu, 1034
EtBr (ethidium bromide)	3,8-diamino-5-ethyl-6-phenylphenanthridiniumbromid, 1%	Roth, 2218.2
EtOH	Ethanol, 99.8%	VWR, 20821.321
Formamide		Roth, 6749.1
Gelatin from bovine skin	Type B	Sigma-Aldrich, G9391
Glycerol	87%	Applichem, A3561
HCl	Hydrochloric acid, 1N	VWR, 1.09057.1000
HEPES	4-(2-hydroxyethyl)-1-piperazineethanesulfonic acid	Roth, 9105.2
Kanamycin sulphate		Roche, 70162526
KCl	Potassium chloride	Roth, 6781.1
KH_2PO_4	Potassium dihydrogen phosphate	Roth, 3904.1
$MgCl_2$•$6H_2O$	Magnesium chloride hexahydrate	Merck, 1.05833.1000
Mounting medium with DAPI	Vectashield Hard Set	Vector Laboratories
Sodium heparin		Neolab, 10475.0001
Na_2HPO_4•$2H_2O$	Disodium hydrogen phosphate dihydrate	Roth, T877.1
$Na_3C_6H_5O_7$•$2H_2O$	Trisodium citrate dihydrate	Sigma-Aldrich, 71405
NaCl	Sodium chloride	VWR, 27810.364
NaH_2PO_4	Sodium dihydrogen phosphate dihydrate	Merck, 1.06342.1000
NaN_3	Sodium azide	Serva, 30175
NaOAc•$3H_2O$	Sodium acetate trihydrate	Roth, 6779.1
NaOH	Sodium hydroxide pellets	Roth, 6771
PEI	Polyethyleneimine	Polysciences, 23966
Phenol red	Phenolsulphonphthalein	Merck 137038
Propidium iodide		Sigma-Aldrich, P4170
Protease-Inhibitor Mix HP	100x	Serva, 39106
SDS	Sodium dodecyl sulphate	Gerbu, 1212
TRIS	Tris-(hydroxymethyl)-aminomethane	Roth, 5429.3
TRITC-lectin	Lectin from *Bandeireia simplicifolia*, TRITC conjugated	Sigma-Aldrich, L5264
Yeast extract		Gerbu, 1133

II.A.12 Disposables

Denotation	*Type*	*Source, ordering number*
20G x 1½ needles	Microlance 3	BD Biosciences
384-well plate	MicroAmp Optical	Applied Biosystems
96-well microtitre plates with agar		GATC
Adhesive film	MicroAmp Optical	Applied Biosystems
Cell culture dishes	56.7/145 cm^2	Thermo Scientific
Cell culture flasks	25/75/175 cm^2	Greiner Bio-One
Cell culture plates	6/12/96-well	Thermo Scientific
Cellulose chromatography paper	Whatman	Whatman
Centrifuge tubes	Falcon, 15/50 ml	BD Biosciences
Conical-bottom tubes	4.5 ml	Greiner Bio-One
Cryogenic vials	CryoTube, 1.0/1.8/3.6/4.5 ml	Thermo Scientific
Cryomolds	Tissue-Tek, intermediate	Sakura Finetek
Electroporation cuvettes	GenePulser/MicroPulser, 0.2 cm gap	Bio Rad
Fat pen	Dako pen	Dako
Glass bottles	50-2500 ml	Brand
Hybridisation transfer membrane	GeneScreen Plus	Perkin Elmer
Large centrifuge tubes	500 ml	Corning, 431123
Microscope slides + coverslips	Superfrost plus	Thermo Scientific
Microtome blades	MX35 Premier+, 34°/80 mm	Thermo Scientific
Miniprep tubes	14 ml, round-bottom, dual-position snap cap	BD Biosciences
Pasteur pipettes		WU
Pipette tips	Micro/200/1000 µl	Greiner Bio-One
Reaction tubes	0.5/1.5/2 ml, safe-lock	Eppendorf
Round-bottom tubes	5 ml	BD Biosciences, 352008
Screw-cap tubes	1.5 ml, conical	Sarsted
Semi-micro cuvettes	3 ml	Greiner Bio-One
Serological pipettes	Falcon, 5/10/25 ml	BD Biosciences
Sterile filter	0.2 µm pore size	Renner
Syringes	2/5 ml	BD Biosciences
	1 ml Soft-Ject Luer	HSW
Tissue culture chambers	CellSTACK, 5/10-stack	Corning
U-bottom cell culture plates	96-well	Greiner Bio-One
Ultracentrifuge tubes	Quick-Seal, 13.5/39 ml	Beckman Coulter

II.A.13 Laboratory equipment

Denotation	*Type*	*Source, ordering number*
Cell counting chamber	Neubauer	Brand
Cell culture incubator	B 5601 EC-CO_2	Thermo Scientific
Contamination monitor	LB 122 C	Berthold
Crosslinker	UV Stratalinker 1800	Stratagene
Cryostat	CM3050 S with MX35 Premier+ microtome blades	Leica Microsystems
Cryostorage system	K series	Tec-Lab

Culture myograph		DMT
Electroporation instrument	Gene Pulser Xcell	Bio Rad
Floor centrifuge	RC 5C Plus (with GS3 rotor)	Sorvall
Flow cytometer	FACSCalibur	BD Biosciences
Fluorescence microscopes	DM IL (with incident light fluorescence unit and DFC 350 FX monochrome camera) DM RD (with incident light fluorescence unit and Hamamatsu ORCA 100 camera)	Leica Microsystems
Freezing container	Cryo 1°C, PC	Thermo Scientific
Gel documentation system	ImageQuant 100	Amersham Biosciences
Gel electrophoresis chambers	Horizontal, mini/midi, with combs	Peqlab
Hybridisation bottles	BigShot III	Fisher Scientific
Hybridising furnace	400 HY-E	Bachofer
HybriDot manifold		Whatman
Light microscope	CK 2	Olympus
Micro-volume spectrophotometer	NanoDrop ND1000	Peqlab
Mobile pipetor for serological pipettes	Pipetboy Acu	Integra
Molecular imager	Storm 860	Molecular Dynamics
Multichannel pipette	Transferpette (8/12 channel)	Brand
Pipettes	Pipetman, 2/20/200/1000µl	Gilson
Power supply	EPS 600	Amersham Biosciences
Preparative ultracentrifuge	Optima LE-80k	Beckmann Coulter
Radioactivity counter	QC 2000	Bioscan
Real-Time PCR System	7300 Fast	Applied Biosystems
Seal former	Sealing of ultracentrifuge tubes	Beckmann Coulter
Spectrophotometer	Ultrospec 3100pro UV/visible	GE Healthcare
Storage phosphor screens		Molecular Imaging
Table-top centrifuge (large)	5810 R (with A-4-62 rotor)	Eppendorf
Table-top centrifuge (small)	Biofuge Fresco	Heraeus
Thermal cycler	GeneAmp 9700 (96-well)	Applied Biosystems
Tube sealer	Sealing of ultracentrifuge tubes	Beckman Coulter
Ultracentrifuge rotors and spacers	50.2/70.1Ti	Beckman Coulter
Ultrapure water system	Milli-Q Biocel A10	Millipore
Ultrasound water bath	Sonorex TK 30	Bandelin
Vacuum concentrator		Bachofer

II.A.14 Software

Denotation	*Application*	*Source, ordering number*
Adobe CS5	Graphic processing	Adobe Systems
CellQuest Pro 6.0	Acquisition of flow-cytometry data	BD Biosciences
FlowJo 7.6	Analysis of flow-cytometry data	Tree Star
ImageQuant 4.1	Scanning of storage phosphor screens	Molecular Dynamics
Geneious 5.3	Sequence alignment	Biomatters
ImageQuant Capture 1.0.1	Gel documentation	GE Healthcare
PyMol 1.4	Molecular visualisation	www.jalview.org

OpenOffice 3.2	Text processing	Oracle
Primer X	Mutagenic primer design	http://www.bioinformatics.org/primerx
SDS 1.4	Analysis of qRT-PCR data	Applied Biosystems
SigmaPlot 10.0	Statistical evaluation of data	Systat Software

II.A.15 Company affiliations

Company name	*City**
Adobe Systems	München
Amersham Biosciences	Freiburg
Applichem	Darmstadt
Applied Biosystems	Darmstadt
Axis-Shield	Heidelberg
Bachofer	Burladingen
Bandelin	Berlin
BD Biosciences	Heidelberg
Beckman Coulter	Krefeld
Berthold	Bad Wildbad
Biomatters	Auckland
Biorad	München
Bioscan	Paris
Brand	Wertheim
Braun	Melsungen
Charles River Laboratories	Sulzfeld
Clontech	Heidelberg
Corning	München
Dako	Hamburg
DMT	Copenhagen
Eurofins MWG	Ebersberg
Fermentas	St. Leon Roth
Fisher Scientific	Schwerte
GATC	Konstanz
GE Healthcare	München
Geneart	Regensburg
Gerbu	Heidelberg
Gilson	Limburg-Offheim
Greiner Bio-One	Essen
Hamamatsu	Herrsching
Heraeus	Hanau
HSW	Tuttlingen
Tec-Lab	Idstein
Integra	Zürich

Company name	*City**
Invitrogen	Karlsruhe
Laboratoire de Thérapie Génique	Nantes
Leica Microsystems	Wetzlar
Lifespan Biosciences	Eching
Merck	Darmstadt
Molecular Dynamics	Krefeld
MPI for Medical Research	Heidelberg
NEB (New England Biolabs)	Frankfurt am Main
Neolab	Heidelberg
Oligo Synthesis Core Facility	University of Freiburg
Olympus	Hamburg
Oracle	München
PAA	Cölbe
Peqlab	Erlangen
Perkin Elmer	Rodgau
Polysciences	Heidelberg
Promocell	Heidelberg
Qiagen	Hilden
Renner	Dannstadt
Roche	Mannheim
Roth	Karlsruhe
Sakura Finetek	Staufen im Breisgau
Sarstedt	Nümbrecht
Sigma-Aldrich	Hamburg
Stratagene	Waldbronn
Systat Software	Erkrath
Talecrid Biotherapeutics	Frankfurt am Main
Thermo Fisher	Langenselbold
Thermo Scientific	Schwerte
Tree Star	Olten
Vector Laboratories	Eching
WU	Mainz
VWR	Darmstadt
Whatman	Dassel

*All companies are located in Germany, except Bioscan or Laboratoire de Thérapie Génique (France), Integra (Switzerland), Biomatters (New Zealand) and DMT (Denmark).

II.B Molecular biological methods

II.B.1 Plasmid and virus DNA purification

Bacterial cells were harvested by repeated centrifugation in suitable plastic vessels (5000 x *g*, 15 min, 4°C) until the entire culture was processed and plasmid DNA was purified by QIAGEN Plasmid Purification Kits according to manual instructions (Table II.B.1-1). Elution of DNA took place in a suitable amount of elution buffer or ddH_2O.

Table II.B.1-1: Bacterial culture volumes and corresponding DNA purification kits

Culture volumes	*Employed kit*	*User guide*
1 ml	PeqGOLD Plasmid Miniprep Kit I	07/2006, A. High copy-number plasmids, steps 2-9
200 ml	QIAGEN HiSpeed Plasmid Maxi Kit	11/2005, steps 4-21, guideline in red
1000 ml	QIAGEN Plasmid Mega Kit	11/2005, pages 25-28, steps 4-15, guideline in blue
5000 ml	QIAGEN Plasmid Giga Kit	11/2005, pages 25-28, steps 4-15, guideline in red

Purification of plasmid DNA previously exposed to enzymatic digestion (Chapter II.B.2), electrophoretic separation (Chapter II.B.6) or PCR (Chapter II.B.8) was done with QIAquick kits noted in Table II.B.1-2 according to manufacturer's recommendations. Unless otherwise specified, elution from spin columns occurred in 30 µl ddH_2O. If the amount of DNA to be purified exceeded the recommended amounts per column, DNA samples were separated on several columns.

Table II.B.1-2: DNA purification kits used for plasmid DNA fragment purification

DNA source	*Employed kit*	*User guide (QIAquick Spin handbook 03/2008)*
Enzymatic digestion	QIAquick Nucleotide Removal Kit	pages 23-24, steps 1-7
PCR	QIAquick PCR Purification Kit	pages 21-22, steps 1-7
Electrophoretic separation	QIAquick Gel Extraction Kit	pages 27-29, steps 2-11

Viral DNA was purified from capsid particles obtained by cell lysis (Chapter II.E.1) or density gradient centrifugation (Chapter II.E.2) with the QIAamp MinElute Virus Spin Kit (04/10, all steps) and DNA was eluted in 60 µl ddH_2O. By purifying 6E+8 gc/sample, a final concentration of ~1E+7 gc/µl or ~55 pg/µl DNA was obtained.

II.B.2 Restriction digestion of plasmid DNA

All restriction enzymes were purchased from Roche, NEB or Fermentas and digestion was carried out in corresponding buffers supplied by the manufacturer at enzyme-specific temperatures for 2 h, unless otherwise noted. In case double-digestion was required and enzymes were not compatible with the same buffer, DNA was purified with the QIAquick PCR Purification Kit (Chapter II.B.1) after the first digestion reaction. Success of digestion was controlled by gel electrophoresis (Chapter II.B.6) and, if required, repeated by adjusting amounts of enzyme, amounts of DNA or incubation time.

A general protocol of a restriction digestion reaction is given in Table II.B.2. If FastDigest enzymes (Fermentas) were used, reaction parameters were set up according to manufacturer's recommendations applying doubled incubation times.

Table II.B.2: Protocol for DNA restriction digestion

Volume	*Final concentration*	*Reagent*
Variable	Max. 10 µg	DNA
5 µl	1x	10x enzyme buffer
5 µl	1x	100x BSA, 1:10 pre-diluted in ddH_2O*
Variable	5-20 U/µg DNA	Restriction enzyme
Ad 50 µl		ddH_2O

*BSA-addition was only required for certain NEB enzymes

II.B.3 Chemical modification of free DNA ends

To enable blunt end ligation of incompatible cohesive DNA ends, a fill-in of 5' or removal of 3' overhangs was performed using the T4 DNA polymerase. The reaction (Table II.B.3-1) was incubated for 15 min at 12°C and was stopped by adding 1 µl 0.2 M EDTA and heating to 75°C for 20 min. DNA fragments were then purified with the QIAquick Nucleotide Removal Kit (Chapter II.B.1).

Table II.B.3-1: Protocol for T4 DNA polymerase-mediated DNA-blunting

Volume	*Final concentration*	*Reagent*
Variable	Variable	Plasmid backbone
5 µl	100 µM	10 mM dNTP, 1:100 pre-diluted in ddH_2O
5 µl	1x	10x NEBuffer 2
5 µl	1x	100x BSA, 1:10 pre-diluted in ddH_2O
1 µl	3 U/µg DNA	T4 DNA polymerase
Ad 50 µl		ddH_2O

To reduce vector re-ligation 5' phosphate groups from plasmid DNA backbones were removed using Antarctic phosphatase. The reaction (Table II.B.3-2) was allowed to take place 30 min at 37°C, followed by an inactivation step at 65°C for 5 min. Dephosphorylated DNA fragments were purified with the QIAquick Nucleotide Removal Kit (Chapter II.B.1).

Table II.B.3-2: Protocol for dephosphorylation of DNA ends

Volume	*Final concentration*	*Reagent*
Variable	Variable	Plasmid backbone
5 µl	1x	10x Antarctic phosphatase reaction buffer
1 µl	5 U/µg DNA	Antarctic phosphatase
Ad 50 µl		ddH_2O

II.B.4 Ligation of plasmid DNA

II.B.4.1 General ligation protocol

Ligation of DNA fragments with cohesive or blunt ends was performed at a fivefold molar excess of insert-to-backbone using either the Rapid DNA Ligation Kit (06/2004, manual page 3, steps 1-3) or the protocol described in Table II.B.4.1 with an o/n incubation at 16°C.

Table II.B.4.1: Protocol for DNA ligation

Volume	*Final concentration*	*Reagent*
Variable	100 ng	Plasmid backbone
Variable	5x molar excess	Insert
2.5 µl	1x	10x T4 DNA ligase reaction buffer
1 µl	400 cohesive end units	T4 DNA ligase
Ad 25 µl		ddH_2O

II.B.4.2 Ligation of oligonucleotides into AAV2 or AAV9 plasmid backbones

Complementary forward and reverse 32-mer oligonucleotides specified in Chapter II.A.4 were synthesized on a 0.01 µmol scale and HPSF-purified at Eurofins MWG. Reconstitution occurred in a ddH_2O volume indicated by MWG to obtain a concentration of 100 pmol/µl. For insertion of oligonucleotides plasmids p5E18-VD-2/9-*SfiI*1759 or pMT-187-XX2 (Chapter II.A.3) were digested with 4 U/µg DNA *SfiI* for 4 h releasing a 15 bp DNA stuffer fragment that was separated from backbone DNA by gel electrophoresis (Chapter II.B.6). The plasmid backbone was recovered from preparative gel and DNA was purified with the QIAquick Gel Extraction Kit (Chapter II.B.1). Two µg each, forward and reverse oligonucleotides were mixed with annealing buffer *ad* 40 µl and annealing reaction was allowed to take place (95°C/5 min, 76°C/20 min and 37°C/20 min). Ligation of 100 ng *SfiI*-linearised plasmid backbones and 10 ng annealed oligonucleotides (23x molar excess) was done with the Rapid DNA Ligation Kit (Chapter II.B.4.1). Ligated plasmids were transformed into *E. coli* (Chapter II.C.2) and correct insertion of oligonucleotides was confirmed by sequencing of single clones (bacterial colonies) propagated by miniprep (Chapter II.C.2) using primers AAV2cap-588ins for AAV2 or AAV9cap-589ins for AAV9 constructs (Chapter II.A.4).

II.B.5 Concentration of DNA

Low DNA amounts of < 100 ng solved in ddH_2O were concentrated in a vacuum concentrator until desired volume was attained. Low (high) DNA amounts solved in elution buffer were precipitated o/n (30 min) at -20°C (RT) with 0.1 volumes 3M NaOAc and 2.5 volumes 100% EtOH. DNA was pelleted and salts were removed by centrifuging once in presence of ice-cold (RT) 70% EtOH in a table-top centrifuge (13.000 x *g*, 15 min, 4°C). Ethanol traces were removed by aspiration and subsequent air-drying and DNA pellets were resuspended in desired volumes of elution buffer or ddH_2O.

II.B.6 Gel electrophoresis of DNA

Electrophoretic separation of DNA was done on agarose gels. As a rule, 0.8-2.5% gels were made to allow a proper separation of DNA fragments from 0.3-8 kb. Briefly, 0.8-2.5% w/v agarose was boiled in 1x TAE buffer, cooled to < 50°C under stirring and 2E-4 volumes EtBr solution were added. Gels were poured into gel electrophoresis chambers with appropriate combs, solidification was awaited and chambers were filled with 1x TAE. Blue Gel Loading Dye (Chapter II.A.6) was 1:6 diluted in DNA samples and 5-10 µl (or up to 50 µl if preparative gels were made) were pipetted in a pocket. Five µl/pocket of O'RangeRuler DNA standards (Chapter II.A.6) covering the expected size range of the analysed DNA were applied and running conditions were set to 5 V/cm electrode distance and 1-2 h running time. Separated DNA fragments were analysed on an ImageQuant 100 gel documentation system and, if necessary, DNA-bands were cut out from preparative gels with a scalpel and were purified (Chapter II.B.1).

II.B.7 DNA quantification

Concentration as well as purity of DNA amounts > 10 ng were determined with a NanoDrop ND1000 micro-volume spectrophotometer. The device was calibrated with 1.5 µl ddH_2O and 1.5 µl DNA solution were measured *versus* solvent. DNA samples were regarded as pure when the 260/280 nm ratio indicating protein contaminations exceeded 1.8.

II.B.8 Polymerase Chain Reaction (PCR)

II.B.8.1 Standard PCR

Distinct DNA regions were amplified via PCR on a GeneAmp 9700 96-well thermal cycler. Table II.B.8.1 provides all information required to perform a standard PCR reaction. Depending on the amount of template DNA the total cycle number was varied between 25 and 35.

Table II.B.8.1: Protocol for a standard PCR

Volumes	Final conc.	Component	Cycling steps	Temperature (°C)/Time (s)
2.5 µl	1x	10x standard *Taq* reaction buffer	Initial denaturation	95/180
0.5 µl	200 µM	10 mM dNTPs	**Denaturation**	95/45
0.5 µl	0.2 µM	10 µM forward primer	**Annealing**	60/30
0.5 µl	0.2 µM	10 µM reverse primer	**Elongation**	72/90
1 µl	0.05-10 ng	Template DNA	Final elongation	72/10
0.125 µl	1.25 U	*Taq* DNA polymerase	Optional	4/∞
To 25 µl		ddH_2O	**Total cycles**	25-35

II.B.8.2 TaqMan quantitative real-time PCR (qRT-PCR)

Prior to PCR amplification, 10 µl of iodixanol-purified virus or vector particles (Chapter II.E.2) or 10 µl ddH_2O as negative control were mixed with 10 µl TE buffer and 20 µl 2 M NaOH solution and were incubated for 30 min at 56°C to allow capsid disintegration. Neutralisation of pH occurred by addition of 960 µl 40 mM HCl solution. Plasmids containing *rep* (viral quantification) or CMV (vector quantification) sequences were quantified photometrically (Chapter II.B.7) and 1:10 serially diluted with ddH_2O to create eight standard samples ranging from 3.5E+10 to 3.5E+3 plasmid copies per ml. A mastermix of 60 µl was prepared containing 40 µl TaqMan Universal PCR Master Mix, 2 µl 5 µM probe, 2 µl 5 µM forward and reverse primer each (Chapter II.A.4) and 14 µl ddH_2O. Ten µl standard dilution were combined with 60 µl mastermix and 3 x 20 µl/well were distributed on a 384-well plate, allowing a triplicate quantification. Before onset of PCR the plasmid copies per well ranged from 1E+8 to 1E+1. An amount of 6.7 µl from samples were quantified in duplicate by adding 40 µl mastermix and distributing 2 x 20 µl/well. The reaction plate was covered with an adhesive film to avoid sample evaporation and was centrifuged (400 x *g*, 5 min, RT) to remove air bubbles from well bottom. The PCR reaction was run on a 7300 Fast Real-Time PCR System with conditions set to an unique 2 min step at 50°C, an initial denaturation step at 95°C for 10 min, followed by 40 cycles of denaturation (95°C, 15 min) and annealing/elongation (60°C, 1 min). Calculation of titres occurred with SDS software by setting the threshold at the beginning of the linear phase, where exponential PCR amplification is close to theoretical 2^n. A total dilution factor of 3.5E+4 was multiplied to the quantified viral genomes/well.

II.B.8.3 PCR-mediated in vitro-mutagenesis of DNA

Manipulation of DNA sequences was performed using the QuikChange II Site-Directed Mutagenesis Kit (revision #064001d, page 8/step 3 to page 10/step 2) with forward and reverse primers (Chapter II.A.4) designed with Primer X software. Five µl PCR product were transformed into *E.coli* as described in the manual of the kit, and grown colonies raised by miniprep (Chapter II.C.2) were sequenced using sequencing primers (Chapter II.A.4) to confirm successful manipulation. More detailed information is provided in Chapters II.E.4.1 and II.F.5.

II.C. Microbiological methods

II.C.1 Propagation of Subcloning Efficiency DH5α Competent Cells

Sterile solutions and working environment were required since antibiotics were omitted at any time. A 5 ml pre-culture containing LB-medium was inoculated using 2.5 µl Subcloning Efficiency DH5α Competent *E.coli* (Chapter II.A.1) thawed on ice. After an o/n incubation in miniprep tubes (150-200 rpm, 37°C), 1 ml pre-culture was used to inoculate a 250 ml main culture.

The main culture was maintained at 37°C until an OD_{600} (see Chapter II.C.2) of 0.5 – 0.6 and was cooled on ice for 10 min prior to centrifugation (3000 x *g*, 5 min, 4°C) in 50 ml centrifuge tubes. The pellet was resuspended in 50 ml ice-cold 0.1 M $MgCl_2$ solution, centrifuged again, resuspended in 50 ml ice-cold 0.1 M $CaCl_2$ solution and incubated for 20 min on ice. After another centrifugation step the pellet was carefully resuspended in 5 ml ice-cold 0.1 M $CaCl_2$/glycerol solution and cells were stored in 100 or 200 µl aliquots at -80°C.

II.C.2 Transformation and maintenance of bacterial cells

All incubation steps involving bacterial growth were carried out at 37°C. Liquid cultures were vigorously agitated (150-200 rpm) in vessels 4x larger than the culture volume to ensure proper aeration. For transformation, Subcloning Efficiency DH5α Competent Cells (Chapter II.A.1) were thawed on ice, a 50 µl aliquot was mixed with 25 ng (100 ng) untreated (ligated) plasmid DNA in a reaction tube and was incubated for 20-30 min on ice. Heat-shock treatment occurred for 90 s at 42°C and was stopped by cooling down on ice for 2-3 min. Five hundred µl SOC medium pre-warmed to RT were added, bacterial suspension was transferred into a miniprep tube and the sample was incubated for 45 min to initiate expression of ampicillin/kanamycin resistance. Depending on the source, 100 µl (untreated plasmid) or 200 µl (ligated plasmid) bacterial suspension were spread on LB-amp/kana agar plates (Chapter II.A.2) and incubated o/n to allow colony formation. A 5 ml LB-amp/kana pre-culture was inoculated with a single bacterial colony and incubated in a miniprep tube o/n. For preparation of smaller DNA amounts (miniprep), 1 ml pre-culture was purified with the PeqGOLD Plasmid Miniprep Kit I (Chapter II.B.1). If higher amounts of plasmid DNA were required, 200 ml (maxiprep), 1 L (megaprep) or 5 L (gigaprep) LB-amp/kana main cultures were inoculated with 0.001 volumes of pre-culture and were raised o/n. For growth control, 100 µl aliquots were 1:10 diluted with fresh LB-medium and optical density was measured *versus* fresh medium at OD 600 nm (OD_{600}) in semi-micro cuvettes with a spectrophotometer. Harvesting of bacterial cells occurred at OD_{600} values of 2.5-3.

II.D Cytological methods

II.D.1 Cell maintenance

II.D.1.1 Primary cells

Primary cells (Chapter II.A.1) are characterized by a limited number of cellular divisions and may experience different biochemical variations upon prolonged *in vitro* propagation. In order to largely avoid this drawback and at the same time to obtain high cellular yields, primary cells were first subjected to expansion until fourth passage and were then cryo-preserved in aliquots of 5E+5 or 1E+6 cells. Therefore, experiments involving these cell types were conducted with cells in passages 4 through 8.

Cryo-preserved HCAEC or HCASMC were purchased from Promocell, while HUVEC were freshly isolated from umbilical veins (Chapter II.F.7). All solutions required for cell maintenance were pre-warmed to 37°C, except the Trypsin/EDTA solution from the DetachKit, which was allowed to reach RT only. Cell culture vessels and media volumes are shown in Table II.D.1.2.

The expansion phase was initiated by fast thawing (water bath, 37°C) and seeding at a density of 7000 cells/cm^2 in appropriate ready-to-use cell culture medium (Chapter II.A.2) in a 75 cm^2 cell culture flask. For HUVEC propagation, flasks were pre-coated with 2% gelatine solution for 5 min at 37°C followed by rinsing twice with 1x PBS. All incubation steps occurred in a cell culture incubator under standard conditions (37°C, 5% CO_2-atmosphere, 95% rel. hum.) with a medium exchange after 24 h, then every other day. Growth of cells was monitored under a light microscope and upon 70-80% confluence, passaging took place. Cells were rinsed once with HepesBSS, detached with Trypsin/EDTA solution and trypsin reaction was neutralized with TNS (all from DetachKit). Cells were transferred to 50 ml centrifuge tubes and pelleted at 220 x *g* for 4 min at RT, supernatant was removed and re-suspension and dilution was done with ready-to-use cell culture medium. If determination of cell number was required, 10 µl of resuspended cells were mixed 1:1 with trypan blue solution, incubated for 1 min and counted in a cell counting chamber, whereas blue stained (= dead) cells were not considered. Further expansion of cells was performed in 175 cm^2 flasks with seeding densities of 7000 cells/cm^2. For cryo-preserving, 5E+5 or 1E+6 cells were resuspended in 0.5 ml and 1 ml 4°C CryoSFM (Chapter II.A.2), respectively, were transferred in cryogenic vials and were gradually cooled (-1°C/min) to -80°C in a freezing container o/n. For long-term storage vials were placed in a liquid nitrogen (LN_2) cryostorage system.

II.D.1.2 Immortalized cells

Passaging of any cell line used in this study (Chapter II.A.1) occurred by default upon reaching ~80% confluence with all solutions pre-warmed to 37°C (see also Table II.D.1.2). Briefly, cell culture medium was removed, cell monolayers were rinsed once with 1x PBS and detached with trypsin. Trypsin-neutralization occurred by adding respective ready-to-use cell culture medium and pelleting, re-suspension, counting and cryo-preserving was done as described in Chapter II.D.1.1. Depending on the cell line and generation time dilutions from 1:5 to 1:15 of ~80% confluent cells were seeded in new cell culture flasks.

Table II.D.1.2: Volumes[1] of media and solutions used per cell culture vessel

	Plates (wells)			Dishes (cm^2)		Flasks (cm^2)			Chambers (stacks)	
Vessel	96-well	12-well	6-well	56.7	145	25	75	175	5	10
Medium	0.1	1	2	n/a	20	4-5	10-12	20-25	500	1000
1x PBS	0.03	0.2	0.5	n/a	10	2	3	5	250	500
Trypsin	0.03	0.2	0.5	n/a	n/a	1	3	5	50	100
Medium[2]	0.03	0.2	0.5	n/a	n/a	1	3	5	Old medium	
HepesBSS[3]		0.2	0.5	2	n/a	1	2	3	n/a	n/a
Trypsin[3]		0.2	0.5	2	n/a	1	2	3	n/a	n/a
TNS[3]		0.2	0.5	2	n/a	1	2	3	n/a	n/a

[1]in ml, [2]ready-to-use cell culture medium used for trypsin neutralization, [3] from DetachKit

II.D.2 Flow cytometry

Flow cytometry analysis was employed to determine the transduction efficiency of AAV vectors of different cell types and the expression of cell surface receptors. Cell samples were collected by removing old medium, rinsing once with 1x PBS, trypsin treatment and trypsin neutralization with corresponding media (see Table II.D.1.2). Detached cells were transferred into conical-bottom tubes and centrifuged (272 x *g*, 5 min, RT). Pellets were resuspended in 150-1000 µl of ice-cold staining solution, transferred into round bottom tubes and kept on ice until FACS analysis. Data acquisition was carried out on a FACSCalibur flow cytometer using CellQuest Pro software. Below, a representative example of the acquisition and analysis process of HEK 293T cells is given. Relevant parameters are specified in table Table II.D.2. The flow cytometer was calibrated using a non-transduced cell sample (negative control) stained with propidium iodide solution (PI).

On a FSC-H/FL3-H plot (Figure II.D.2 **A**), events were discriminated according to their size (forward scatter height, FSC-H) and incorporation level of propidium iodide (FL3-H channel), which is lower in intact cells. Sub-populations of events regarded as live cells were gated by assigning them to region R1. Consequently, events laying outside of region R1 represented artefacts (cell fragments, cell clumps, dead cells) and were excluded from further analysis. The subset of live cells gated in R1 was plotted on a FSC-H/SSC-H plot (Figure II.D.2 **B**). The side scatter height (SSC-H) allows for a more precise discrimination between single cells and cell clumps. Events regarded as single cells were gated by assigning them to region R2 thus excluding cell clumps from further analysis. Subsequently, the „spill-over“ of intense fluorescence signals from FL1 into FL2 channel was compensated. This step is necessary as only evaluation of events occurring in the FL1 channel (= EGFP-positive cells) is possible. First, the background fluorescence of gated cells (R1 + R2) from the negative control was set at 10^1 relative fluorescence units (RFU) for both channels. A positive control containing cells transduced with scAAV-CMV-EGFP was then used to correct FL1-to-FL2 „spill-over“ of intense EGFP signals (Figure II.D.2 **C**). The sample flow-rate was set between 50-300 events/second by adjusting flow speed and/or sample volume and for every sample 0.5-1E+4 live single cells were collected.

Table II.D.2: Common parameters in flow cytometry analysis

Channel	Parameter	Description
FSC-H	Forward scatter height	Correlates with cell volume (size)
SSC-H	Side scatter height	Depends on inner complexity of a cell (granularity)
FL1-H	Fluorescence height	Detects EGFP, FITC* fluorescence (filter 530/30)
FL2-H	Fluorescence height	Detects PE* fluorescence (filter 585/42)
FL3-H	Fluorescence height	Detects PI* fluorescence (filter 670 LP)

*Examples of detectable fluorescent molecules: EGFP = green fluorescent protein, FITC = fluorescein isothiocyanate, PE = phycoerythrin, PI = propidium iodide

Evaluation of transduction efficiencies was carried out with the FlowJo software. Gated events were plotted on a FL1-H histogram and histogram overlays of negative and positive control were generated (Figure II.D.2 **D**). Events within the overlapping histogram area of positive (orange line) and negative control (black line) were regarded as „false negative signals“ and two marker regions M1 and M2 joining at the intersection point of the overlays were set. All events within marker M2 were defined as EGFP-positive cells and were calculated by the software as percentage of gated events (% EGFP-positive cells). M2-values from negative control were defined as „false positive signals“ and were subtracted from each analysed sample.

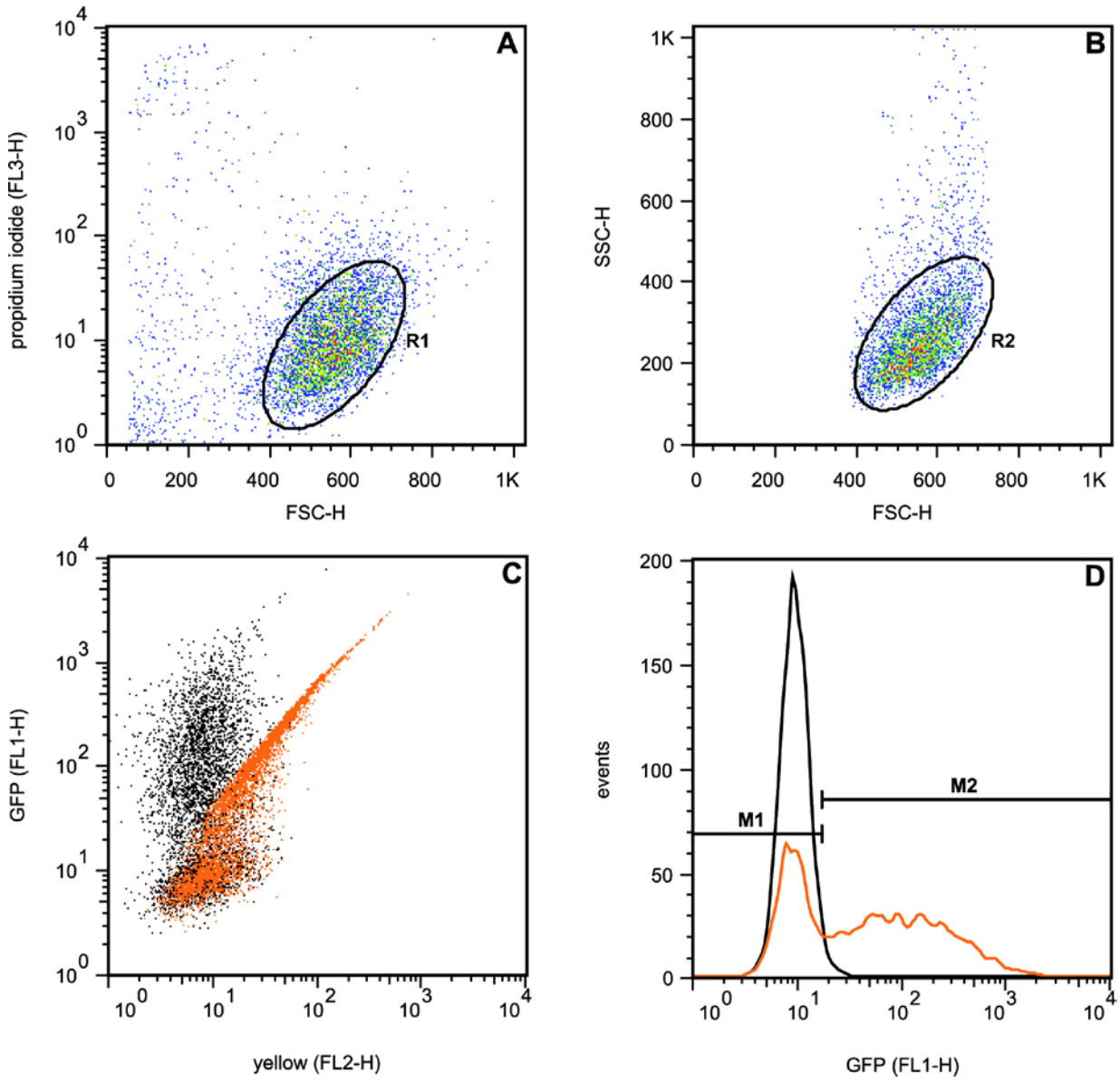

Figure II.D.2: Workflow for data acquisition by flow cytometry. (**A**) Data obtained from negative control (untreated cells stained with PI) was plotted on a FSC-H/FL3-H scatter-plot and live cell populations were gated by assignment to region R1. The distribution of cells is given in false colours, whereas red indicates a high and blue a low density. (**B**) The R1-subset of cells was plotted on a FSC-H/SSC-H scatter-plot and single cells were gated by assignment to region R2. (**C**) Fluorescence channels FL1-H and FL2-H were set to 10^1 RFU using the negative control and FL1-to-FL2 „spill-over" (orange dots) was corrected (black dots) using cells transduced with AAV. (**D**) Gated events (R1 + R2) from negative (black line) and positive control (orange line) were overlaid on a FL1-H histogram and marker regions M1 and M2 were drawn joining at the intersection point of the overlays. By definition, marker M2 contains EGFP-positive cells.

II.E. Virological methods

II.E.1 AAV vector production

Recombinant scAAV vectors were produced by applying two different protocols. For wild type AAV2 or AAV9 vectors, plasmids pDP2rs and pDP9rs were used, respectively (Chapter II.A.3). Mutant AAV vectors were produced using plasmid pDGΔVP and pMT-187-XX2 (AAV2) or p5E18-VD2/9-*Sfil*1759 (AAV9) containing distinct oligonucleotide inserts (Chapter II.A.4 and II.B.4.2) enabling peptide display behind VP1 residue 588 (AAV2) or 589 (AAV9). Plasmid dsAAV-CMV-EGFP containing a CMV-EGFP expression cassette flanked by ITRs or, alternatively, plasmid dsAAV-CMV-EGFPΔG67 expressing a non-fluorescent EGFP variant was packaged into AAV vectors.

Depending on the desired size of production 10, 20 or 40 145cm^2 cell culture dishes or, alternatively, instead of 20 or 40 dishes, 5- or 10-stack tissue culture chambers corresponding in surface were employed. For transfection of plasmids, polyethyleneimine (PEI) was aseptically dissolved in ddH_2O to 0.323 g/L, freeze-thawed 6 times (LN_2/37°C) and stored in aliquots at -80°C. In general, cells were propagated for 24 h prior to transfection allowing proper adhesion to the dishes and plasmids were PEI-transfected at a N/P-ratio of 20[231].

For transfection 5E+6 HEK 293T cells per 145 cm^2 cell culture dish were seeded in 20 ml appropriate medium (Chapters II.D.1.2 and II.A.2). The next day, two mastermixes were prepared separately with solutions pre-warmed to 37°C according to Table II.E.1 (values account for one dish), were mixed under vigorous stirring and were incubated for 10 min at RT to allow precipitation of PEI and DNA. Transfection occurred by adding 4 ml of combined mastermixes to each dish followed by an incubation of 48 h under standard conditions. In case of tissue culture chambers entire medium was carefully removed, mixed with the mastermix in appropriate-sized glass bottles and reapplied to the cells. After incubation, cells were collected from dishes in 500 ml large centrifuge tubes by washing-off with present medium and were pelleted (220 x *g*, 4 min, RT). Then, the pellets were washed once with 1x PBS. Cell collection from tissue culture chambers was done by removal of old medium and trypsin treatment (see Table II.D.1). Additionally, chambers were rinsed twice with 1x PBS to ensure complete removal of cells.

Lysis was performed by re-suspension of cell pellets in 5 ml (from up to 20 dishes or a 5-stack chambers) or 20 ml (from up to 40 dishes or a 10-stack chambers) MNT buffer followed by 4 freeze-thaw-cycles (LN2/37°C). Cell lysates were treated for 1 min at 48W in a ultrasound water bath and incubated with 100 U Benzonase (Chapter II.A.5) per ml of lysate for 30 min at 37°C. Repeated centrifugation (5000 x *g*, 10 min, 4°C) removed cellular debris completely and AAV-containing supernatant was stored at -20°C until further processing.

Table II.E.1: Transfection mastermixes for AAV vector production

	Volume (µl)	Amount/ concentration	Plasmids (mutant scAAV vectors)	Plasmids (wild type scAAV vectors)
Mastermix 1	Variable	35 µg	pDGΔVP	pDP2rs or pDP9rs
	Variable	10 µg	dsAAV-CMV-EGFP or dsAAV-CMV-EGFP(ΔG67)	dsAAV-CMV-EGFP or dsAAV-CMV-EGFP(ΔG67)
	Variable	12 µg	pMT-187-XX2 or p5E18-VD2/9-*SfiI*1759	n/a
	Ad 1 ml		ddH_2O	ddH_2O
	1 ml	300 mM	NaCl	NaCl

	Substance	Concentration		
Mastermix 2	PEI	0.323 g/l	456 µl	360 µl
	ddH_2O		544 µl	640 µl
	NaCl solution	300 mM	1 ml	1 ml

II.E.2 AAV vector purification by density gradient ultracentrifugation

Cell lysates (Chapter II.E.1) were thawed and were pipetted into 13.5 ml (5 ml lysates) or 39 ml (20ml lysates) ultracentrifuge tubes with the aid of a Pasteur pipette placed into the tube. Iodixanol solutions were prepared freshly according to Table II.E.2 were applied into the tubes with the lowest gradient concentration loaded first, followed by increasingly higher concentrations. After loading, the order of solutions inside the tube were: cell lysate, 15%, 25%, 40% and 60% iodixanol, top to bottom. The addition of phenol red into 25% (reddish colour) and 60% iodixanol (yellowish colour) facilitated discrimination between individual layers. Tubes were heat-sealed using a seal former and tube sealer and were balanced to ±0.01 g using fresh MNT buffer taking into account the weight of centrifuge rotor spacers.

For ultracentrifugation, 39 ml (13.5 ml) tubes were loaded into 50.2 Ti rotors (70.1 Ti rotors) and centrifugation was carried out at 375.000 x *g* for 2 h 15 min at 10°C. Tubes were then fixed with an extension clamp on a support stand, a 20G 1½ needle was plunged atop the tube for air balance and the 40% iodixanol fraction containing full capsid particles was carefully aspirated by lateral puncture using another 20G 1½ needle and a 5 ml syringe, yielding volumes of ~1.0 ml (small gradient) or ~2.5 ml (large gradient). The 40% iodixanol fraction was not retrieved entirely due to a partially mixed layer interface between 25% and 40% iodixanol containing also empty capsid particles and small amounts of cell debris. Vector particle-containing fractions were stored in 1.5 ml screw-cap tubes at 4°C (short-term) or -20°C (long term).

Table II.E.2: Iodixanol solutions and their components

	Concentration	Total volume*	Iodixanol	PBS-MK	PBS-MKN	Phenol red
Small gradient	60%	1.5 ml	1.5 ml	-	-	~ 15 µl
	40%	1.5 ml	1 ml	0.5 ml	-	-
	25%	2 ml	0.83 ml	1.17 ml	-	~ 10 µl
	15%	3 ml	0.75 ml	-	2.25 ml	-

	Concentration	Total volume[1]	Iodixanol	PBS-MK	PBS-MKN	Phenol red
Large gradient	60%	4 ml	4 ml	-	-	~ 30 µl
	40%	4 ml	2.66 ml	1.34 ml	-	-
	25%	5 ml	2.08 ml	2.92 ml	-	~ 20 µl
	15%	7 ml	1.75 ml	-	5.25 ml	-

*Volumes required for the purification of a 5ml (small gradient) or a 20ml (large gradient) cell lysate sample

II.E.3 Quantification of AAV infectious titres

HEK 293T cells were seeded at a density of 1E+4 cells/well in a 96-well cell culture plate in 100 µl corresponding cell culture medium (Chapters II.D.1.2 and II.A.2) containing only 5% FBS. The next day, the virus stock was 1:10 serially diluted by transferring 11 µl virus solution between wells and mixing. Each dilution was analysed in duplicate. Infection was allowed to take place in a cell culture incubator for 2 h at 37°C and internalized virus particles were amplified by super-infection with 20 µl cell culture medium (5% FBS) containing wild type Adenovirus 5 (Ad) at a multiplicity of infection (MOI) of 10 IU/cell added to each well. Further incubation was carried out until a ~50% Ad-induced cytopathic effect was observed (usually within 2-3 days). For lysis, cells were freeze-thawed three times (-80°C/37°C) without removing the medium and 100 µl 1.5 M NaOH solution was added to each well.

Plates were centrifuged (300 x *g*, 5 min, RT) to avoid carry-over of cellular debris and 180 µl supernatant were transferred to the HybriDot manifold avoiding air bubbles. Prior to transfer of supernatant, a trimmed hybridisation transfer membrane enveloped by two pieces of cellulose chromatography paper was soaked in 1x PBS and the HybriDot manifold was assembled. Transfer occurred by applying vacuum until the entire supernatant passed the membrane. The membrane was removed from manifold and viral DNA was denatured by placing the membrane on a fresh chromatography paper soaked with denaturation buffer (10 min, RT). Alkaline conditions were neutralized by placing the membrane on another chromatography paper soaked with neutralization buffer (10 min, RT) and the membrane was air-dried. DNA was cross-linked to its surface with a crosslinker at 120 mJ. Prior to addition of radioactively labelled DNA, the membrane was placed in a hybridisation bottle and was pre-treated with 10-15 ml hybridisation solution in a hybridisation furnace (>1 h at 42°C).

A DNA fragment for radioactive labelling was prepared by *NcoI*/*HindIII*-digestion (Chapter II.B.2) of plasmid p5E18-VD-2/9 (Chapter II.A.3). The 1.257 kb *rep*-fragment was gel-purified (Chapters II.B.6 and II.B.1), and 250 ng were used for α-^{32}P dCTP radioactive labelling following the Random Primed DNA Labelling Kit protocol (02/2008, steps 2-4) with following modifications: DNA solution was completed *ad* 23 µl with ddH_2O and 4 µl each dNTPs, reaction mixture and Klenow enzyme were added. The mixture was completed by adding 5 µl α-^{32}P dCTP (50 µCi) and radioactive labelling was allowed to take place. After EDTA treatment/heating, unincorporated nucleotides were removed with the Mini Quick Spin Oligo Columns according to manual recommendations (version 09/2004, pages 6-7). Radiation of the eluate containing purified labelled oligonucleotides was determined with a radioactivity counter and probes yielding >10^6 cpm were heat-treated (10 min at 95°C) and cooled instantly on ice to maintain single strand state. The entire amount of probe (~50 µl) was mixed with 450 µl hybridisation solution and pipetted to the pre-treated membrane. Hybridisation of probe and cross-linked DNA was allowed to take place in a hybridisation furnace (o/n at 42°C).

The hybridisation solution was removed and excess radioactive contamination was washed off by repeated incubation in 10-15 ml washing solution (10-15 min at 42°C, hybridisation furnace). After each washing step, labelling intensity was roughly estimated by removing the membrane from the hybridisation bottle and measuring radiation with a contamination monitor. Upon reaching values of ~1.000 cpm, membranes were shortly air-dried, wrapped in cling-film and were mounted on a storage phosphor screen. After 5-24 h exposure, read-out of screens was performed on a molecular imager with ImageQuant software.

The infectious titre of analysed virus stocks was estimated by counting blackened dots. Theoretically, one infectious AAV particle per well is sufficient to generate a detectable radioactive signal upon amplification by Ad super-infection. Since serial dilutions of 1:10 lowering the amount of infectious particles to ~one/cell were made, each additional dot represents a tenfold higher infectious titre. Hence, 5 blackened dots represent a titre of 10^4 IU translating into 10^6 IU/ml.

II.E.4 Production of an AAV9 random peptide heptamer library

Detailed molecular biological techniques used for the cloning strategy in this chapter are described in Chapter II.B and II.C and more detailed information on plasmids or primer/oligonucleotides is given in Chapters II.A.3 and II.A.4, respectively.

II.E.4.1 Plasmid library

Creation of an AAV9 library plasmid backbone

A 975 bp fragment of the wtAAV9 *cap* ORF was synthesized (Geneart, plasmid pGA4) harbouring two incompatible *SfiI* restriction sites at nucleotide positions 1759 through 1786 of *cap*9 separated by two adenine molecules. Modified 975 bp *cap*9 fragment (*cap*9mut) was excised with *XcmI* and *BsiWI* from pGA4 and was inserted into equally-cut p5E18-VD-2/9, resulting in p5E18-VD-2/9-*SfiI*1759. Correct insertion of the 975bp fragment into p5E18-VD-2/9-*SfiI*1759 was analysed by a double-digestion with *SfiI* and *BsiWI*. This plasmid served on the one hand as an intermediate construct for the generation of the ITR-positive plasmid library and on the other hand was used for insertion of oligonucleotides (Chapter II.B.4.2) to create AAV9 vectors displaying distinct peptides behind VP1 residue 589. In contrast, AAV2 vectors displaying peptides behind VP1 residue 588 were generated using plasmid pMT-187-XX2.

For generation of the ITR-positive plasmid library, several subcloning steps had to be performed due to unavailable restriction sites. In the first step p5E18-VD-2/9-*SfiI*1759 was digested with *HindIII* and *EcoRV*, releasing a 2774bp fragment containing the entire modified *cap*9 ORF as well as a part of the *rep*2 ORF and was cloned into equally-digested pMT-187-XX2. This step is necessary since p5E18-VD-2/9 lacks *XbaI* recognition sites required in a later step. To enable the *HindIII*/*EcoRV*-digestion of pMT-187-XX2, the *EcoRV*-site was generated by *in vitro*-mutagenesis using IVM-F/R primers following the manufacturer's protocol and successful mutagenesis was verified by *EcoRV*-digestion. The resulting plasmid was termed pMT-187-XX2-*rep*2/*cap*9mut. Then, the entire *rep*2/*cap*9mut sequence was excised from ITR-negative pMT-187-XX2-*rep*2/*cap*9mut with *XbaI* and was ligated into equally-cut ITR-positive plasmid pSSV9 resulting in library plasmid backbone pKV-AAV9Lib/BB. Sequencing using primer AAV9cap-589ins confirmed the presence of the modified *cap*9 fragment.

Creation of an oligonucleotide library

For generation of an oligonucleotide library, degenerated single-stranded oligonucleotide NNK-Oligo was synthesized encoding a random seven-residue peptide insert flanked by two incompatible *BglI* restriction sites (Oligonucleotide Synthesis Core Facility). Second strand synthesis of NNK-Oligo was done with the Sequenase DNA Sequencing Kit 2.0 (page 8, steps 1-2, 6) and second strand primer NNK-Oligo-2nd according to manual recommendations with the following modifications: 2 µg oligonucleotide and 4 µg primer were inserted into the reaction and incubation (step 6) took place at 37°C for 1 h. Unincorporated nucleotides were removed with the QIAquick Nucleotide Removal Kit and the double-stranded oligonucleotide library was eluted in 80 µl elution buffer (diluted 1:3 with ddH_2O, first elution in 50 µl, second in 30 µl) per column and stored at -20°C until further use.

Ligation of plasmid backbone and oligonucleotide library

Prior to ligation, oligonucleotide library and backbone plasmid pKV-AAV9Lib/BB were digested for 4 h with *BglI* or *SfiI*, respectively, using 10 U enzyme/µg DNA each. *SfiI*-digestion released a 15 bp stuffer fragment within pKV-AAV9Lib/BB rendering it compatible to the *BglI*-digested oligonucleotide library. Backbone or insert were purified by gel-isolation and the QIAquick PCR Purification Kit, respectively, and elution occurred twice in the same 50 µl elution buffer 1:3 diluted with ddH_2O. To determine the optimal insert-to-backbone molar ratio, test-ligations were prepared. Reactions specified in Table II.E.4.1 were completed to a total volume of 20 µl with ddH_2O, were heat-incubated 2 min at 65°C and chilled on ice for 10 min. Ligation reaction was completed as in Chapter II.B.4.1 but with 1000 U ligase and reaction was allowed to take place. For concentration, ligated plasmids were ethanol-precipitated, resuspended in 50 µl elution buffer 1:10 diluted with ddH_2O and DNA concentration was determined. One µl containing 10 ng of library plasmid ligated at any ratio was mixed with 25 µl ElektroMAX™ DH5α-E Competent Cells thawed on ice and transformed by electroporation (1.8 kV, 25 µF, 200 Ω, electroporation cuvettes cooled on ice) using the Gene Pulser Xcell electroporation instrument. Transformed bacteria were instantly collected in SOC medium pre-warmed to 37°C resulting in a total volume of 1 ml and incubated under vigorous shaking for 1 h at 37°C. Serial 1:10 dilutions of bacterial culture ranging from 1:1 to 1:10.000 were prepared with SOC and 100 µl of each were plated on LB-amp agar plates. The transformation efficiency E_T was determined by counting colonies the next day according to formula (1):

$$(1)\ E_T = \frac{\text{counted CFU} \times 1\mu\text{g DNA}}{\text{x µg transformed DNA}} \times \frac{1\text{ml}}{\text{x ml plated}} \times \text{dilution factor}\ (\text{CFU/µg DNA})$$

A large-scale ligation 20x the amounts of the test-ligation specified in Table II.E.4.1 was attempted at a ratio of 1:30, since this ratio yielded the highest transformation efficiency. After ethanol-precipitation the DNA pellet was resuspended in 400 µl 1:10 ddH_2O-diluted elution buffer and concentration was determined. For reason of costs, new transformation parameters using less competent cells were applied. One electroporation approach consisted now of 2 µl (100 ng) library plasmid, 20 µl competent cells and was collected after electroporation in SOC medium resulting in a total volume of 2 ml. To exclude a lowering of transformation efficiency, one approach was analysed in advance as described above. Additionally, several colonies were picked, were raised by miniprep and plasmid DNA was sequenced to verify the correct insertion of library oligonucleotides using primer AAV9cap-589ins. The transformation of the large-scale ligation contained in total 104 approaches (see above). To facilitate handling, two approaches were combined into one cuvette for electroporation. Transformations from 13 cuvettes were pooled and were incubated under vigorous shaking 1 h at 37°C, resulting in a total of 4 separate batches (1 batch = 13 cuvettes = 26 approaches). Again, aliquots from each batch were taken and transformation efficiency was analysed as described above.

Each batch was then completed with LB-amp medium to 250 ml and plasmids were amplified under shaking o/n at only 30°C and 200 rpm until cultures reached an OD_{600} of ~0.2. The plasmid library termed pKV-AAV9Lib was purified using the HiSpeed Plasmid Maxi Kit and stored at -20°C.

Table II.E.4.1: Plasmid-to-insert ratios used for test-ligations

Ratio	Backbone (ng)	Insert (ng)
1:10	500	18.9
1:30		56.7
1:100		189.0
Control		-

II.E.4.2 Production of the transfer shuttle library (TSL)

TSL particles were produced by PEI-transfection of library plasmid pKV-AAV9Lib, codon-optimized wtAAV2 helper plasmid pRSV-VP3co or non-optimized wtAAV9 plasmid p5E18-VD-2/9, respectively, and pDGΔVP into HEK 293T cells. Different stoichiometric amounts of plasmids (Table II.E.4.2) were assayed to determine the optimal ratio leading to maximum genomic and infectious titres, at the same time saving library plasmid. Transfection of 5E+6 cells per plasmid combination occurred as described in Chapter II.E.1 by adjusting the PEI volume to the absolute amount of plasmids. Following combinations were assayed: TSL productions using wtAAV2 (Table II.E.4.2, code ABC), wtAAV9 (code ABD) or no helper plasmid (code AB) and TSL productions without library plasmid (codes AC and AD, only red highlights). TSL particles were harvested and purified (Chapters II.E.1 and II.E.2) and quantification of genomic titres (Chapter II.B.8.2) and infectious titres (Chapter II.E.3) was performed. The optimization process revealed a plasmid ratio of 1:1:15 (µg pKV-AAV9Lib, pRSV-VP3co and pDGΔVP, respectively) to result into maximal infectious titres. Using this protocol, the main TSL productions were upscaled 20x to 10E+8 HEK 293T cells yielding an absolute infectious titre of 5E+7 IU each.

Table II.E.4.2: Plasmid combinations used for optimisation of transfer shuttle library production

Code	**Plasmids**	**Absolute amounts (µg)**								
A	pDGΔVP					15				
B	pKV-AAV9Lib	1	2	5	1	2	5	1	2	5
	Ratio BC/BD		**1:1**			**1:5**			**1:10**	
C	pRSV-VP3co	1.5	3.0	7.4	7.4	14.8	37.0	14.8	29.6	74.0
D	p5E18-VD-2/9	1.1	2.1	5.4	5.4	10.7	26.8	10.7	21.4	53.5

II.E.4.3 Production of the virus library

The final AAV9 virus library expressing random heptapeptides behind VP1 residue 589 was generated by infection of HEK 293T cells with the TSL at a MOI of 0.5 IU/cell. Two small-scale productions using TSL prepared with wtAAV2 or wtAAV9 helper plasmids were attempted using one dish (5E+6 cells) each. Only one large-scale production using the entire remaining TSL prepared with wtAAV2 helper plasmid was produced using twenty dishes (1E+8 cells). The cells were seeded the day before (Chapter II.D.1.1) in appropriate medium and the TSL was applied to the cells. Half of cell culture medium (10 ml) was removed from each dish and was replaced with fresh medium lacking FBS containing the TSL. Thus, thorough mixing of viscous iodixanol solution and medium was possible and total FBS was reduced to 5%. After an incubation of 4 h, cell culture medium was removed and cells were carefully rinsed once with 1x PBS. Twenty ml fresh medium containing 5% FBS and 5 IU/cell Ad were supplied to each dish and super-infection was allowed to take place until a ~50% cytopathic effect induced by Ad (cell rounding, pending detachment) was observed (48-72 h). Library particles were then harvested and purified (Chapters II.E.1 and II.E.2) and quantification of genomic titres was performed (Chapter II.B.8.2).

II.E.5 Characterization of plasmid and virus library

Randomness, functional diversity and amino acid usage of plasmid or virus library were analysed by sequencing of randomly assigned clones. Plasmid or viral DNA was PCR-amplified (Chapter II.B.8.1) using AAV9cap F2/R primers (Chapter II.A.4). Virus DNA was supplied as a template by adding 1 µl virus stock solution directly to the PCR reaction. The primer pair used here yields a 467 bp-fragment from the mutated AAV9 *cap* gene that includes the oligonucleotide insertion site and binding site of sequencing primer AAV9cap-589ins (Chapter II.A.4). PCR-amplification using *Taq*-polymerase resulted in adenylation of DNA 3' ends enabling T/A-overhang ligation with the TOPO TA Cloning Kit for Sequencing (version O, 04/2006, pages 5, 10/steps 1-8). Four µl PCR product were used for ligation into TOPO vector as described in the user guide and One Shot DH5α-T1^{R} Chemically Competent Cells supplied with the kit were transformed. Prior to plating of 50 µl bacterial suspension, 40 µl X-gal solution were spread on LB-amp agar plates for blue-white selection of insert-positive clones and plates were pre-incubated for 30 min at 37°C. The next day a 96-well microtitre plate with agar was inoculated with single white colonies and clones were sequenced using AAV9cap-589ins.

II.F Transduction and infection of cells

II.F.1 *In vitro* selection of the AAV9 random peptide display library on HCAEC

For *in vitro* biopanning of AAV9 random peptide libraries, 1E+6 HCAEC were seeded in 175cm^2 cell culture dishes in 20 ml corresponding medium (Chapter II.A.2). After an o/n incubation under standard conditions (Chapter II.D.1.1), the libraries were applied in different attempts at MOIs 10, 100 and 1000 gc/cell by medium replacement. After a 4 h exposure medium was removed, cells were rinsed once with 1x PBS to remove unbound virus particles and 20 ml fresh medium with 20 IU/cell Ad was supplied for super-infection. Incubation was continued until a cytopathic effect was observed. At a MOI of 20 IU Ad/cell HCAEC displayed a typical cell rounding after 48 h but remained still adherent. It was assumed that 48 h exposure to Ad should suffice for AAV replication. Cells were washed twice with 1x PBS and harvested by trypsin treatment (Chapter II.D.1.1). Cell pellets were washed twice with 1x PBS to remove the majority of library particles in the supernatant and intracellularly enriched variants were purified using 1 ml MNT buffer as described in Chapter II.E.1. Purification by density gradients was omitted to avoid particle loss. Titration of genomic copies was performed by qRT-PCR (Chapter II.B.8.2) and absence of contaminating wtAAV9 genomes was confirmed by gel analysis (2.5% agarose, Chapter II.B.6) of purified (Chapter II.B.1) and PCR-amplified (Chapter II.B.8.1) viral DNA using AAV9cap-F/R primer pair (Chapter II.A.4). This primer pair yields a 270 bp PCR fragment from wtAAV9 and 297bp fragment from the mutated AAV9 *cap* gene. The enriched library was subjected to further three selection rounds using the parameters described above and after the third and fourth round a total of 16 single clones from each attempt using a specific MOI were generated and sequenced (see Chapter II.E.5) to further characterise enriched peptide motives.

II.F.2 *In vitro* gene transfer studies with wild type and selected AAV vectors

In vitro AAV treatment of cells occurred usually in the 12-well plate format with parameters described in Table II.F.2. All parameters of each group (experimental code) were combined unless specific affiliations were indicated by an arrow. Cells were seeded the day before in 1 ml of corresponding medium (Chapters II.D.1.1 and II.A.2) at desired densities and were incubated o/n to allow cell attachment to the well bottom. The next day, cells were exposed to wild type or mutant scAAV-CMV-EGFP vectors displaying peptides behind VP1 residue 588 (AAV2) or 589 (AAV9) by mixing vector stock solution at desired MOIs and replacing old medium with 500 µl fresh medium containing maximum 5% FBS and vector. After exposure, vector-containing medium was aspirated, cells were rinsed once with 500 µl 1x PBS and, if necessary, incubation was continued in presence of 500 µl fresh medium. At the end of the incubation time, transduction efficiency of vectors was analysed by flow cytometry as described in Chapter II.D.2. In the chapters below, details or deviations to the protocol described here are indicated.

Table II.F.2: Parameters applied for AAV treatment of cells

Experiment code	Cell type	Seeding density (cells/well)	Exposure MOI (gc/cell)	Vector (serotype/peptide[1])	Exposure time (h)	Incubation time (ad h)	n[2]
1	HCAEC	5E+4	1E+4	2/NDVRAVS	4	48	3
2	HCAEC	5E+4	1E+4	2/NDVRAVS	4	48	3
3	HCAEC	5E+4	5E+3	2/NDVRAVS	4	24, 48, 72	3
4	HCAEC	5E+4	5E+3	2/NDVRAVS	2, 4, 8, 24, 48, 72	72	3
5	HCAEC	7.5E+4	1E+4	2, 9/wild type 2, 9/NDVRAVS	72	72	4
6	HCAEC H5V	→ 7.5E+4, → 1E+5	1E+3 and 1E+4	9/see AI[3]	48	48	4 1
7	HCAEC HCASMC HEK 293T HeLa 911 HepG2	→ 7.5E+4 → 7.5E+4 → 1.5E+5 → 2E+5 → 1.5E+5 → 2E+5	2.5E+3	9/wild type 9/SLRSPPS 9/RGDLRVS	48	48	3
8	HCAEC HCASMC HEK 293T 911	→ 5E+4 → 5E+4 → 1.5E+5 → 1.5E+5	2.5E+3	9/SLRSPPS	48	48	3
9	HUVEC	5E+4	1E+3, 1E+4, 5E+4, 1E+5	9/SLRSPPS	2	48	3
10	HCAEC	5E+4	5E+3	2, 9/see AI[3]	48	48	3
11	HCAEC	7.5E+4	5E+3, 25x-100x (see experimental codes)	9/SLRSPPS 9/RGDLRVS 9/PSLPSRS 9/SDLRRGV	4	48	3

[1]Peptides displayed behind VP1 residue 588 (AAV2) or 589 (AAV9), [2]number of replicates performed each sample

Experimental codes (additional information)

1 Exposure occurred in 0.5 ml (131 µl/cm^2), 1 ml (263 µl/cm^2) or 1.5 ml (394 µl/cm^2) medium

2 Exposure occurred in presence or absence of 1%, 5%, 10% (vol/vol) iodixanol, including iodixanol from vector stocks

6 Wild type, TEWDQPF, RGDLRVS, NLHSPPA, SLRSPPS, SIRSPPS, RGDFRVG, NNVRGFV, NFTRLSA, NDVRAVS

8 CMV-EGFP, 163-EGFP or 313-EGFP expression cassettes were encapsidated in scAAV9-SLRSPPS vectors

10 Wild type, RGDLRVS, NLHSPPA, SLRSPPS, NDVRAVS, NSSRDLG, NSVSSAS

11 Vectors packaging CMV-EGFP were applied at MOI 5E+3 gc/cell and vectors packaging CMV- EGFPΔG67 were applied at 25x, 50x, 75x and 100x excess MOI

II.F.3 Transcriptional targeting

Detailed information on required cloning techniques is given in Chapters II.B and II.C. For generation of plasmid constructs that put EGFP under the control of the murine VE-cadherin promoter (EMBL databank accession no. Y10887), plasmid dsAAV-CMV_{enh}-MLC_{260}-EGFP was used as a basis (Chapter II.A.3). A plasmid backbone for insertion of the 163 or 313 bp VE-cadherin promoter fragments was prepared by *PpuMI*/*HindIII*-digestion of dsAAV-CMV_{enh}-MLC_{260}-EGFP, that released the myosin light chain promoter fragment (MLC_{260}) but retained the CMV enhancer sequence (CMV_{enh}). The *PpuMI* recognition site is located between the 3' end of the CMV_{enh} and the 5' end of MLC_{260}, while the *HindIII* site is situated at the 3' end of MLC_{260}. The cadherin promoter was provided within plasmid pBLCAT3. Since no *PpuMI*/*HindIII* sites were present, artificial synthesis was required by PCR. Primer pairs were designed that allowed PCR-amplification of either the 163 bp or the 313 bp fragment from the cadherin promoter, at the same time adding a *HindIII* site downstream of the +24 nucleotide position (Chapter II.A.4, VE-Cad-R, bold highlights) or a *PpuMI* site upstream of the -139/-289 nucleotide position (Chapter II.A.4, VE-Cad-F1/VE-Cad-F2, bold highlights). The endogenous *HindIII* recognition sequence present at the -289 site of the cadherin promoter was destroyed upon creation of a *PpuMI* site by PCR (Chapter II.A.4, VE-Cad-F2, underlined bases). Purified PCR fragments were rendered compatible for ligation into backbone plasmid by *PpuMI*/*HindIII*-digestion, eventually creating plasmid dsAAV-CMV_{enh}-163-EGFP and dsAAV-CMV_{enh}-313-EGFP. These plasmids were used for production AAV9 vectors displaying peptide SLRSPPS (Chapter II.A.4) behind VP1 residue 589 (Chapters II.E.1, II.E.2 and II.E.3). Transduction of cells was performed with parameters described in Table II.F.1, code 8. At the end of the incubation time, transduction efficiency of vectors was analysed by flow cytometry as described in Chapter II.D.2.

II.F.4 *In vitro* neutralization of AAV transduction

In a u-bottom 96-well cell culture plate that facilitates accurate pipetting of low volumes, serial 1:2 dilutions of intravenous immunoglobulin (IVIG) and ADK9 (Chapter II.A.7) or no serum (positive transduction control) were made in a total of 30 µl/well using HEK 293T cell culture medium lacking FBS (Chapter II.A.2). Additional 30 µl serum-free medium containing wtAAV2, wtAAV9 or selected scAAV9-CMV-EGFP vectors displaying peptide sequences RGDLRVS, SLRSPPS or NDVRAVS were added to the serial dilutions resulting in a preliminary MOI of 2.25E+4 gc/cell and neutralization reaction was allowed to occur for 45 min at room temperature. The final concentration of ADK9 antibody in the lowest dilution (1:10) represented 0.4 ng. Forty out of 60 µl antibody-treated vector solution resulting in final MOIs of 1.5E+4 gc/cell were added to 1E+4 HEK 293T cells seeded the day before in a 96-well plate in 100 µl corresponding medium (Chapter II.D.1.1). Cells were incubated for a total of 48 h and transduction efficiencies were evaluated by flow-cytometry as described in Chapter II.D.2.

II.F.5 Capsid competition assay

The capsid competition assay was performed by co-incubation of vectors harbouring fluorescent EGFP expression cassettes and competing vectors containing non-fluorescent EGFPΔGly67. A non-fluorescent EGFP reporter gene variant was generated by subcloning of the EGFP ORF from plasmid dsAAV-CMV-EGFP into plasmid pEBFP-C1 (Chapter II.A.3). This step was beneficial for the mutagenesis reaction since it reduced the total size of the plasmid and avoided the presence of ITRs. *KpnI*/*NotI*-digestion released EGFP and EBFP, respectively, and the EGFP fragment was ligated into pEBFP-C1 backbone. To abolish EGFP fluorescence, glycine residue G67 was removed by PCR mutagenesis (Chapter II.B.8.3) using EGFPΔG67 forward and reverse primers (Chapter II.A.4). Sequencing using EGFP-N sequencing primer (Chapter II.A.4) confirmed correct deletion of G67 codon. The EGFPΔG67 ORF was cloned back into dsAAV-CMV backbone with *KpnI*/*NotI* resulting into dsAAV-CMV-EGFPΔG67. A more detailed description of molecular biological techniques required for the cloning steps is provided in Chapter II.B and II.C. Plasmid dsAAV-CMV-EGFPΔG67 was compared to fluorescent dsAAV-CMV-EGFP by co-transfection with plasmid pDP2rs (Chapter II.A.3, transfection control) into HeLa cells (see Chapter II.E.1 for details on transfection). After a 24 h incubation fluorescence signals were monitored with a fluorescence microscope.

For the capsid competition assay, 7.5E+5 HCAEC were exposed to scAAV9-CMV-EGFP mutants displaying SLRSPPS or RGDLRVS alone or co-incubated with mutant scAAV9-CMV-EGFPΔGly67 vectors displaying peptide sequences RGDLRVS or SLRSPPS, as well as mutants displaying the scrambled counterparts SDLRRGV and PSLPSRS (Chapter II.A.4). Before use, all vectors were tested individually on HCAEC at MOI 5E+3 gc/cell to ensure the absence (EGFPΔGly67) or presence (EGFP) of fluorescence signals. The transduction assay was performed using parameters described in Table II.F.2, code 11. At the end of the incubation time, transduction efficiency of vectors was analysed by flow cytometry as described in Chapter II.D.2.

II.F.6 Heparin competition assay

The assay was performed by exposing 1E+5 HCAEC or 2.5E+5 HepG2 cells to wild type or scAAV9-CMV-EGFP vectors displaying peptide sequences RGDLRVS or SLRSPPS at MOI 5E+3 gc/cell in presence or absence of 210 IU sodium heparin solution. Medium was replaced with 500 µl/well cell culture medium containing vectors and – in case of heparin application – 2.5 µl 280 mg/ml heparin stock solution (see also Chapter II.F.2). A wild type scAAV2-CMV-EGFP vector was used as positive control. The exposure time was set to 4 h and further incubation in presence of fresh medium was conducted *ad* 48 h. Transduction efficiency of vectors was analysed by flow cytometry as described in Chapter II.D.2.

II.F.7 *In situ* gene transfer studies with wild type and selected AAV vectors

II.F.7.1 Gene transfer of murine Arteria mesenterica endothelium

Female immunocompetent NMRI mice 6-8 weeks of age were purchased by the German branch of Charles River Laboratories. All animal procedures were carried out in accordance with the guidelines outlined by the local committee for animal experiments (DKFZ Heidelberg and Regierungspräsidium Karlsruhe). The experiments described in Chapter II.F.7 were performed in collaboration with Anja Feldner and Ender Serbest at the Institute for Physiology and Pathophysiology, Heidelberg, Germany.

Isolation and preparation of *Arteria mesenterica* pieces

The animals were sacrificed by cervical dislocation and were fixated on their backside with a pin each limb. Skin and abdomen were opened by a longitudinal cut along the *linea alba* from the groin to the *sternum* using surgical instruments. Two small transversal cuts at either end of the longitudinal cut exposed the viscera. The colon was spread and mesenteric artery secondary branch pieces ~5 mm in length were isolated after careful removal of adipose and connective tissue. The vessels were inserted into a culture myograph and artery ends were knotted to the cannulae using surgical suture to avoid vector leakage. The infusion system was operated by an 1 ml syringe that was attached to the tubing of one cannula.

In situ-exposure of murine mesenteric artery endothelial cells (MMAEC)

Artery pieces mounted on the culture myograph were perfused with 50 µl endothelial cell culture medium (used for HCAEC, Chapter II.A.2) with or without 2.3E+9 gc/µl scAAV9-CMV-EGFP vector that displayed peptide SLRSPPS behind VP1 residue 589. The supply chamber was filled with medium until the artery pieces were covered and exposure was carried out for 48 h at 37°C. After vector treatment, the arteries were rinsed with 1x HBSS (w/ Ca^{2+} and Mg^{2+}) and endothelium was counter-stained by perfusion with 50 µl 1x TRITC-lectin solution and 15 min incubation at RT in the dark. After rinsing with 50µl 1x HBSS, artery pieces were removed from the infusion system and were mounted on microscope slides. Transduction of MMAEC was evaluated with a fluorescence microscope at 20x magnification and EGFP and TRITC signals were acquired separately.

In vivo-exposure of murine mesenteric artery endothelial cells (MMAEC)

Mice were injected each 200 µl 4.6E+11 gc scAAV9-CMV-EGFP vector that displayed peptide SLRSPPS behind VP1 residue 589 or mock via tail vein using 27G x ¾ needles (n = 2). Two weeks later the animals were sacrificed and mesenteric artery pieces were stained and evaluated as described above.

II.F.7.2 Gene transfer of human Vena umbilica endothelium

All experimental sets were performed in triplicate using human umbilical cords from independent donors. Cords were obtained from surrounding hospitals in Heidelberg and were kept at 37°C until use but not for longer than 8 h. A total of 12 cords were required to perform the final experiments below. Table II.F.7.2 gives an overview over the amount of cords needed for each experimental group.

Table II.F:7.2: Amount of human umbilical cords needed for in situ/in vitro gene transfer studies on HUVEC

	Amount of cords needed	Experimental replicates
In vitro-exposure	1	n = 3 each MOI
In situ-exposure	6	n = 3 for wtAAV9 and AAV9-SLRSPPS each
CD31 staining	1	n = 3
Vector gc quantification *in vitro*	1	n = 3 each MOI
Vector gc quantification *in situ*	3	n = 3 for AAV9-SLRSPPS

Isolation of HUVEC from umbilical veins

Residual blood clots were removed by gently dispersing the cords and veins were rinsed with RT 1x HANKS buffer. HUVEC isolation occurred by perfusion with 3.125 mg/ml dispase solution and incubation at 37°C for 30 min. Detached cells were collected by gently dispersing the cords and flushing veins with 1x HANKS buffer. After pelleting (220 x *g*, 4 min, RT), cells were resuspended in medium and maintained in 25 cm^2 flasks (see Chapter II.D.1.1) in corresponding medium (Chapter II.A.2) for 96 h with medium exchange occurring every other day. If a higher amount of cells was required, *in vitro*-propagation was extended to > 96 h as described in Chapter II.D.1.1.

In vitro-exposure of HUVEC

HUVEC were isolated as described above without vector pre-treatment and were cultivated until the desired cell number was achieved. Cells were seeded as described in Chapter II.D.1.1 and treated with AAV9-SLRSPPS vector as described in Chapter II.F.2, code 9. Transduction efficiency was analysed by flow cytometry as described in Chapter II.D.2.

In situ-exposure of HUVEC

Cleaned umbilical veins were perfused with HUVEC medium (Chapter II.A.2) supplied with scAAV9-CMV-EGFP wild type or mutant vector displaying peptide sequence SLRSPPS. Umbilical veins had diameters of 0.4-0.5 cm translating into a volume of ~0.125-0.196 cm^3 (or µl) volume for a 1 cm long fragment. Therefore, perfusion occurred with 250 µl vector solution/cm of vessel containing 4.3E+8 vector gc. To avoid leakage of vector solution, cord ends were sealed by knotting with surgical suture.

After 2 or 24 h exposure at 37°C, vector solution was removed and veins as well as parts of the cord potentially contaminated with vector solution were rinsed thoroughly with 1x HANKS buffer. Transduction of HUVEC by wild type or mutant scAAV9-CMV-EGFP vectors was analysed by cryo-fixation and cross-sectioning as described below or after dispase-isolation by flow cytometry as described in Chapter II.D.2.

Cryo-fixation and cross-sectioning of umbilical veins

Umbilical veins were carefully removed from cords after 24 h vector treatment and cut into small pieces of about 0.5 cm. For cryo-fixation the vessel pieces were embedded in cryomolds using cryo-embedding compound and were frozen and stored at -80°C. Cross-sections were prepared in a cryostat at 10 µm thickness and were mounted on microscope slides and stored at -20°C. For endothelial counter-staining, cross-sections were 20 min air-dried, encircled with a fat pen, 50 µl 1x TRITC-lectin solution each section were added and the reaction was allowed to take place for 15 min at RT in the dark. After rinsing with 50µl 1x HBSS, the sections were covered with coverslips using mounting medium with DAPI and transduction of HUVEC was evaluated with a fluorescence microscope at 20x magnification by separately acquiring EGFP, TRITC and DAPI signals.

CD31-staining of isolated HUVECs

Endothelial origin of isolated and cultivated cells was confirmed in a separate attempt by labelling endothelial marker protein CD31 with a FITC-conjugated PECAM-1 antibody (Chapter II.A.7). HUVEC were isolated from umbilical veins as described, but were not exposed to vector before. After 96 h *in vitro*-propagation, cells were rinsed once with 1x PBS, 2-3 ml non-enzymatic cell dissociation solution pre-warmed to 37°C was applied and cell detachment was monitored under a light microscope. The sample was separated in two portions and after centrifugation (220 x *g*, 4 min, RT), cells were resuspended in 50 µl PECAM-1 antibody diluted 1:2 with 1x PBS or in 50µl 1x PBS only. Binding of PECAM-1 to CD31 was allowed to take place in the dark for 45 min at 4°C. Unbound antibodies were removed by centrifugation and washing once with 1x PBS and presence of CD31 was analysed by flow cytometry as described in Chapter II.D.2.

Quantification of intracellular vector genome copies

For quantification of intracellular genome copies umbilical veins were *in situ*-exposed to scAAV9-CMV-EGFP displaying peptide SLRSPPS for 2 h and HUVECs were isolated by dispase treatment as described before. The isolated cell sample was divided in two parts. One part was propagated in HUVEC medium in a 25 cm^2 flask as described (Chapter II.D.1.1) while the other was prepared for qRT-PCR quantification of genomes. A propagation of cells < 20 h prevented growth but enabled counting of adherent cells, since contaminating erythrocytes or other non-adherent cells were removed by rinsing with 1x HANKS.

It was assumed that the doubled number of counted cells after < 20 h propagation would correspond to the total amount of cells isolated the day before. Quantification of intracellular gc from the other part of isolated HUVEC occurred by isolation of total DNA with the DNeasy Blood & Tissue Kit according to the manufacturer's recommendations (07/2006, pages 25-26, steps 1c-8). DNA was eluted twice in the same 100 µl AE buffer supplied with the kit. In a separate attempt, HUVECs were *in vitro*-exposed to the vector (Chapter II.F.2, code 9), were collected using trypsin (Chapter II.D.1), and total DNA was purified with the DNeasy Blood & Tissue Kit. Vector genome copies among total DNA were quantified via qRT-PCR (Chapter II.B.8.2) using CMV primers and probe (Chapter II.A.4) and were calculated as genome copies/cell.

II.G Statistical methods

For statistical evaluation data obtained by FACS analysis (% EGFP-positive cells, Chapter II.D.2) was provided in duplicate (n = 2), triplicate (n = 3) or quadruplicate (n = 4). SigmaPlot software was used to calculate mean values, standard deviation (SD) and significance level (p-values) of samples, whereas SD and p were only calculated for samples with n > 2. An unpaired Student's t-test was performed to calculate p-values and differences of means with $p < 0.05$ and $p < 0.01$ were regarded as significant or highly significant, respectively. All charts were generated using SigmaPlot and were further designed with Adobe Illustrator CS 5.

III. RESULTS

III.A *In vitro* transduction of cells by AAV – preliminary experiments

AAV transduction of cells *in vitro* can be influenced by various experimental parameters. To establish a reliable readout of transduction efficiencies, four parameters were analysed by incubating human coronary artery endothelial cells (HCAEC) with a self-complementary (sc) Adeno-associated virus serotype 2 (AAV2) vector displaying endothelium-targeted peptide NDVRAVS behind VP1 residue 588[195]. The vector encapsidated a CMV-EGFP expression cassette enabling analysis of transduction efficiency by flow cytometry. HCAEC were used as a cell model since library selection and related experiments were carried out predominantly on this cell type. The terms exposure and incubation subsequently used to describe cell treatment differ by the presence (exposure) or absence (incubation) of vector in cell culture medium.

III.A.1 Influence of medium volume during exposure

Exposure of cells to AAV occurs in cell culture vessels supplied with vector-containing medium and the applied volume influences the rate of vector-to-cell contacts. Since transduction depends on interaction of vectors and cell surface molecules, application of unnecessary high volumes will reduce the rate, resulting in lower transduction that in turn could render analysis of less efficient vectors difficult. At the same time, media volumes must be applied that ensure optimal maintenance of cells over several days. HCAEC were exposed to the vector mixed with 0.5 ml/well, 1 ml/well and 1.5 ml/well (12-well plates) corresponding to 131 µl/cm^2, 263 µl/cm^2 or 394 µl/cm^2, respectively (Chapter II.F.1, code 1). The volumes included the range of 200-300 µl/cm^2 recommended by the manufacturer of the cell culture plates. Exposure in 0.5 ml/well yielded significantly ($p < 0.01$) the highest transduction of HCAEC (Figure III.A **A**). Notably, no morphological changes of HCAEC or other cell types maintained in this volume for a maximum of 4 d could be observed. Thus, future *in vitro* transduction experiments were performed in a medium volume of 131 µl/cm^2 unless otherwise noted.

III.A.2 Influence of iodixanol during exposure

In this study, AAV vector or virus purification occurred via step gradient (isopycnic) ultra-centrifugation using iodixanol, a biologically inert contrast agent normally used for coronary angiography. Full capsids sedimented within the 40% iodixanol layer. Depending on titre of AAV stock and applied MOI, different amounts of iodixanol solution were mixed to medium, changing its viscosity. Since rate of vector-to-cell contact not only depends on amount of vector but also on medium viscosity, a high iodixanol incidence enforced by low vector stock titres could reduce the rate, thereby influencing transduction efficiencies.

To investigate the role of iodixanol concentrations, HCAEC were exposed to the vector in medium supplied with 1%. 5% and 10% total iodixanol concentrations (Chapter II.F.1, code 2). The presence of 10% iodixanol significantly ($p < 0.01$) reduced transduction efficiency by ~10% when compared to the 1% iodixanol sample (Figure III.A **B**). Only ~4 % reduction was observed between 5% and 1% iodixanol samples ($p < 0.02$). The presence of 10% iodixanol in 0.5 ml medium requires mixing of 125 µl vector stock solution containing 40% iodixanol. Assuming typical experimental parameters of 5E+4 HCAEC/well and a MOI of 1E+4 gc/cell, a low vector stock titre of 4E+9 gc/ml is necessary to obtain final iodixanol concentrations of 10%. To avoid falsification of efficiencies by high iodixanol concentrations, vector preparations below 5E+10 gc/ml were not used for transduction studies, thus enabling total iodixanol concentrations of < 1%.

III.A.3 Influence of incubation time on transduction

Successful transduction of cells implicates the presence of decapsidated transgene DNA within the nucleus. Post-entry processing of vector particles can vary in time and efficiency thus influencing the abundance of vector genomes within the nucleus. Here, the time required for a complete transgene expression post vector-exposure was analysed by pulse-treatment of HCAEC with vector and continued incubation in absence of vector (Chapter II.F.1, code 3). Obviously, the amount of vector that has entered the cell during the 4 h vector exposure, is processed completely during the first 24 h of continued incubation, since no increase of transduction efficiency can be monitored upon extending incubation time to 72 h (Figure III.A **C**). This experiment however, must not necessarily represent other vectors or cell types used in this study and therefore an incubation time of 48 h was generally regarded as adequate for *in vitro* transduction experiments unless noted otherwise.

III.A.4 Influence of exposure time on transduction

As shown in III.A.3, post-entry processing of AAV2-NDVRAVS particles within HCAEC occurs during one day leading to maximum transgene expression. The uptake of all functional vector particles from medium into the cell, however, may take more than 4 h exposure time. To analyse this effect, exposure time of HCAEC to the vector was increased gradually from 2 to 72 h. After corresponding time points medium was replaced and incubation was continued up to 72 h allowing analysis of transduction in an exposure time-dependent manner (Chapter II.F.1, code 4). An increase of transduction was observed during the first 48 h of exposure, which plateaued at 48/72 h (Figure III.A **D**). Thus, it was assumed that a total exposure time of 48 h should generally allow a comparable analysis of transduction efficiency between different vectors and was therefore applied subsequently for *in vitro* transduction experiments unless otherwise noted.

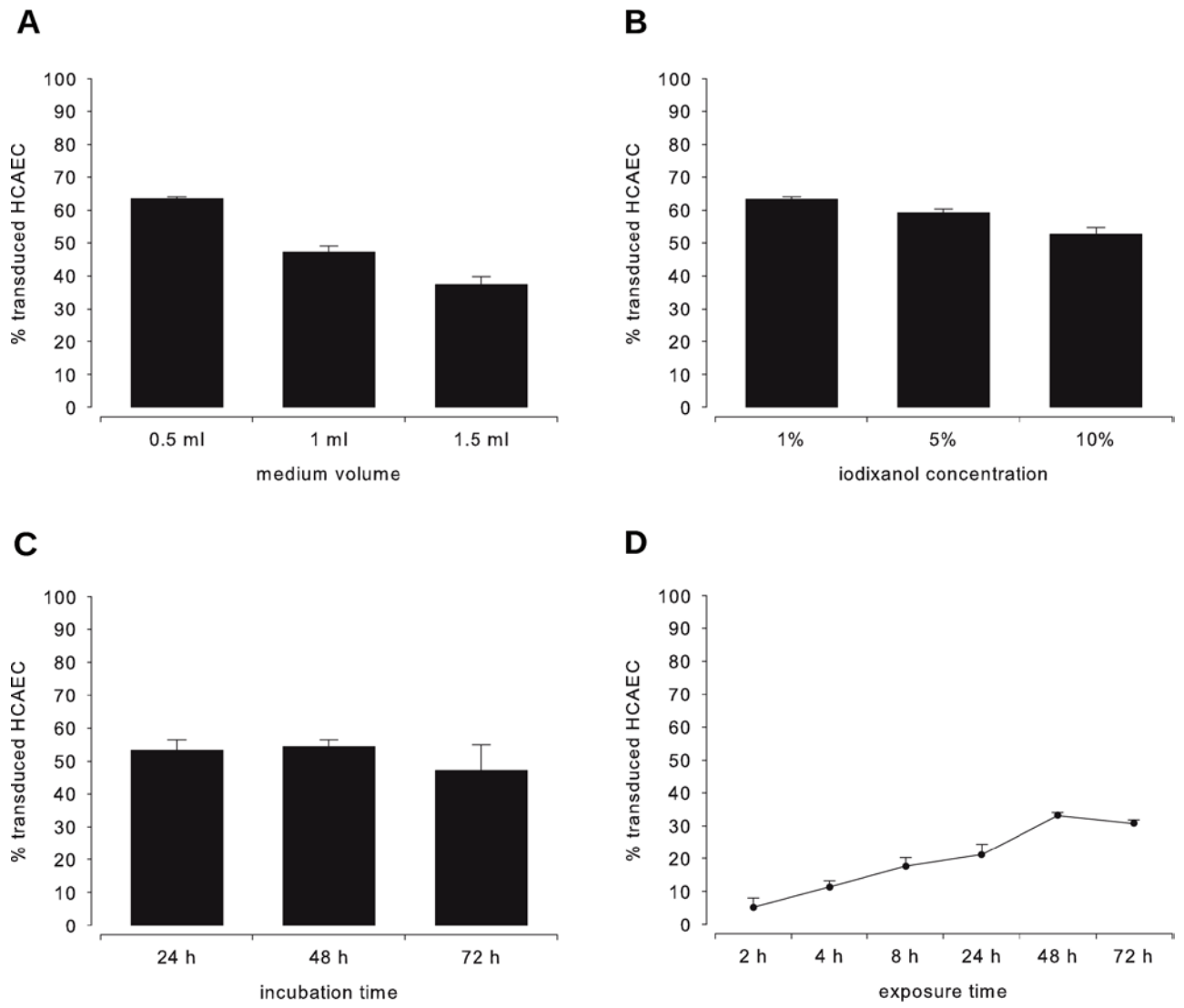

Figure III.A: Four different parameters affecting *in vitro* AAV transduction. Human coronary endothelial cells (HCAEC) were exposed to a scAAV2-CMV-EGFP vector displaying NDVRAVS behind VP1 residue 588 and exposure was terminated by removal of vector-containing medium. EGFP-expression was allowed to be established by continued incubation in presence of fresh medium. Transduction efficiencies obtained by flow cytometry analysis are given in % transduced HCAEC as means + SD (n = 3). **(A)** Influence of medium volume was assessed by pulse-exposing cells 4 h to vector using a MOI of 1E+4 gc/cell in 0.5 ml, 1 ml, or 1.5 ml medium. EGFP-expression was determined 48 h thereafter. **(B)** Absolute iodixanol amounts of 1%, 5% or 10% as well as vector at MOI 1E+4 gc/cell were mixed with medium and cells were exposed for 4 h. Influence of iodixanol presence was analysed after a continued 48 h incubation. **(C)**. An exposure of 4 h to vector at MOI 5E+3 gc/cell followed by continued incubations *ad* 24 h, 48 h, or 72 h in presence of fresh medium indicated the time necessary for complete EGFP-expression. **(D)** Time-dependent transduction of cells incubated with vector at a MOI of 5E+3 gc/cell was investigated by applying variable exposure times of 2 h, 4 h, 8 h, 24 h, 48 h or 72 h. Incubation in presence of fresh medium was performed *ad* 72 h (except for the 72 h sample).

III.B Design of an adequate peptide display site on the AAV9 capsid surface

III.B.1 Theoretical considerations

Artificial modulation of tropism and transduction efficiency requires knowledge of functional capsid surface domains and their corresponding amino acid residues. Resolution of AAV2 atomic structure by x-ray crystallography[94] together with identification of membrane-attached heparan sulphate proteoglycan (HSPG) as a primary receptor for AAV2 binding and infection[92] as well as isolation of capsid regions involved in HSPG-binding[90,91] enabled a more precise design of AAV2 capsid mutants with altered tissue tropism and improved transduction efficiencies. Insertion of a random peptide heptamer library displayed behind VP1 arginine residue 588 (R588) and selection thereof on HCAEC resulted in enrichment of peptide sequences that conferred improved transduction efficiencies of AAV2 vectors for this cell type[195]. R588 is localized at the shoulder of the three-fold protrusions (Figure III.B.1-1 **A-C**, red highlights) that are formed partially by VP1-3 loop IV (subloop 4), according to canine parvovirus (CPV) sequence alignment[110]. By another definition R588 is part of the variable region VIII (VR VIII, Figure III.B.1-1 **D-F**, red highlights) as first determined by Padron e*t al*.[100]. A corrected version of VRs is shown in Govindasamy *et al*.[96] or Figure III.B.1-2.

Lacking structural information of the AAV9 capsid at the onset of the project as well as unknown capsid binding sites and cellular receptors limited the possibilities by which rational peptide insertion sites could be predicted for AAV9. A VP1 sequence alignment of AAV serotypes 1 to 9 revealed VR VIII and other VRs to be shared by all analysed serotypes[100], suggesting that these regions could be generally involved in differential AAV tropism. ClustalW2 analysis of AAV2 and AAV9 VP1 sequences (NCBI database accession numbers YP_680426.1 and AAS99264, respectively) performed online at EBI (http://www.ebi.ac.uk/ Tools/msa/clustalw2) pinpointed an alanine residue at position 589 (A589) to correspond to R588 from AAV2 (Figure III.B.1-2, blue highlights). It was therefore assumed, that display of foreign peptides behind A589 could also influence the tropism of AAV9.

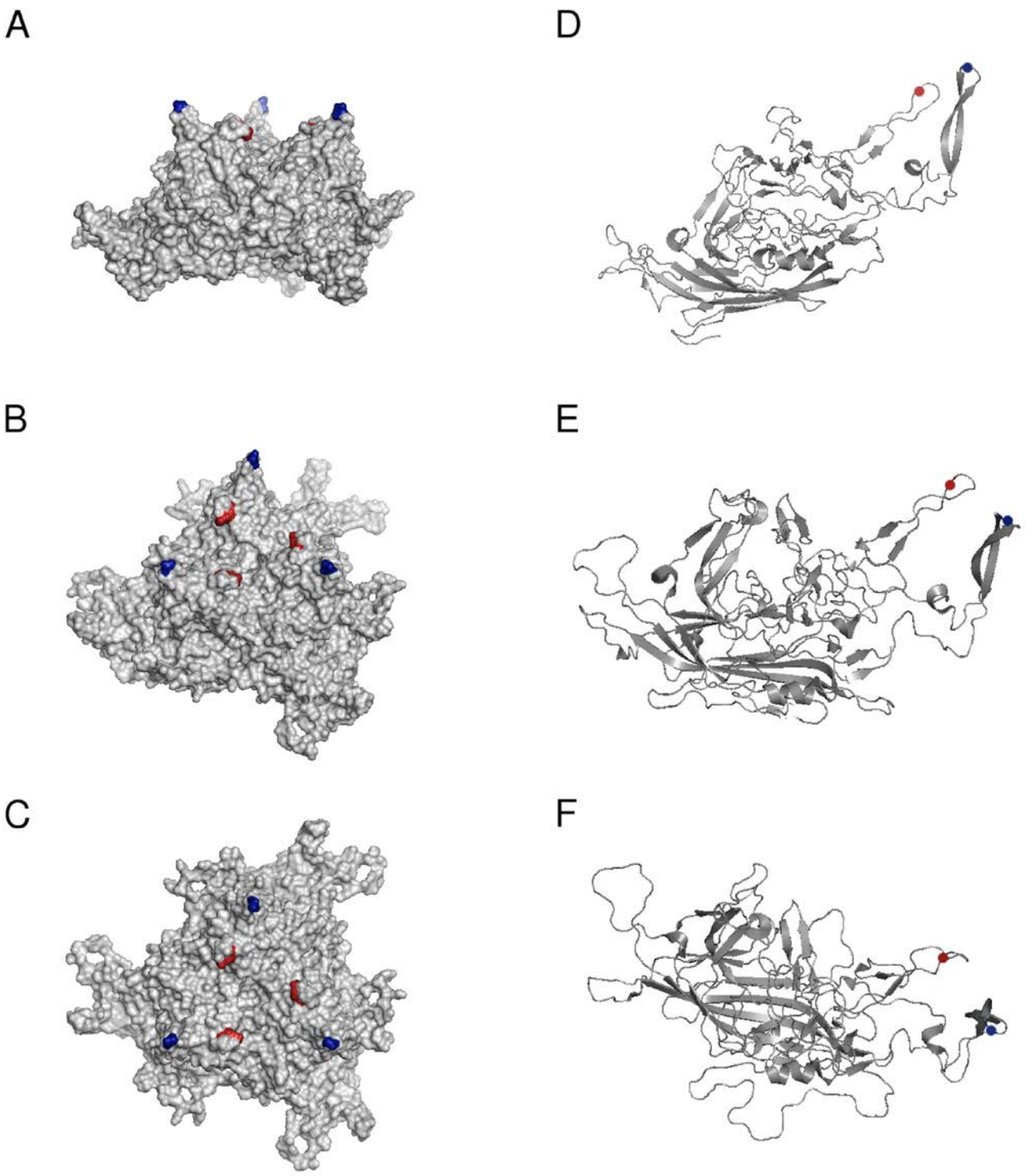

Figure III.B.1-1: In silico modelling of an AAV2 VP mono- or trimer. A trimer (**A**, **B**, **C**) or a monomer (**D**, **E**, **F**) were modelled using PyMol software and data from protein data bank (PDB). AAV2 accession number is 1LP3. For orientation, T454 located at the tips of the three-fold protrusions formed by VR IV were labelled blue. Red-labelled R588 is located at the inward-oriented side of the shoulder (easily visible in **A**), that is formed by VR VIII. VP monomer and trimer are displayed from the perspective of a capsid cross-section (**A**, **C**), a ~45°C inclination towards the observer (**B**, **E**) or from top (**C**, **F**). Fusion of 20 such trimer subunits forms the AAV2 icosahedral capsid.

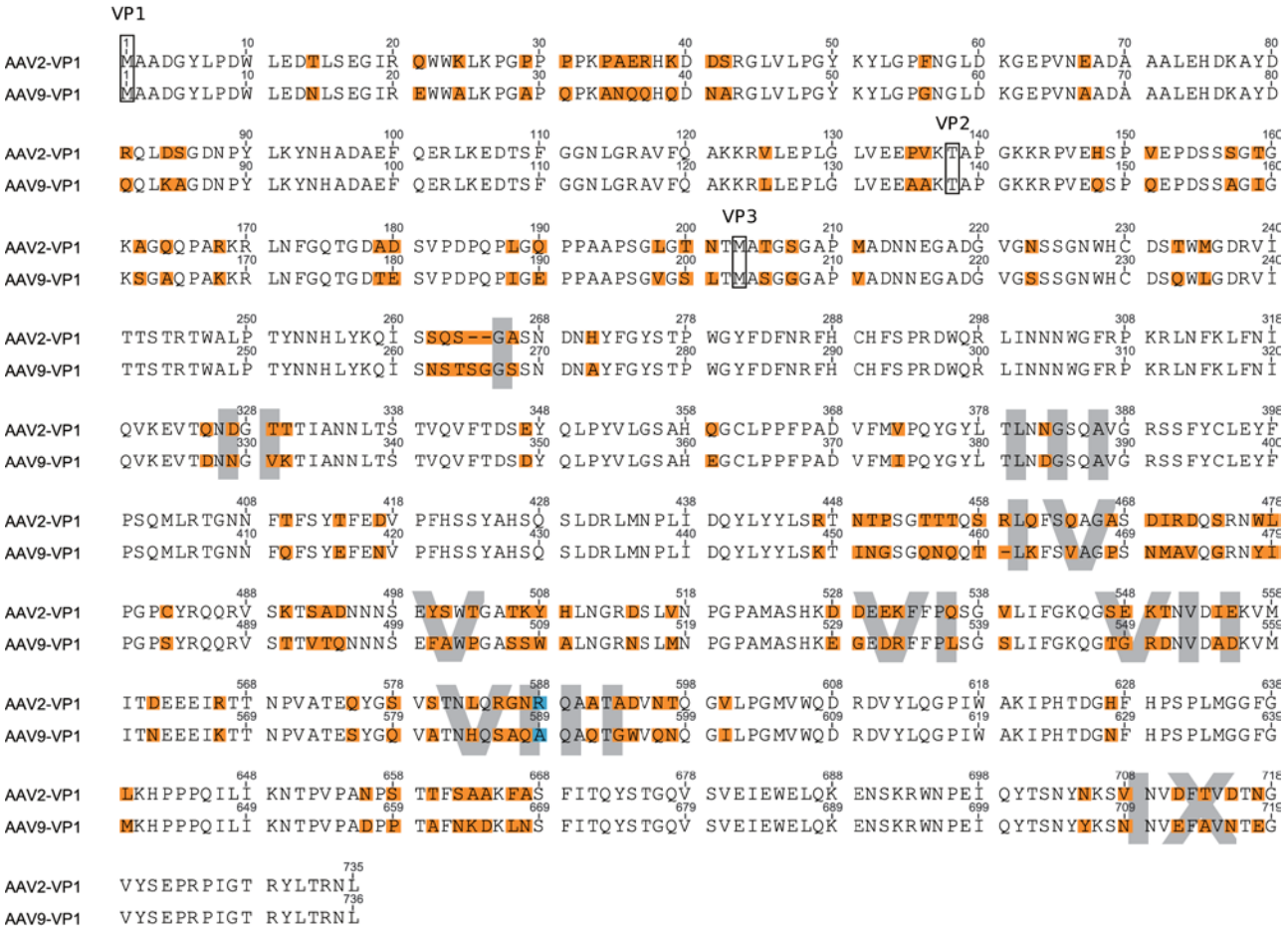

Figure III.B.1-2: Alignment of AAV2 and AAV9 VP1 peptide sequences. Sequence information was retrieved from NCBI (accession numbers YP_680426.1 and AAS99264 for AAV2 and AAV9, respectively) and ClustalW2-alignment was performed at EBI. Sequence editing was done with Geneious software and the illustration was manually modified with Adobe Illustrator CS5. The respective amino acids encoded by start codons of VP1-3 are framed in a box. Identical sequences of both serotypes are unlabelled while variable residues are highlighted orange. In addition, nine variable regions (VR) defined by Govindasamy *et al.*[96] are indicated with Roman numerals. VR VIII of AAV2 sequence contains R588 and is paralleled by A589 from AAV9 (blue highlights). Discrepancies in numbering arise from additional or missing amino acids within VRI and IV.

III.B.2 Adequacy of candidate residue A589 for peptide insertion

The generation of a random peptide library displayed on the AAV capsid surface is laborious and cost-intense. The poor predictive accuracy for the outcome of AAV9 capsid modifications demanded the testing of VP1 residue 589 as a site for foreign peptides display before the virus library was produced. The sequence of the AAV9 *cap* gene was modified according to Müller *et al.*[195] to allow insertion of oligonucleotides. Subsequently, AAV2 or AAV9 vectors displaying endothelium-targeted peptide NDVRAVS were generated to analyse the transduction efficiency of HCAEC.

III.B.2.1 Modification of the AAV9 cap ORF for oligonucleotide insertion

The introduction of two *SfiI* restriction sites by base exchange (Chapter II.E.4.1) enabled cloning of oligonucleotides into plasmid backbone p5E18-VD-2/9-*SfiI*1759 (Chapter II.B.4.2) allowing display of foreign peptides behind AAV9 VP1 residue 589 (Figure III.B.2.1). The modification induced several amino acid exchanges/insertions within the wtAAV9 *cap* ORF: A587G, Q592A, and two new amino acids G and A flanking the peptide heptamer insertion (Figure III.B.2.1, red highlights). The anatomy of the oligonucleotide insertion site had two advantages: first, cloning of oligonucleotides occurred in an oriented fashion, since the two *SfiI* recognition sequences were not religation compatible (GGCC-**AAGCA**-GGCC *versus* GGCC-**CAGGC**-GGCC). Second, the two adenosine nucleotides separating the *SfiI* recognition sequences induced a frame-shift in the AAV9 *cap* open reading frame (ORF) creating an early stop codon downstream of the insertion site. Hence, production of AAV particles from plasmids lacking oligonucleotide inserts was prohibited. *SfiI*-cleavage of the 15 bp stuffer fragment from p5E18-VD-2/9-*SfiI*1759 (Figure III.B.2.1 arrows) and ligation of an distinct oligonucleotide or a oligonucleotide library restored the frame and production of AAV capsids displaying foreign peptides behind VP1 residue 589 was possible. *SfiI*-treatment of oligonucleotides encoding peptide heptamers was not necessary since the single-stranded 21-mers were flanked by several nucleotides generating *SfiI*-compatible overhangs.

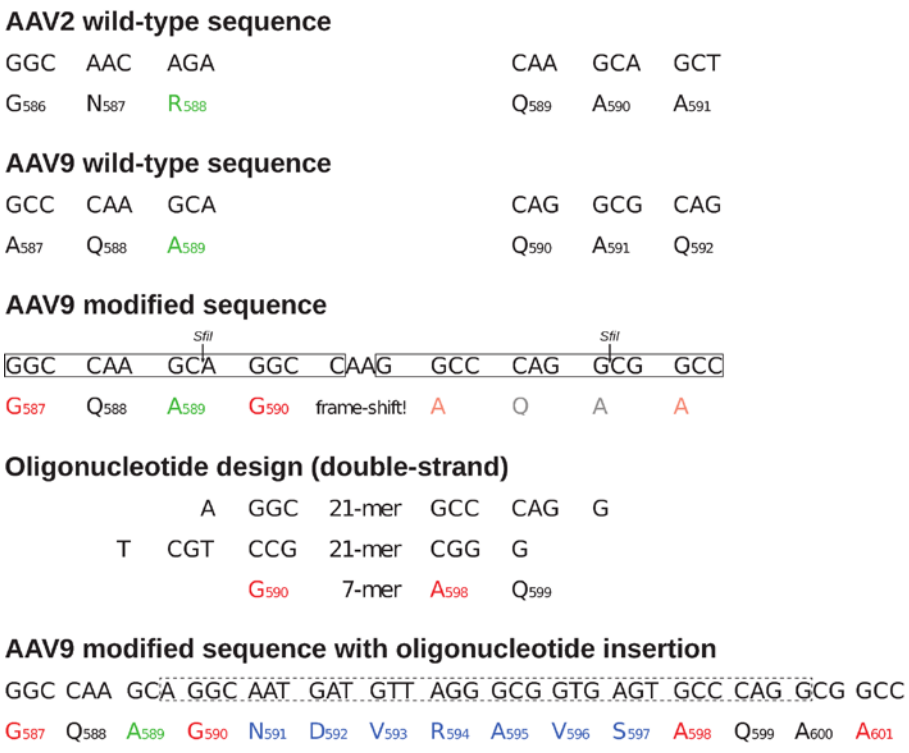

Figure III.B.2.1: Design of an oligonucleotide insertion site within the AAV9 *cap* gene. A representative section of the AAV9 *cap* ORF encompassing VP1 residue 589 is shown in a 5' to 3' orientation (see also Figure III.B.1-2). Sequence alignment revealed wtAAV9 alanine residue A589 to correspond to AAV2 arginine residue R588 (green highlights). Modification of the wtAAV9 *cap* ORF allowed insertion of two incompatible *SfiI* recognition sites (framed boxes). Only 4 amino acid residues were affected (red highlights), leaving the residual *cap* ORF unchanged.

The oligonucleotides encoding distinct peptide heptamers or the peptide library were flanked by nucleotides that would create *SfiI* compatible sticky ends upon annealing. Separation of *SfiI* recognition sites by two adenines induced a frame-shift within the *cap* ORF. Correct insertion of a 32-mer (dashed box) restored the frame-shift and enabled capsid formation from VP proteins displaying inserted peptide heptamers.

III.B.2.2 Transduction efficiency of AAV9 vectors displaying peptides selected with AAV2 libraries

Wild type or mutant scAAV9-NDVRAVS vectors displaying endothelium targeted peptide NDVRAVS behind VP1 residue 589 were produced and their transduction efficiency of HCAEC was compared to wtAAV2 and AAV2-NDVRAVS (Chapter II.F.1, code 5). While wtAAV2 and wtAAV9 showed transduction efficiencies of 19.2±10.7% and 12.4±3.9%, respectively, AAV2- and AAV9-NDVRAVS improved efficiencies to 71.7±15.7% and 74.2±8.9% transduced cells, respectively (Figure III.B.2.2), confirming the theoretical assumption that peptide display behind VP1 residue 589 modulates tropism and increases transduction efficiency of AAV9 vectors. Therefore, VP1 residue 589, comparable to VP1 residue 588 of AAV2, is suitable for introduction of foreign peptides or a peptide library.

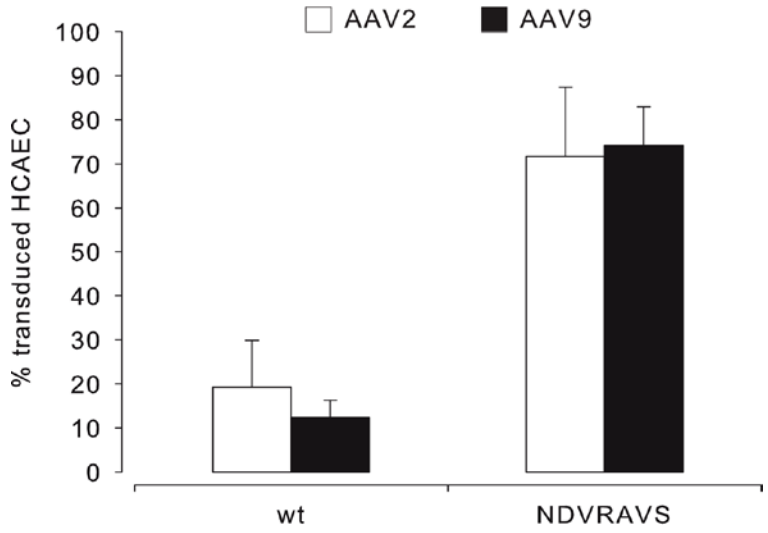

Figure III.B.2.2: Transduction efficiencies of wild type and mutant AAV2 and AAV9 vectors. HCAEC were exposed for 72 h to AAV2 (white bars) or AAV9 (black bars) wild type or mutant vectors displaying peptide NDVRAVS behind VP1 residues 588 or 589, respectively. Each construct was analysed at MOI 1E+4 gc/cell using two independent vector productions. Transduction efficiencies obtained by flow cytometry analysis is given in % EGFP-positive cells as means + SD (n = 4).

III.C Generation and characterization of an AAV9 random heptapeptide display library

After verifying the role of VP1 residue 589 as a potential peptide insertion site, the AAV9 random peptide display library production was attempted. A three step procedure described by Müller *et al*.[195] was applied: first, the plasmid library was created by introduction of a randomized oligonucleotide library into a plasmid backbone containing the modified AAV9 genome (see Chapter III.B.2.1). In the second step, the plasmid library together with a helper plasmid encoding wtAAV *rep* and *cap* and a wild type Adenovirus serotype 5 (Ad) helper plasmid were transfected into HEK 293T producer cells to obtain transfer shuttle library (TSL) particles. The mosaic AAV capsids of the TSL are formed by wild type and mutant VPs that randomly package the genomes present in the respective cell. In the third step, the TSL was used to re-infect HEK 293T cells at a MOI of 0.5 IU/cell, ensuring theoretical uptake of one viral genome/cell. Subsequent super-infection with Ad lead to synthesis of virus library particles from VP proteins that were transcribed from only one genome present in a cell, ensuring the display of heptamer sequences that correspond to the packaged genomes. A schematic overview of the three production steps is given in Figure III.C and Chapters III.C.1-III.C.3 provide more detailed information about the individual steps and implications related to them.

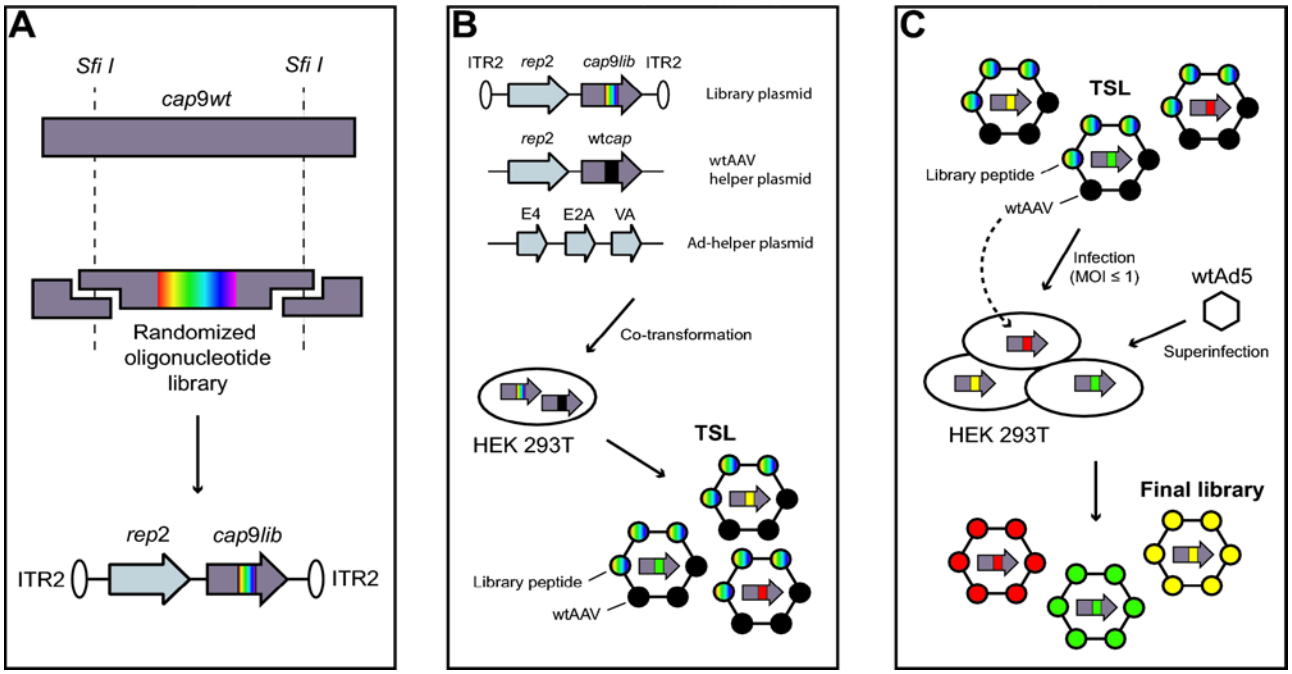

Figure III.C: Schematic representation of the AAV9 library production steps. (**A**) The randomized oligonucleotide library was cloned into the library plasmid backbone via *Sfi*I-digestion. The library plasmid contains AAV2 ITRs (ITR2), the *rep* gene from wtAAV2 (*rep*2) and the modified AAV9 *cap* gene (*cap*9lib). (**B**)The library plasmid, wtAAV helper plasmid providing wild type AAV2 or AAV9 VP proteins and a helper plasmid containing essential Ad genes E4, E2A and VA were triple-transfected into HEK 293T producer cells. Thus, the transfer shuttle library (TSL), mosaic capsid particles consisting of wild type and mutant VP proteins displaying random heptamers is produced. (**C**) The TSL is applied at a MOI 0.5 IU/cell to ensure infection of HEK 293T cells with only one particle/cell. Wild type VP proteins present on the TSL shells provide a theoretically an infection of HEK 293T from each TSL particle (dashed arrow line).

Super-infection with Ad (wtAd5) enables amplification of internalized TSL genomes and generation of pure virus library particles that display peptide heptamers encoded by the encapsidated genomes.

III.C.1 The plasmid library

III.C.1.1 Design of the randomized oligonucleotide library

The degenerated genetic code discloses the opportunity to modify the DNA sequence of a protein without affecting its peptide chain. In most cases, prohibiting the appearance of a certain base at the third position of the codon lowers the occurrence of that particular amino acid. Exemplary, changing the NNN architecture to NNK reduces the codons of arginine by half (CG**G**, CG**T**, AG**G**, see Table S2), as N permits all 4 bases within the first two codon positions and K limits the third position bases to G and T. This modification also affects the number of stop codons, which in case of NNK are reduced by one third, at the same time prevailing the occurrence of all amino acids. Therefore, the NNK architecture was chosen as a basis for the synthesis of the random peptide display library. Theoretically, a peptide chain consisting of seven amino acid residues featuring all 20 amino acids yields 1.28E+9 (20^7) different sequences.

III.C.1.2 Plasmid library complexity

A crucial step in the generation process of the plasmid library that can reduce the complexity is posed by the insert-to-backbone ratio used for ligation of oligonucleotide library and plasmid backbone (pKV-AAV9Lib/BB). The complexity is estimated by counting of bacterial colonies after transformation (transformation efficiency) and is given in colony forming units (CFU)/µg transformed DNA (see Chapter II.E.4.1). Assuming the transformation of only one library plasmid copy per bacterial cell that later forms a colony, the total amount of colonies is an approximation for the complexity. To test the most feasible insert-to-backbone ratio, three different test-ligations without or with 10x, 30x or 100x molar excess of oligonucleotide library to backbone were prepared. Counting of colonies assigned highest complexity to the attempt using the 30x excess of insert with a background from re-ligation of empty plasmid backbones of 0.17% (Table III.C.1.2, left panel). The 20x up-scaled ligation attempt using this ratio yielded a total of 6.02E+7 CFU/µg plasmid (Table III.C.1.2, right panel) translating into 6.02E+8 CFU/10 µg that represents at the same time the total plasmid library complexity.

Table III.C.1.2: Estimation of plasmid library complexity by calculation of transformation efficiencies

Excess Insert	CFU/µg[1] plasmid	Background[2] (%)
10x	2.09E+7	0.28
30x	3.47E+7	0.17
100x	7.80E+6	0.74
Control	5.80E+4	1

Batch[1]	CFU/µg plasmid	Mean CFU/µg
1	5.35E+7	6.02E+7
2	3.90E+7	
3	5.64E+7	
4	9.20E+7	

[1]see Chapter II.E.4.1, [2]quotient of „control“ and „excess inserts“

The NNK-architecture of the plasmid library allows only G or T nucleotides at the third codon position and thus reduces the total amount of codons from 64 to 32. This influences also the theoretical occurrence O_T of stop codons (equation (2)) that are reduced from 35% for NNN (x = 3, y = 60) to 21.9% for NNK (x = 1, y = 32) within the peptide heptamer.

$$(2)\quad O_T = \frac{x\ \text{stop codons}}{y\ \text{total codons}} \times 7\ \text{residues} \times 100$$

Still, the amber stop codon can be encoded and its occurrence within the heptamer lowers the complexity of the plasmid library. Within 79 sequenced plasmid library clones 30 stop codons were identified (37.9%), exceeding the calculated O_T of the NNK or NNN architectures. In total, 28 sequences (35.4%) contained one or more stop codons at random positions within the heptamer rendering them infeasible for virus production (Figure S1 **A**). Therefore, the plasmid library complexity of 6.02E+8 CFU/10 µg was corrected by factor 0.354 to its functional complexity of 3.89E+8 clones.

III.C.1.3 Amino acid distribution of peptide heptamers encoded by the plasmid library

The theoretical mean occurrence of a NNK-encoded amino acid over the entire peptide heptamer was calculated with equation (3) as a quotient of codons encoding that amino acid and total available codons:

$$(3)\quad O_T = \frac{x\ \text{codons}}{y\ \text{total codons}} \times 7\ \text{residues} \times 100$$

In case of alanine the theoretical mean occurrence is 6.3% (x = 2, y = 32). In reality, after counting alanine appearances within 79 analysed sequences, its mean occurrence was 5.4% (see Table S1). Theoretical and real mean occurrences were calculated for the remaining amino acids and are summarized in Figure III.C.1.3. Overall, the occurrence of amino acids within the plasmid library (Figure III.C.1.3, dotted line) fits theoretical calculations (continuous line), with exception of cystein (C), phenylalanine (F), valine (V) and tyrosine (Y) that seem to be slightly over-represented. A more disclosed amino acid distribution shown in Figure S1 **A** reveals no accumulation or consecutive repetition of more than 2 amino acids. Together, the plasmid library can be regarded as sufficiently complex with an exhaustive amino acid usage that is represented in an residue-unbiased manner.

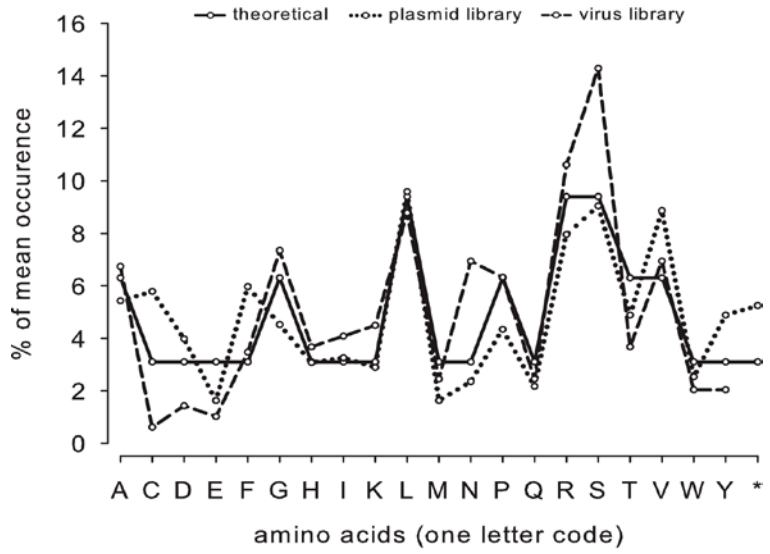

Figure III.C.1.3: Representation of amino acids within plasmid and virus library. Individual clones from plasmid (79) or virus library (70) were sequenced and amino acid distribution for each residue within the heptapeptide was determined. The occurrence of each amino acid at any position was calculated as percentage and the average over the entire heptamer is plotted here as % of mean occurrence for each amino acid. Theoretical means (continuous line) were assessed by calculating the probability an amino acid would to occupy a residue according to the NNK-architecture of the library oligonucleotide. Data for the plasmid and virus library are given in dotted and dashed lines, respectively. * = stop codon (amber).

III.C.2 The transfer shuttle library (TSL)

A categorical feature of the TSL is a high infection efficiency of the producer cell line, since this eventually represents the key to a high virus library complexity. Transfection of the plasmid library alone would yield TSL viruses from VP proteins encoded by several *cap* variants from the plasmid library and viral genomes would be encapsidated in mosaic capsid particles, as in case of Perabo *et al*.[194]. Such particles potentially display different infective properties and if applied for infection, a preferential uptake of some TSL particles over other may occur, lowering the final library complexity. Co-transfection of an ITR-negative helper plasmid containing the wtAAV2 *cap* ORF cleared this imbalance in case of AAV2-based TSL productions. WtAAV2 vectors have a strong transduction efficiency of HEK 293T cells and transcapsidation of the TSL with wtAAV2 VP proteins theoretically ensures an approximately equal efficiency of infection for each TSL particle.

However, wtAAV9 vectors display only a very low transduction of HEK 293T cells (Figure III.F.1) and transcapsidation with wtAAV9 VPs may lower the general TSL infectiousness and complexity. A transcapsidation of the AAV9 TSL with wtAAV2 VPs may solve the problem, however, at the risk of a lowered packaging efficiency as observed for transcapsidation of AAV subgroups A and C[187]. Hence, TSL test-productions with wtAAV2 and wtAAV9 VPs at variable ratios of 1:1, 1:5 and 1:10 library to wild type VPs (Table III.C.2) were attempted to analyse the most feasible combination. In theory, a stoichiometric plasmid ratio of 1:1, 1:5 or 1:10 would result in TSL particles assembled from 30:30, 12:48 or 6:54 VPs from wtAAV9 and wtAAV2, respectively.

In addition, different amounts of plasmid library pKV-AAV9Lib per cell were assayed. In the following description TSL productions from **wtAAV2** or **wtAAV9** helper plasmids (pRSV-VP3co and p5E18-VD-2/9, respectively) are referred to as **2-TSL** or **9-TSL**, respectively. The use of Ad helper plasmid pDGΔVP is not mentioned explicitly below.

No DNase-resistant particles (DRP) were detectable from 2-TSL (code AC) or 9-TSL (code AD) control productions performed in absence of library plasmid proving a helper plasmid stock free of wild type-contaminations. Another control production using library plasmid only (code AB) yielded genomic titres comparable to productions employing helper plasmids (codes ABC, ABD), albeit with a reduced infectiousness of HEK 293T. Insertion of foreign peptide heptamers behind VP1 residue 589 obviously does not hamper efficient genome packaging and formation of infectious particles from VP protein library variants but the reduced infectiousness indicates the need of wtAAV VP proteins as described above. The infectiousness of TSL particles was tested on HEK 293T cells (Chapter II.E.3), since this cell type was also used for the production of the final virus library. Although expected, no differences of infectiousness between 2-TSL or 9-TSL particles were present (codes ABC and ABD). Comparable genomic titres of 2-TSL and 9-TSL productions prove an efficient packaging capacity of transcapsidated AAV particles. Independent of helper plasmid, a slight decrease of TSL infectiousness was detected when higher amounts of library plasmid or a higher library to helper plasmid ratio was employed. According to these results a stoichiometric library to helper plasmid ratio of 1:1 together with the application of only 1 µg library plasmid for 5E+6 cells (1 dish, see Chapter II.E.4.2) resulted in TSL particles with the maximum infectiousness of HEK 293T cells (Table III.C.2, framed boxes).

Table III.C.2: Genomic and infectious titres of TSL produced at different plasmid ratios

Code	Ratio[1]	pKV-AAV9Lib (µg)			Infectious titre (IU/ml)			Genomic titre (gc/ml)		
AB	1:1	n/a	n/a	5	n/a	n/a	1E+4	n/a	n/a	1.1E+9
AC	1:1	n/a	n/a	5	n/a	n/a	0	n/a	n/a	0
AD	1:1	n/a	n/a	5	n/a	n/a	0	n/a	n/a	0
	1:1	1	2	5	1E+6	1E+6	1E+5	1.4E+9	1.5E+9	2.8E+9
ABC	1:5	1	2	5	1E+5	1E+5	1E+4	2.3E+9	1.1E+9	1.6E+9
	1:10	1	2	5	1E+6	1E+5	1E+5	6.9E+8	1.9E+9	1.4E+9
	1:1	1	2	5	1E+6	1E+5	1E+5	2.2E+9	2.5E+9	7.4E+9
ABD	1:5	1	2	5	1E+5	1E+6	1E+5	1.9E+9	5.2E+8	2.6E+8
	1:10	1	2	5	1E+5	1E+4	1E+5	1.5E+9	4.4E+9	9.1E+8

Codes: A = pDGΔVP, Ad-helper plasmid; B = pKV-AAV9Lib, library plasmid; C = pRSV-VP3co, wtAAV2 helper plasmid; D = p5E18-VD-2/9, AAV9 helper plasmid; [1]code B to C or D

III.C.3 The virus library

III.C.3.1 Virus library titres and complexity

Using the production parameters established in Chapter III.C.2, 2-TSL and 9-TSL productions were upscaled to 20x of the amounts of test productions (see Chapter II.E.4.2). These productions yielded comparable absolute genomic and infectious titres (see Table III.C.3.1). The functional complexity of the plasmid library of 3.89E+8 was reduced to 5E+7 for both TSL, as the complexity can not exceed the amount of infectious particles present in a virus stock. To generate the final virus library, the HEK 293T producer cell line was infected using the TSL productions at MOI 0.5 (Chapter II.E.4.3). First, two small-scale library productions employing TSL of either origin were produced and analysed. Determination of infectious titre was not possible due to a inhomogeneous infectiousness of library particles. The absolute genomic titre of both small-scale library productions yielded 3E+9 gc each and confirmed similar production efficiency from both TSL backgrounds. Due to reasons explained later in Chapter III.C.4 only the 2-TSL was used for the large-scale final library production. This final library yielded an absolute genomic titre of 4.6E+11 gc or 4.6E+3 gc/cell which is comparable to those of AAV vectors displaying peptides (Chapter III.E.1), suggesting a easily scalable and hence cost-effective production method. Again, the infectious titre can not be analysed directly, but since the entire TSL with a complexity of 5E+7 was employed in the production process, a final library complexity of up to 5E+7 can be expected, taking into account the loss of variants during production and purification steps.

Table III.C.3.1: Genomic and infectious titres of upscaled TSL and virus library

Absolute titres	**PL**[1]	**TSL**[2] (pRSV-VP3co)	**TSL** (p5E18-VD-2/9)	**VL**[3]
Genomic (gc)	n/a[4]	3.8E+12	3.2E+12	3E+9
Infectious (IU)	n/a	5E+7	5E+7	n/a
Complexity	3.89E+8	5E+7	5E+7	n/a

[1]plasmid library, [2]transfer shuttle library, [3]virus library from both TSL sources, [4]not assayed

III.C.3.2 Amino acid distribution of peptide heptamers encoded by the virus library

Sequencing of 70 individually assigned clones (Chapter II.E.5) allowed the analysis of amino acid usage and randomness of peptide heptamer inserts. A decreased average presence of cysteine (C), aspartic (D) and glutamic acid (E) and threonine (T) was detected, while presence of asparagine (N) and serine (S) was slightly increased when compared to theoretical means (Figure III.C.1.3, Supplementary Table 1). Notably, N was strongly over-represented at the first (25.7% vs theoretical 3.1%) and S at second and sixth residue (both 18.4% vs theoretical 9.6%). The biggest differences in mean occurrence between plasmid and peptide library (Figure III.C.1.3) were observed for amino acids C (5.2%), N (4.5%) and S (5.3%).

Similarly, involved heptamer residues were the first (N), second and fifth to seventh (all S). Despite this slight bias for the presence of certain amino acids, the virus library can be regarded as sufficiently complex with an acceptable amino acid usage and distribution.

III.C.4 Wild type contamination of the AAV9 random peptide display library

The lack of ITRs flanking the AAV genomes of helper plasmids avoids packaging of wtAAV genomes during TSL production. However, an exchange of wild type and mutant *cap* sequences by intracellular DNA recombination between helper and library plasmid would create wild type genomes flanked by ITRs leading to a wild type contamination of TSL and final virus library particles. Such a wild type contamination lowers the library complexity and leads to co-selection of wtAAV on wild type-permissive cells, thus impairing the selection process. To compensate this drawback, the codon-optimized helper plasmid pRSV-VP3co bearing a synthetic wtAAV2 *cap* gene was developed and enabled the production of a wild type-free AAV2 peptide library[201]. No codon-optimized wtAAV9 helper plasmid was available for the creation of an AAV9 random peptide library, rendering DNA recombination between p5E18-VD-2/9 helper and pKV-AAV9LIB library plasmids probable.

All plasmids involved in AAV9 library production, TSLs and final virus libraries were subjected to PCR analysis (Chapter II.F.1) to detect the presence of contamination with wtAAV9 sequences. The primer pair AAV9cap-F/R amplifies a 270 bp fragment within the wtAAV9 *cap* ORF or a 297 bp fragment within an AAV9 *cap* ORF containing an oligonucleotide insertion. Easy discrimination of fragments is possible by electrophoretic separation on a 2.5% agarose gel. Stocks of pRSV-VP3co and pDGΔVP were free of wild type contamination and plasmid p5E18-VD-2/9 showed the expected 270 bp wtAAV9 fragment (Figure III.C.2, “Plasmids”). Library plasmid pKV-AAV9Lib, however, reproducibly showed along with the typical library fragment at 297 bp also a faint wild type fragment at 270 bp, indicating primordial wild type-contamination. The persistence of the contamination in both TSLs and the final virus libraries (Figure III.C.2, “TSL” and “Library”) prove that the wild type-contamination of the plasmid library stock originates from wild type genomes containing ITRs. Consequently, an AAV9 random peptide display library free of wtAAV9 contamination using this plasmid library stock was not possible. High overall library plasmid production costs lead to the decision to continue the project with the present plasmid library. It was assumed that the low permissiveness of wtAAV9 towards HCAEC (see Chapter III.B.2.2) would exclude a co-selection of wtAAV9 and would allow enrichment of distinct virus variants, as shown for the selection of a wtAAV2-contaminated AAV2 library on human saphenous vein ECs[201]. The less intense 270 bp fragment from the library production using 2-TSL (pRSV-VP3co) suggests contamination to a lower degree. Thus, only the 2-TSL was used for the large-scale production of the final virus library which then was employed for selection of endothelium-targeted peptides.

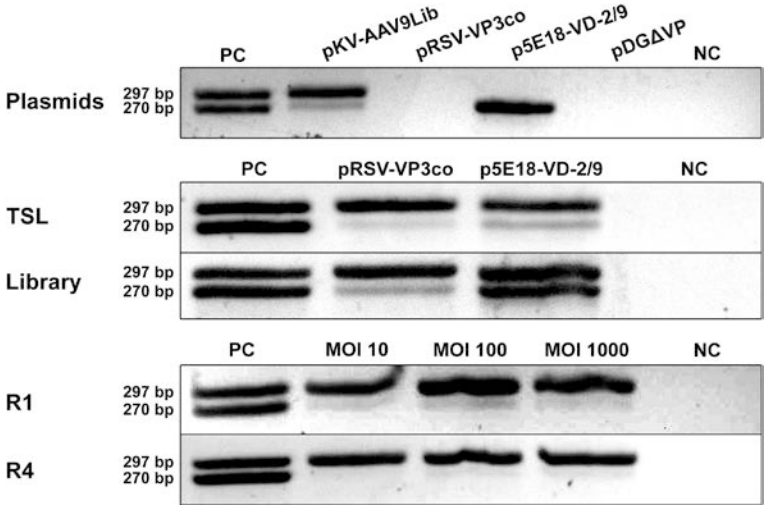

Figure III.C.4: Detection of wtAAV9-contaminations during the virus library production. PCR-amplification of DNA occurred with primer pair AAV9cap-F/R that amplifies a 270 bp fragment of wtAAV9 *cap* ORF or a 297 bp fragment from *cap* ORFs containing an oligonucleotide insert. Five µl PCR products previously mixed with 6x Gel Loading Dye Blue were loaded on a 2.5% agarose gel and electrophoresis was run for 2 h at 5 V/cm electrode distance. For positive control (PC), 100 pg of plasmids p5E18-VD-2/9 or p5E18-VD2/9-*SfiI*1759 with an oligonucleotide insert were PCR-amplified separately and 5 µl PCR reaction each were mixed and loaded on the same lane, facilitating discrimination between wild type and library fragments. One µl ddH_2O instead of DNA template was used as negative control (NC). Ten ng of each plasmid employed in library production (Plasmids) or ~55 pg purified DNA from 2-TSL and 9-TSL, unselected virus library (Library) and virus library selected once (R1) or four times (R4) at MOIs 10, 100 and 1000 gc/cell on HCAEC were inserted into the PCR reaction. For a better visualisation the gel photography is displayed as a black/white-inversion and brightness/contrast were adjusted to enable visualization of faint bands.

III.D. *In vitro* selection of the AAV9 random peptide display library on HCAEC

The AAV9 peptide library consists of a multitude of capsid variants (Figure III.D-1) that may display different levels of transduction efficiencies. Selection therefore will favour the propagation of virus particles that have beneficial attributes related to the infection process of the host cell. Peptide display on the capsid surface does not only influence binding to cell surface receptors and endocytosis, but modulates also the downstream processing of viral particles, like endosomal release, nuclear import, uncoating or packaging of replicated genomes. Only capsid variants that master all these steps with good efficiency will be enriched during repeated selection of the library on host cells (Figure III.D-1, red hexagons). But also less efficient variants will propagate during the initial selection round, for instance variants with poor binding and internalisation properties but efficient in the downstream processing (Figure III.D-1, green hexagons). Such variants can be theoretically eliminated by application of several consecutive selection rounds. In addition, defective viruses that bind to receptors but fail to enter the cell represent a potential source of contamination as they would mix with efficient variants during library purification by cell lysis. To largely avoid the presence of such false positive variants, purification of enriched virus particles involved trypsination of cells, which is expected to remove cell surface receptors and with them bound viral particles (Figure III.D-1, orange hexagons).

An important role for proper amplification of internalized AAV particles plays the MOI used for super-infection of cells with Ad. Excessive amounts of Ad will lead to an untimely cell lysis lowering the titre of AAV library particles.

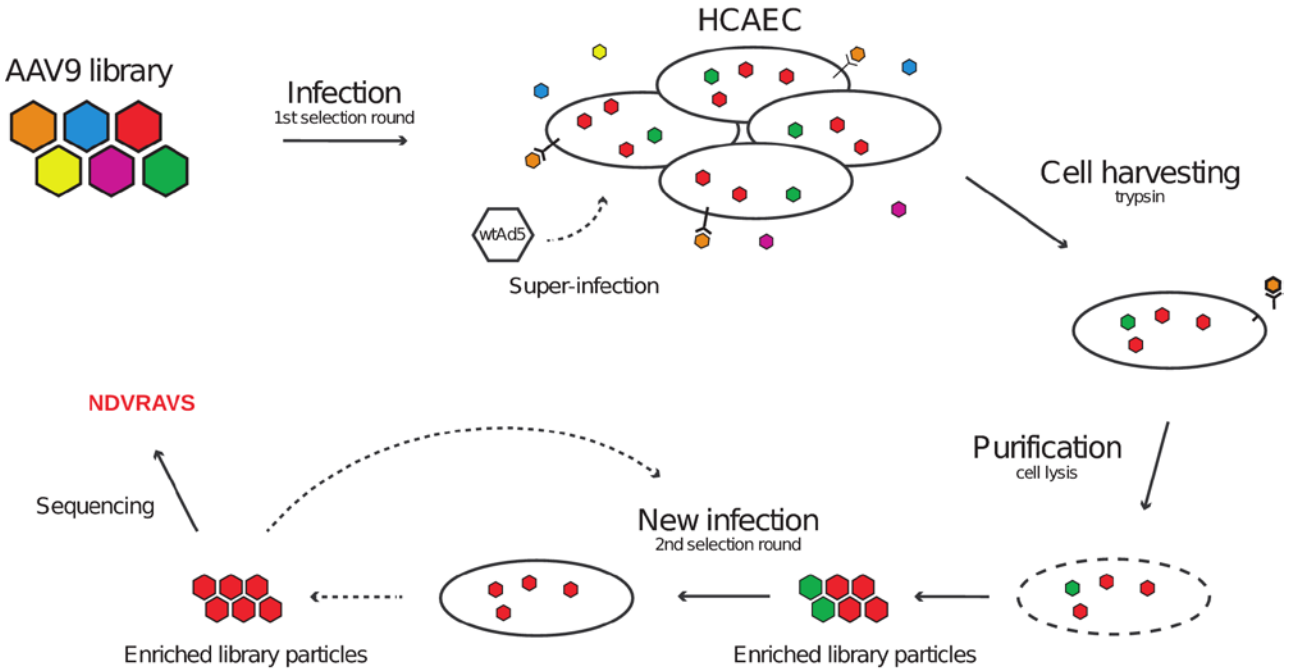

Figure III.D-1: Schematic representation of the selection process of the AAV9 library *in vitro*. HCAEC were exposed for 4 h to the library at MOIs of 10, 100 and 1000 gc/cell in separate attempts (Infection). After exposure, unbound library particles (yellow, blue, violet) were removed and fresh medium containing Ad was supplied (Super-infection). Super-infection with Ad lead to the amplification of internalized library particles which then were purified by cell lysis. Prior to lysis, cells were harvested using trypsin, thereby removing bound but not internalized library particles (orange). Purified enriched library particles were re-applied to HCAEC for a new selection round (New infection). After the third and fourth selection round, DNA clones were prepared and were sequenced to reveal the sequence of the enriched library peptide.

The AAV9 peptide library was selected four consecutive rounds on HCAEC, each round using three different MOIs of 10, 100 and 1000 gc/cell in separate attempts (Chapter II.F.1). Preliminary experiments performed with variable MOIs of Ad on HCAEC revealed a 50% cytopathic effect after 48 h incubation at MOI 20 IU/cell. It was assumed that these parameters would be acceptable for a proper amplification of internalized library particles. After the third and fourth selection round aliquots of purified viral DNA were PCR-amplified, sub-cloned into plasmids and transformed into bacteria. Independently assigned single colonies were analysed to reveal enriched peptide heptamer sequences (Chapter II.E.5). Independent of selection round or applied MOI, peptide sequence RGDLRVS represented the most prominent peptide (Figure III.D-2). Second most common peptides were NFTRLSA and SLRSPPS with a more restricted distribution. Notably, some peptides shared certain residues or had similar sequences ($RGD^{LRVS}/_{FRVG}$, $^{S}/_{T}{}^{L}/_{I}R^{S}/_{A}PP^{S}/_{A}$) while others were differed in amino acid composition (DAKWDYR, GAIPDLR).

These results prove that three to four selection rounds of the AAV9 library on HCAEC yielded a consistent enrichment of certain peptide sequences independent of applied MOI or wtAAV9 contamination of the library. PCR-analysis of the library after the first and the fourth selection round showed a low wild type-contamination, confirming the assumption that co-selection of wtAAV9 in non-permissive cells is less likely to happen (Figure III.C.4). Remarkably, any of the enriched peptides descended from the same DNA clones in an MOI or selection round-independent manner. In contrast, enriched peptides from a HCAEC-selected AAV2 library[195] were from different DNA clones (not shown).

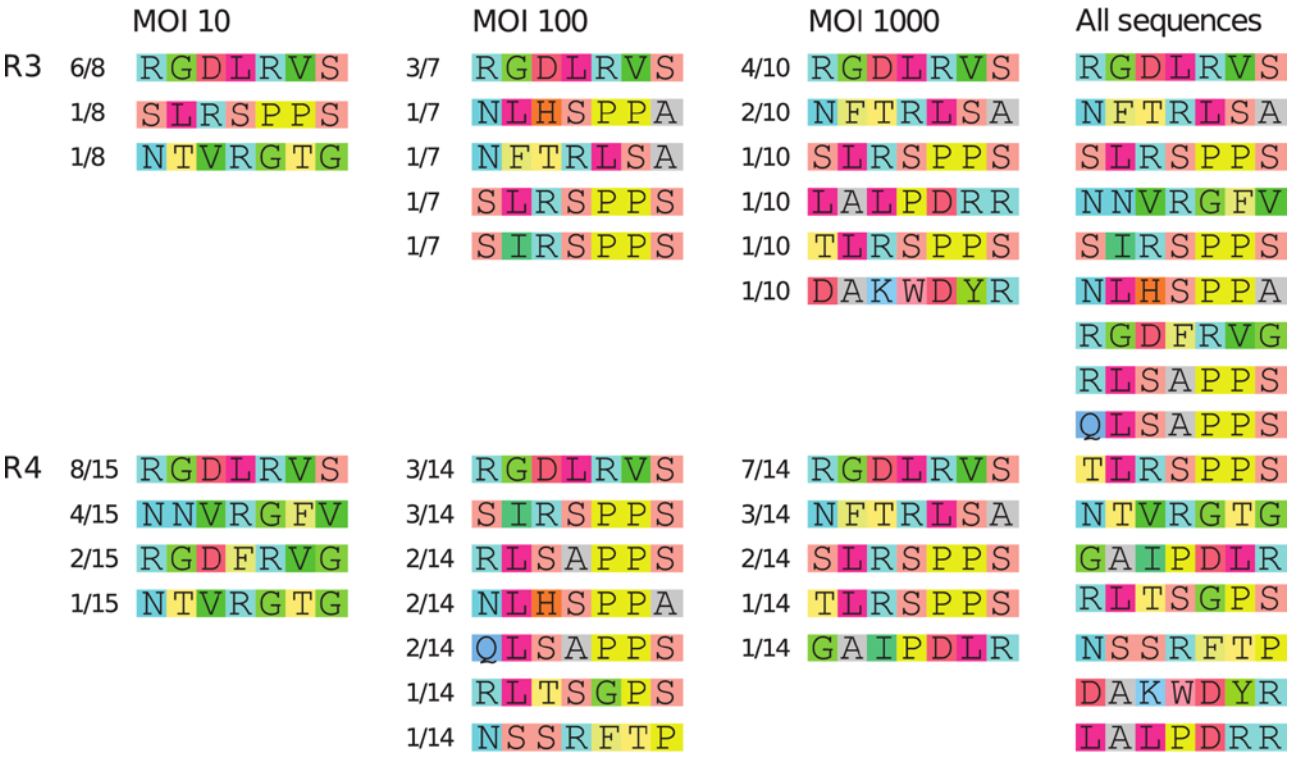

Figure III.D-2: Peptide sequences detected after selection of the AAV9 random peptide library on HCAEC. Nucleotide sequences from independently assigned clones were translated into protein sequences using Geneious software and amino acids were highlighted in unique colours. Peptide sequences are displayed as amount of peptides/total analysed clones each applied MOI (gc/cell). A compilation of all detected peptides is shown in "All sequences" in a most to less abundant fashion, top to bottom. R3, R4 = selection round 3, 4.

III.E *In vitro* efficiency of AAV9 vectors displaying enriched peptide sequences

The efficiency of a targeted vector system is the first of three parameters that determines its quality as a gene transfer vector. The enrichment of library variants after 3-4 selection rounds does not reflect the effective transduction efficiency they would confer to an AAV vector since a strong enrichment reflects a good virus uptake but not necessarily a good intracellular processing. Selection of an AAV2 random peptide library on HCAEC yielded peptides with high abundances (NSSRDLG, NSVSSIA) after three selection rounds but the less represented NDVRAVS conferred to AAV2 vectors the highest transduction efficiencies of HCAEC[195].

Therefore, investigation of more and less abundant peptide sequences is advisable. As a second selection criterion the sequence of enriched peptides was considered. Below, an assortment of several enriched peptides were characterized by vector titre and transduction efficiency on HCAEC.

III.E.1 Vector production efficiency

Mutant AAV vectors harbouring an EGFP reporter gene controlled by the Cytomegalovirus promoter (CMV) were produced by transfection of plasmids pDGΔVP providing Ad-helper genes, dsAAV-CMV-EGFP providing the CMV-EGFP expression cassette flanked by ITRs and p5E18-VD2/9-*SfiI*1759 (or pMT-187-XX2) that provide *rep*2 and *cap*9 (*cap*2) ORFs with oligonucleotide insertions enabling expression of peptide heptamers behind amino acid residue 588 (AAV2) and 589 (AAV9), respectively (Chapter II.B.4.2). For a better comparison, the titres of vector productions were normalized to the amount of genome copies obtained from a single producer cell (gc/cell).

Independent of serotype, wild type vectors yielded the highest titres of 2E+4 gc/cell (Table III.E.1) translating into absolute titres of 1E+12 gc obtained from 5E+7 HEK 293T cells (10 dishes, small gradient, see Chapter II.E.1). AAV9 vectors containing peptide inserts ranged from 5.8E+3 to 1.4E+4 gc/cell. The titre of only one AAV9 vector that displayed peptide sequence SDLRRGV was reproducibly below 1.0E+3 gc/cell (5E+10 gc) and its production was upscaled to 5E+8 cells (20 dishes) to meet the requirements described in Chapter III.A.2. Peptide SDLRRGV represents a randomized sequence of peptide RGDLRVS, the most prominent peptide after four selection rounds of the AAV9 library on HCAEC (Figure III.D-2). SDLRRGV has not been subjected to selective pressure and probably reduces the stability of AAV9 vectors it is displayed on, thus creating lower vector titres. However, this did not happen for peptide PSLPSRS (1.1E+4 gc/cell) that represents a randomized sequence of enriched SLRSPPS. The titres of AAV2 vector productions employed in this study were generally slightly lower. Together, peptide displaying AAV9 vectors yield genomic titres about 0.5 log steps below their wild type counterpart, a result comparable to AAV2 vectors, proving that display of peptide heptamers behind VP1 capsid residue 589 does not impair packaging efficiency of AAV9 vectors.

Table III.E.1 Productions of mutant AAV vectors and their titres

Peptide	AAV2 vectors (gc/cell)	AAV9 vectors (gc/cell)
Wild type	2.0E+4	2.0E+4
NDVRAVS	2.4E+3	9.4E+3
NSSRDLG	2.6E+3	8.2E+3
NSVSSAS	1.0E+3	9.4E+3
SLRSPPS	7.8E+3	1.2E+4
RGDLRVS	7.2E+1	7.6E+3
NLHSPPA	1.2E+3	1.5E+4
TEWDQPF	-	1.0E+4
RGDFRVG	-	6.4E+3
NNVRGFV	-	5.8E+3
NFTRLSA	-	8.0E+3
SIRSPPS	-	1.2E+4
SDLRRGV	-	1.3E+3
PSLPSRS	-	1.1E+4

III.E.2 Transduction efficiency

A total of seven enriched peptide sequences detected after the third and fourth selection round were chosen for a closer characterisation: RGD$^{LRVS}/_{FRVG}$, $^{SLR}/_{SIR}$SPPS, NFTRLSA, NNVRGFV and NLHSPPA. To assess the potential of enriched peptides to transduce HCAEC or H5V, a murine malignant hemangiosarcoma endothelial cell line derived from heart capillaries, cells were exposed to vectors from the same stock and transduction efficiencies were compared to those of wtAAV9, AAV9-NDVRAVS, as well as to AAV9-TEWDQPF, which displays a random (non-selected) control peptide (Chapter II.F.2, code 6). In case of HCAEC, two independent vector stocks each construct were assayed in duplicate to compensate fluctuations in transduction efficiency among different productions. WtAAV9 and AAV9-TEWDQPF vectors showed a very low (2.3±1.6%) to absent transduction of HCAEC at MOI 1E+4 gc/cell. In contrast, AAV9-NDVRAVS improved transduction efficiency to 58.4±5.1% (Figure III.E.2 **A**). Almost all mutant AAV9 vectors displaying any of the selected peptides significantly outperformed endothelium-targeting NDVRAVS vector at MOIs 1E+3 ($p < 0.05$) and 1E+4 gc/cell ($p < 0.001$), except NFTRLSA and NNVRGFV which showed no significant differences to NDVRAVS at MOI 1E+3 gc/cell. Peptides $^{SLR}/_{SIR}$SPPS and NLHSPPA enabled by trend the highest transduction efficiencies at MOI 1E+4 gc/cell when compared to the other enriched peptides.

A reduction of applied vector dose could be achieved with mutant AAV9 vectors on HCAEC. The most efficient peptide SLRSPPS yielded at MOI 1E+3 gc/cell efficiencies of 46.8±25.8% on HCAEC, a cell type that is refractory to wtAAV transduction and normally requires higher vector does for efficient transduction[195,201]. In contrast, transduction efficiencies of H5V were far below those detected for HCAEC, although no significance could be calculated, since only one attempt was undertaken for each construct and MOI (Figure III.E.2 **B**).

The results obtained so far point out several aspects. *In vitro* selection of an AAV9 library on HCAEC yields peptides that outperform transduction efficiency of wtAAV9 and, more important, of the most potent peptide NDVRAVS obtained by selection of an AAV2 library on HCAEC. It's worth mentioning that AAV9-NDVRAVS tested here has an efficiency similar to AAV2-NDVRAVS (Chapter III.B.2.2) and thus both vectors can be compared directly. Furthermore, no correlation could be detected between abundance of a peptide after several selection rounds and the transduction efficiency it confers to the vector. Less represented SLRSPPS yielded significantly ($p < 0.01$) higher efficiencies than most abundant peptide RGDLRVS, an observation that has been also made for AAV2-NDVRAVS and most abundant peptides AAV2-NSSRDLG/NSVSSIA[195]. Due to this outcome, most abundant or most efficient peptide RGDLRVS and SLRSPPS, respectively, were regarded as the most interesting selected peptides in this study.

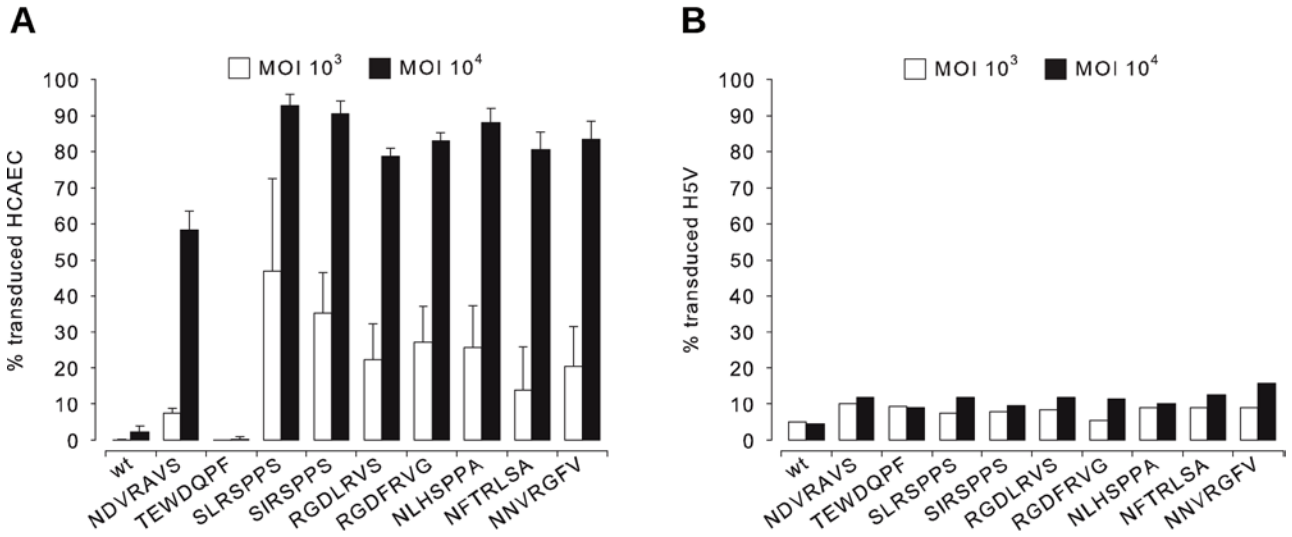

Figure III.E.2: Transduction efficiencies of wild type and mutant scAAV9-CMV-EGFP vectors. (**A**) HCAEC (**B**) H5V. CMV-EGFP bearing wild type and mutant vectors displaying enriched peptides behind VP1 residue 589 were exposed at MOIs 1E+3 (white bars) or 1E+4 (black bars) gc/cell for 48 h and transduction efficiencies were determined by flow cytometry. Besides peptide NDVRAVS (positive control) from selection of an AAV2 library on HCAEC and a non-selected random peptide TEWDQPF (negative control), seven other peptides were chosen based on their frequency of occurrence. Efficiencies for HCAEC are given in % EGFP-positive cells as means + SD (n = 4, two independent vector productions) and efficiencies for H5V are given in % EGFP-positive cells as single values.

III.F. *In vitro*-specificity of AAV9 vectors displaying enriched peptide sequences

The improvement of AAV9 transduction by display of endothelium-targeted peptide sequences raised the question whether also cell specificity, the second crucial parameter that determines the quality of a gene therapy vector, would be increased. Cell specificity can largely be obtained when the displayed peptide retargets AAV towards a cell surface receptor expressed uniquely on the target cell, since a receptor commonly expressed on several cell types will broaden AAV tropism.

III.F.1 Target cell specificity

Transduction efficiencies of wild type and mutant AAV9 vectors displaying SLRSPPS and RGDLRVS were assessed on several cell types (Chapter II.F.2, code 7). At a MOI of 2.5E+3 gc/cell, wtAAV9 vectors showed efficiencies of below 10% on primary cells (HCAEC, HCASMC) or cell lines (HEK 293T, HeLa, 911 and HepG2). Both, AAV9-SLRSPPS and AAV9-RGDLRVS increased transduction efficiencies of other cell types as they did for HCAEC, although to a different degree depending on the inserted peptide. Remarkably, transduction patterns of AAV9-SLRSPPS and AAV9-RGDLRVS correlated with the type of the investigated cells. AAV9-SLRSPPS significantly ($p < 0.01$) outperformed AAV9-RGDLRVS on primary cells (HCAEC, HCASMC) while AAV9-RGDLRVS showed higher transduction efficiencies on cell lines ($p < 0.01$ for HEK 293T, HeLa, and HepG2; $p < 0.05$ for 911). Overall, AAV9-SLRSPPS seems to be more specific to HCAEC than AAV9-RGDLRVS. Nonetheless, retargeting of AAV9 vectors towards HCAEC by display of foreign selected peptides on the capsid surface does not restrict *in vitro* tropism, probably because vector mutants target cellular surface receptors commonly expressed on several cell types.

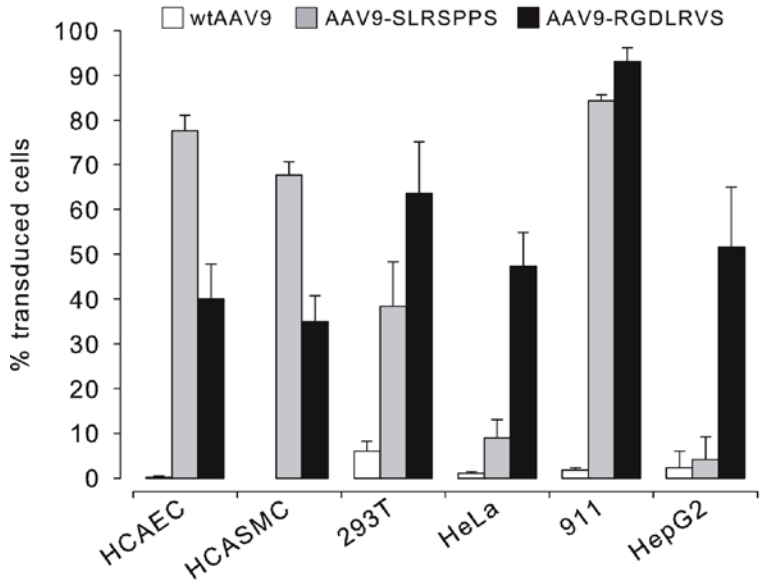

Figure III.F.1: Transduction efficiencies of wild type and two scAAV9-CMV-EGFP mutants of different cells. CMV-EGFP bearing wild type and mutant vectors AAV9-SLRSPPS and AAV9-RGDLRVS were applied for 48h at MOI 2.5E+3 gc/cell and transduction efficiencies of primary (HCAEC, HCASMC) or immortalized cells (HEK 293T, 911, HeLa, HepG2) were determined by flow cytometry. Efficiencies are given in % EGFP-positive cells as means + SD (n=4, two independent vector productions).

III.F.2 Improvement of target cell specificity by transcriptional targeting

Transgene expression limited to the desired cell type is of high interest, since the broad tropism of AAV promotes gene delivery to foreign tissues and could entail deleterious, even toxic effects. Given that restriction of AAV9 tropism towards HCAEC by retargeting is insufficient, control of transgene expression can be exercised by the use of cell- or tissue-specific promoters. The non-regulated CMV promoter used to control EGFP expression in this study is inadequate for transcriptional targeting, in that it is constitutively activated in multiple cell types. In the past, a set of murine and human endothelium-specific promoters have been characterized (reviewed by[232]). Robust transgene expression obtained from the 313 bp fragment of the murine VE-cadherin promoter in bovine aortic ECs (BAEC) but not in murine fibroblasts (NIH-3T3)[233] and availability of a plasmid source containing the entire VE-Cadherin promoter (EMBL databank accession no. Y10887) favoured the choice of this promoter as a candidate for transcriptional targeting in HCAEC.

To enforce endothelium-specific EGFP expression, the CMV core promoter was replaced by the 163 bp fragment containing the basal transcriptional machinery or the 313 bp fragment containing additionally the major specific inhibitory region of the VE-Cadherin promoter (Chapter II.F.3). However, the CMV enhancer element was not removed and potentially acted also in combination with the 163/313 bp fragments. CMV, 163, or 313-EGFP expression cassettes were packaged into an AAV9 vector that displayed peptide SLRSPPS, which is regarded as the most potent peptide of the present study (Figure III.E.2 **A**). The level of transgene expression was then analysed on AAV9-SLRSPPS permissive primary (HCAEC, HCASMC) or immortalized cells (HEK 293T, 911; Chapter II.F.2, code 8). Transgene expression directed by both the 163 bp and the 313 bp fragment occurred by trend at slightly elevated levels compared to CMV in HCAEC, however their activity in non-ECs could not be completely downregulated (Figure III.F.2). EGFP-expression levels driven by the 163/313 bp fragments in human coronary artery smooth muscle cells were similar to CMV and robust expression was also present in immortalized cells (HEK 293T, 911), although at a ~50% reduced efficiency in case of the 163 bp fragment. Taken together, the employment of the short 163 bp or 313 bp fragments from murine VE-cadherin promoter yielded only poor improvement of endothelium-specific transgene expression over CMV, however, their size may be advantageous in contrast to CMV, since they occupy less space within the transgene expression cassette, leaving more space for larger transgenes.

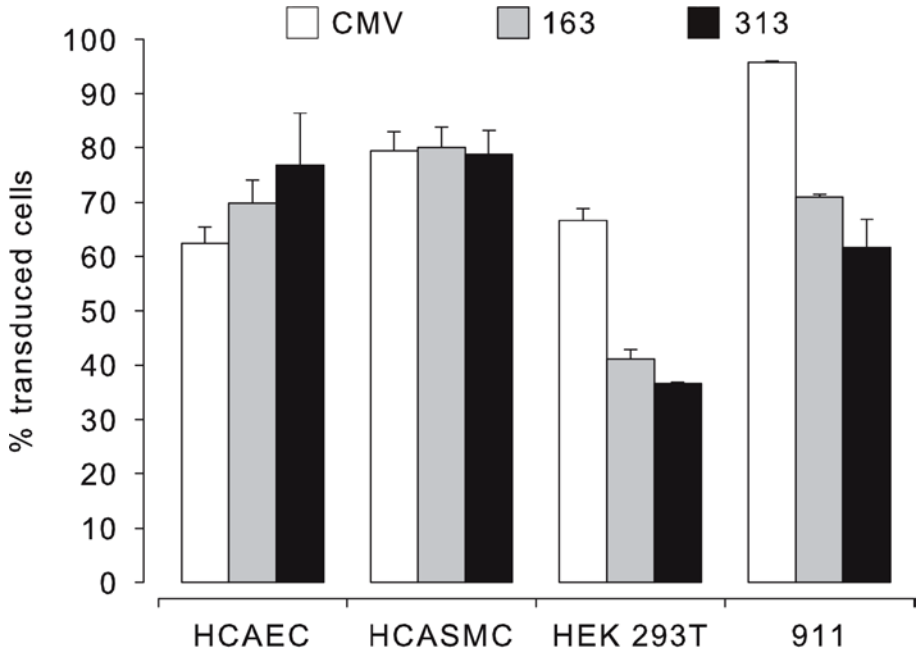

Figure III.F.2: Transcriptional targeting of HCAEC by the murine VE-cadherin promoter. The transcriptional activity of the 163 bp and the 313 bp fragment of the murine vascular endothelial (VE) cadherin promoter was compared to the CMV promoter on primary cells (HCAEC, HCASMC) or cell lines (HEK 293T, 911). Cell types were chosen according to their susceptibility towards the AAV9-SLRSPPS vector (see Chapter III.E.3) that packaged either the CMV-EGFP or the 163/313-EGFP expression cassettes containing the CMV enhancer region. Exposure of cells took place at MOI 2.5E+3 gc/cell for 48 h. The 163 bp fragment of the VE-cadherin promoter contains the basal transcriptional machinery and the 313 bp fragment additionally the major specific inhibitory region necessary for endothelium-specific activation. Efficiencies are given in % EGFP-positive cells as means + SD (n = 3).

III.G Serotype specificity of AAV vectors displaying enriched peptide sequences

The selection of a randomized peptide heptamer library displayed on the AAV2 capsid surface on HCAEC yielded peptides that improved AAV2 and AAV9 vector transduction of this cell type over both wild types (Chapter III.B.2.2 and[195]). This raised the question whether display of peptides derived from selection of AAV2 libraries on the AAV9 capsid would not be sufficient for AAV9 retargeting towards endothelium, avoiding a laborious and expensive generation and selection of an AAV9 library. An attempt to answer this question was posed by analysis of transduction efficiencies from vectors of either serotype that displayed peptides derived from AAV2 and AAV9 library selections on HCAEC. A set of peptides selected in the context of an AAV2 library[195] or the AAV9 library on HCAEC were chosen according to highest abundance after 3-4 selection rounds or highest efficiency (Table III.G). The peptides were cross-displayed on AAV2 or AAV9 CMV-EGFP vectors behind VP1 residues 588 or 589, respectively, and transduction of HCAEC using parameters described in Chapter II.F.2 (code 10) was analysed by flow cytometry. Below, library source (**X**) and vector serotype context (**Y**) of peptides are given as "**X**-peptide-**Y**".

Table III.G: List of most abundant/efficient peptides from AAV2/AAV9 library selections on HCAEC

	AAV2 library selection	AAV9 library selection
Most abundant peptides	NSSRDLG, NSVSSAS	RGDLRVS
Most efficient peptides	NDVRAVS	SLRSPPS, NLHSPPA

Either serotype showed as usual basal transduction efficiencies of HCAEC below 10% (Figure III.G). Overall, **9**-peptides-**9** yielded higher transduction efficiencies of HCAEC when compared to **2**-peptides-**2**. Most importantly, **9**-peptides-**9** significantly ($p < 0.01$) outperformed **2**-peptides-**9**, proving the advantage of an AAV9 library selection. In contrast, **9**-peptides-**2** yielded very low to absent transduction and **2**-peptides-**9** performed similarly to **2**-peptides-**2**, as seen in case of NSSRDLG and NSVSSAS, which represent the peptides with the highest abundance after a three round AAV2 library selection. An unexpected outcome was represented by cross-display of the most potent peptides from both AAV-library selections, NDVRAVS and SLRSPPS. The efficiency of **9**-SLRSPPS-**2** was absent, while **2**-NDVRAVS-**9** yielded results similar to **2**-NDVRAVS-**2** (see also Figure III.B.2.2). This outcome substantiates that the peptides are not solely responsible for the modulation of transduction efficiency but depend on the capsid context of the serotype they are displayed on.

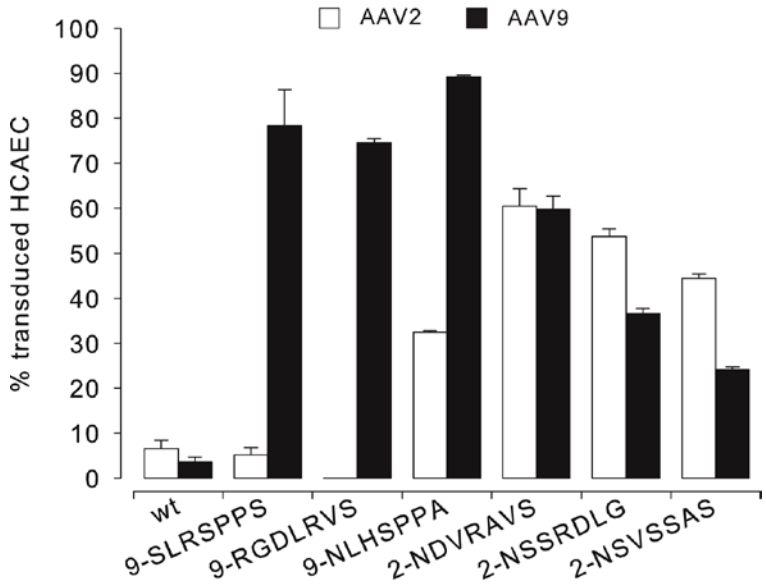

Figure III.G: Transduction efficiencies of AAV2 and AAV9 cross-displayed peptides. Most abundant and most efficient peptides yielded by selection of AAV2 or AAV9 peptide libraries on HCAEC were chosen and cross-displayed on AAV2 or AAV9 vectors behind VP1 residues 588 and 589, respectively. The library source of a peptide is indicated with a 2 or a 9 prefix and the vector serotype the peptides are displayed on is given in the legend. HCAEC were exposed to vectors at MOI 5E+3 gc/cell for 48 h and transduction efficiencies analysed by flow cytometry are given in % EGFP-positive cells as means + SD (bars, n = 3).

III.H *In vitro* immune evasion of AAV9 vectors displaying enriched peptide sequences

The third quality-related parameter of a gene transfer vector is reflected by its ability to evade neutralization by host immune system. Pre-existing antibodies within human or animal serum sensitively alter the outcome of a gene transfer attempt by binding to AAV capsids and impairing transduction of target tissue. Removal of antigenic epitopes from surface-exposed capsid domains could represent a solution to this issue. In contrast to AAV9, epitopes of several binding and neutralizing antibodies have been mapped for AAV2 assigning them to more exposed structures of the capsid surface[174,173]. It is therefore imaginable, that insertion of foreign peptides at the exposed AAV9 capsid site including VP1 residue 589 not only affects targeting and transduction efficiency but also recognition by neutralizing antibodies. To test this hypothesis, the effect of antisera on transduction efficiency of a set of wild type and mutant AAV vectors was analysed *in vitro*. HEK 293T cells are well permissive for wtAAV2, mutants AAV9-SLRSPPS/RGDLRVS and to a lesser extent also for wtAAV9 (Figure III.F.1) and thus were adducted as a cell model. Intravenous immunoglobulin (IVIG), pooled human antisera on the one hand, and ADK9, a murine monoclonal antibody raised against wtAAV9 capsids on the other, were pre-incubated with vectors at several dilutions. Subsequently, cells were exposed to pre-treated vectors (Chapter II.F.4). Present or absent transduction efficiencies were regarded as reciprocal neutralization values, whereas vector transduction in absence of neutralizing antibodies was set to 100% (controls). As a threshold, neutralization of transduction was assumed when transduction efficiency of samples treated with IVIG or ADK9 was reduced by 50% to that of controls.

WtAAV2 and AAV2-NDVRAVS vectors that displayed in absence of IVIG transduction efficiencies of >98%, were neutralized throughout the entire range of dilutions (Figure III.H **A**). Similarly, wtAAV9 vectors were neutralized by both, IVIG and ADK9 up to dilutions of 1:1280. However, AAV9 mutants SLRSPPS and RGDLRVS improved *in vitro* antibody evasion over wtAAV9, wtAAV2 and AAV2-NDVRAVS about four and eight times, respectively, (~1:320 and ~1:160, Figure III.H **A**) and were only affected by IVIG (Figure III.H **A, B**). These results suggest that besides an efficient endothelium-targeting, the AAV9 vectors displaying selected peptides also confer improved (*in vitro*) evasion from neutralizing antibodies, rendering AAV9 more suitable as a serotype backbone for targeted peptide display than AAV2.

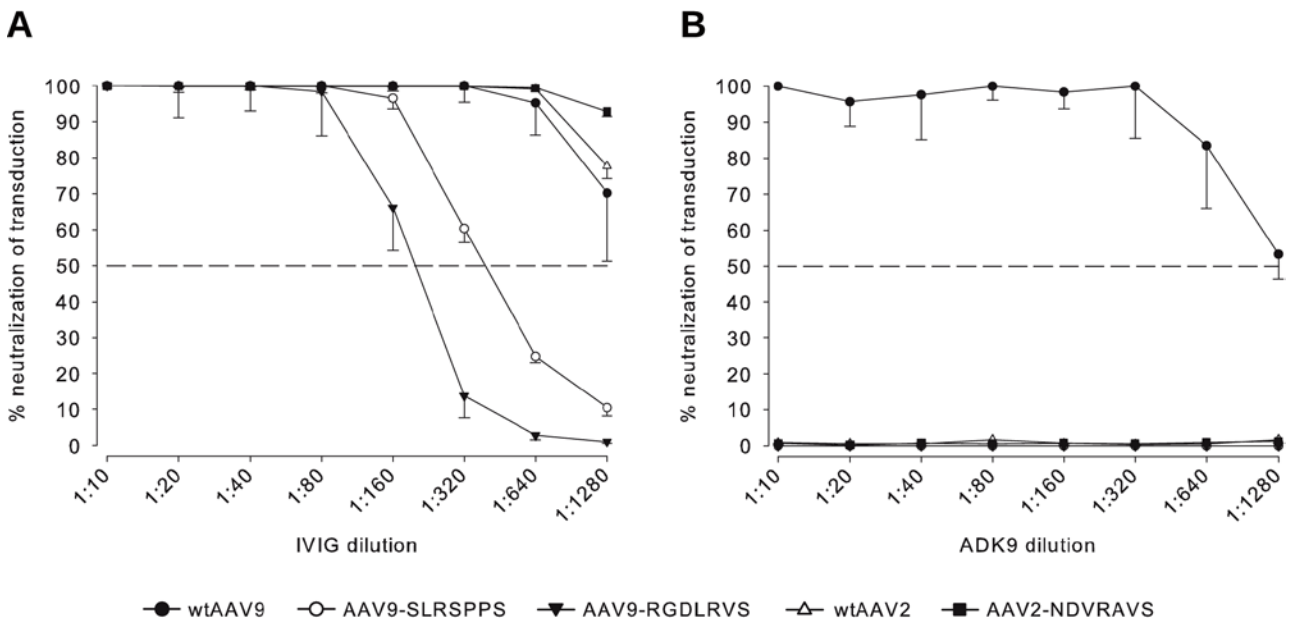

Figure III.H: Neutralization of AAV-transduction by IVIG or ADK9. HEK 293T cells were exposed for 48 h to wild type or mutant scAAV-CMV-EGFP displaying SLRSPPS, RGDLRVS or NDVRAVS at MOI 1E+4 gc/cell. Vectors were previously treated with serial dilutions of IVIG (**A**) or ADK9 capsid antibody (**B**). Neutralization of transduction was assumed when efficiency dropped below 50% of values obtained with vectors in absence of serum or antibody (not shown). Efficiencies determined by flow cytometry (% EGFP-positive cells) were calculated as means - SD (n=3) and are shown here as reciprocal % neutralization of transduction - SD. The dilution of IVIG or ADK9 at which immune escape has occurred by definition can be extrapolated at the intersection of continuous and dashed lines (50% threshold).

III.I. Secondary characterisation of endothelium-targeted peptides

The results obtained so far from transduction experiments involving AAV vectors that display endothelium-targeted peptides pointed out some interesting aspects: (I) AAV9-SLRSPPS and AAV9-RGDLRVS vectors selected in this study showed differential transduction efficiencies when incubated with different cell types (Figure III.F.1). Primary cells were transduced more efficiently by AAV9-SLRSPPS while immortalized cells showed a higher permissiveness towards AAV9-RGDLRVS. This finding, together with the disparity of the peptide sequences raised the impression of a differential transduction pathway, that was closer characterized using a capsid competition assay. (II) Also the differential transduction pattern of different cell types these two peptides confer to AAV9 attracted attention to arginines present within their sequences. AAV9 does not possess arginine residues within VR VIII (Figure III.B.1-2) but gains them by displaying the peptides. Thus, the hypothesis of an AAV9 retargeting towards HSPG, the attachment receptor of arginine-bearing AAV2, was analysed using a competition assay with soluble heparin.

III.I.1 Modulation of transduction in presence of a competing vector

The successful transduction of a cell depends on pre- and post-entry efficiency of vectors. On the pre-entry part, the rate of endocytosis is regulated both by capsid properties that influence the binding of the vector to one or more dedicated cell receptor(s) and the abundance of the receptor(s) on the cell surface. On the post-entry part, the capsid is the main factor determining the intracellular processing efficiency of the vector. Thus, vectors based on two different capsids can exploit diverse starting points or pathways for efficient transduction, that are not mutually exclusive. The disparity of SLRSPPS and RGDLRVS peptides that conferred to AAV9 vectors a differential transduction pattern of several cell types prompted a closer investigation of whether the vectors would use identical or different pathways. To elucidate the differences, a competition assay using both vectors was performed. Competition occurs only when the vectors use a common pathway or parts of it, for instance extracellular receptors or checkpoints involved in intracellular processing. A vector supplied in excess, i.e. the **competitor**, will out-compete the **analyte** vector upon targeting the same pathway, thus exhibiting superior transduction or lowering that of the analyte, but will not interfere in case completely different transduction pathways are employed. In the present case the readout was focused on the analyte whose uptake in to the cell would be lowered in case of a common pathway usage. To enable distinguishing, the analyte vector encapsidated a CMV-EGFP expression cassette, while the competitor packaged a non-fluorescent CMV-EGFPΔG67 transgene (Chapter II.F.5). Thus, only cell transduction originating from analyte vectors was measured by flow cytometry.

The hypothesis of differential transduction pathway usage of AAV9-SLRSPPS and AAV9-RGDLRVS was analysed on HCAEC by assigning to either vector the role of the analyte supplied at MOI 5000 gc/cell or the competitor supplied at 25x-100x excess MOI. Transduction efficiencies of either analyte vector in absence of competitor were set to 100% (Figure III.I.1 **A**, white bars). First, the assay was validated by co-incubating analyte and competitor vectors with identical capsids using a 75x excess MOI for the competitor. Transduction in presence of competitor decreased from 100% to 58.2±3.8% for AAV9-SLRSPPS and 56.7±5.0% for AAV9-RGDLRVS, validating the assay (Figure III.I.1 **A**, light grey bars). Then, analyte vectors were co-incubated with 75x excess competitor vectors that displayed the scrambled sequences PSLPSRS and SDLRRGV, respectively. In contrast to the previous experiment, the transduction efficiency of analyte vectors was not significantly altered (Figure III.I.1 **A**, dark grey bars). This control experiment showed that the lowering of analyte transduction does not arise from unspecific steric inhibition exercised by massive competitor presence but rather is vector (or peptide sequence) specific. This outcome was further supported by the finding, that an increase of competitor excess from 25x to 100x gradually lowered transduction of HCAEC for both analytes to a certain point of saturation that was achieved at 75x excess (Figure III.I.1 **B**).

Importantly, co-incubations of analyte and competitor vectors with adverse capsids supplied at 75x excess lowered the transduction efficiencies to 60.8±2.8% for AAV9-SLRSPPS and 51.7±4.2% for AAV9-RGDLRVS, respectively (Figure III.I.1 **A**, black bars), proving a competition effect between these two mutants and the usage of a common pathway or parts of it.

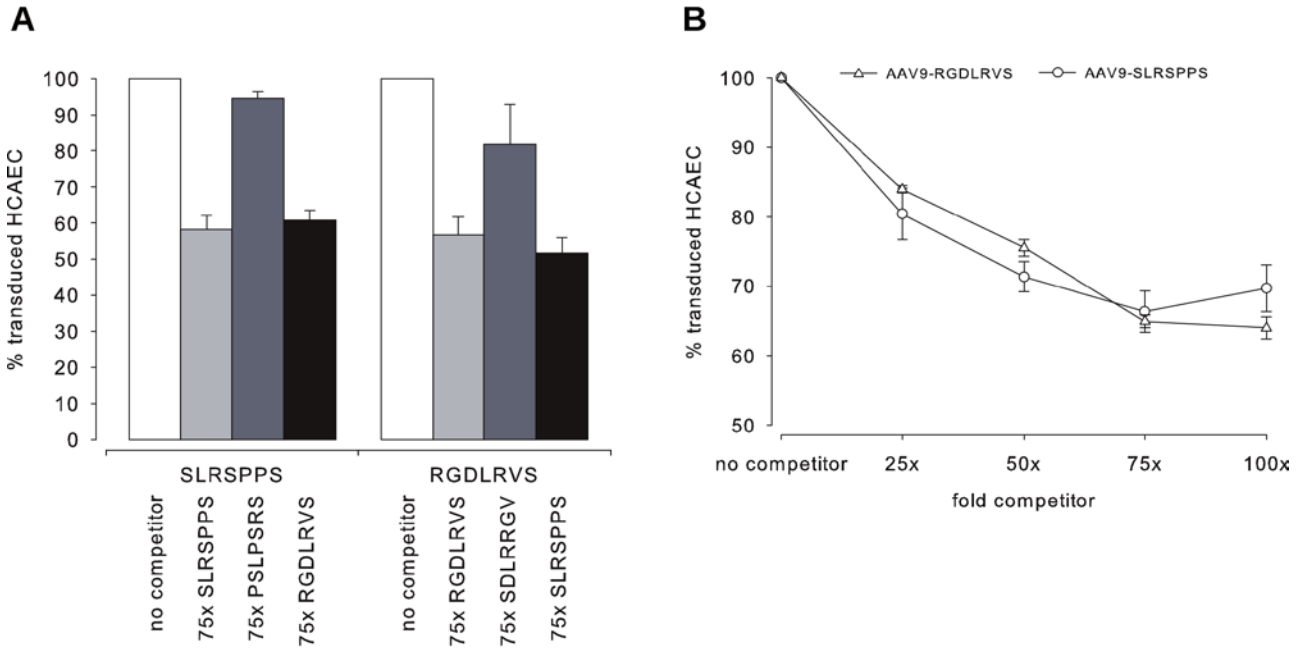

Figure III.I.1: Transduction efficiencies of mutant AAV9 vectors in presence of competitors. (**A**) Transduction efficiencies of analyte vectors displaying peptides SLRSPPS or RGDLRVS behind VP1 residue 589 were analysed on HCAEC. Each analyte was incubated at MOI 5000 gc/cell in absence (no competitor, transduction set to 100%) or presence of competitor vectors displaying SLRSPPS, scrambled peptides PSLPSRS and SDLRRGV or RGDLRVS supplied at 75x excess MOI. Co-incubations were terminated by medium exchange after 4 h and incubation in presence of fresh medium was continued *ad* 48 h. Transduction efficiencies were analysed by flow cytometry and are given in % EGFP-positive cells as means + SD (bars, n = 3). (**B**) AAV9 analyte vectors displaying SLRSPPS and RGDLRVS were co-incubated in absence (no competitor, transduction set to 100%) or presence of competitor vectors displaying RGDLRVS and SLRSPPS, respectively, supplied at 25x-100x excess MOI and data was evaluated as in (**A**). Dots represent means ± SD (n = 3).

III.I.2 Modulation of transduction in presence of soluble heparin

In case of AAV2, a cluster of several basic arginines, R588 among them, represent binding sites for HSPG receptor. Mutants lacking one or several of these arginine residues exhibit a lowered infectiousness[91,90]. As both, SLRSPPS and RGDLRVS deliver arginine residue(s) to the otherwise arginine-negative AAV9 capsid at this site, the question arose whether the enriched peptides could have retargeted AAV9 to the HSPG receptor. To answer this question, HCAEC and HepG2 cells were exposed to wild type or mutant AAV9 displaying SLRSPPS or RGDLRVS in presence or absence of solute heparin.

HCAEC is only poorly permissive for transduction by both serotypes (< 10%, Figure III.I.2, EC). Since HepG2 (Hep) is expressing HSPG, wtAAV2 in contrast to wtAAV9 efficiently transduced this cell type in the absence of heparin (94.8±1.5%) but failed to do so in its presence. Heparin did not alter the transduction patterns of SLRSPPS on any cell type but did for RGDLRVS to a small, but significant extent ($p < 0.05$ for HCAEC and $p < 0.01$ for HepG2). In case of SLRSPPS and probably also RGDLRVS, the gain-of-arginines through display of selected peptides does not retarget AAV9 towards a HSPG-dependent transduction pathway.

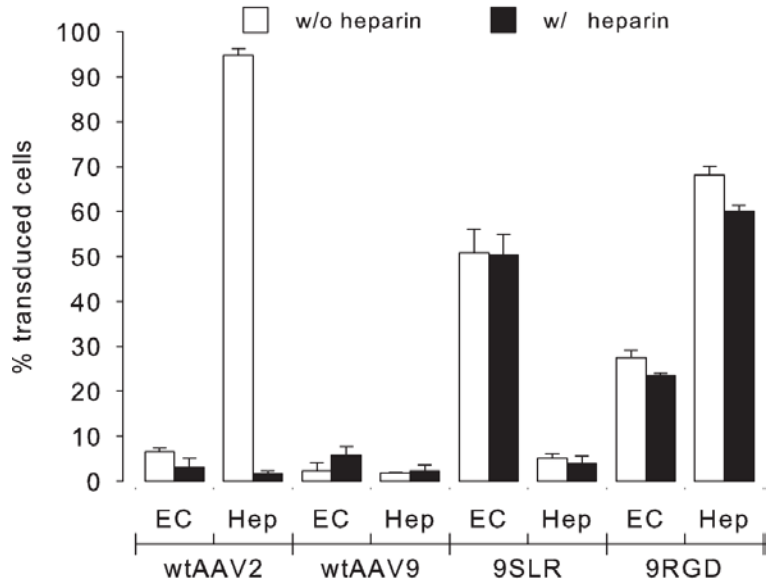

Figure III.I.2: Transduction of cells by wild type and mutant AAV vectors in presence or absence of heparin. Wild type AAV2 or wild type and mutant AAV9 vectors displaying peptides SLRSPPS (9SLR) and RGDLRVS (9RGD) behind VP1 residue 589 were incubated at MOI 5E+3 gc/cell with HCAEC (EC) or HepG2 (Hep) in presence or absence of 210 IU solubilised heparin. Exposure was terminated after 4 h and cells were incubated *ad* 48 h in presence of fresh medium. Transduction efficiencies were analysed by flow cytometry and are given in % EGFP-positive cells as means + SD (bars, n = 3).

III.J *In vivo* efficiency of AAV9 vectors displaying enriched peptide sequences

In vitro-selection of the AAV9 library on HCAEC yielded vector AAV9-SLRSPPS, that in combination with the short 163 bp fragment of the murine VE-Cadherin promoter could represent a powerful tool for *in vitro* gene transfer studies on ECs. However, the promising results obtained so far on cultivated ECs can not be extrapolated to cells embedded in their natural context of a blood vessel. The most evident difference between the cultivated and naturally occurring ECs is their state of proliferation: cultivated ECs divide, naturally occurring ECs remain under normal circumstances quiescent. Also, the artificial environment cultivated cells are exposed to poorly mimics the context of a blood vessel with mural cells blood components interacting with the EC monolayer. This differences may affect the *in vivo* transduction of ECs by AAV.

To elucidate the feasibility of this study's endothelium-targeted vectors *in vivo*, an adequate model had to be chosen. A broad palette of animal models and evaluation techniques has been developed in the past for preclinical studies on AAV vector transduction. Due to lower overall costs, broad availability, easy handling and low-dosed vector application by tail vein injection, mice were favoured over other animals in this study. Several evaluation tools were considered: *in vivo*-imaging of whole organ transduction in live animals, analysis of isolated and sectioned organs by immune-histochemistry (IHC) and real-time PCR-quantification of vector genomes isolated from organs. These techniques allow reliable investigation of AAV transduction, albeit with a certain detection limit that strongly depends the amount of present vector genomes. However, the low number of ECs that are widely disseminated throughout the filigree vascular system of a mouse and a difficult isolation in sufficiently high amounts might easily undercut the detection limits of the mentioned techniques rendering them less suitable for the present study. Additionally, the poor transduction efficiency of H5V using AAV9 vectors displaying selected peptides at the high MOI of 1E+4 gc/cell (see Figure III.E.2 **B**), could point out a low transduction efficiency of murine ECs, further impairing evaluation. Therefore, a technique was employed that allowed a more direct visualisation of endothelium.

III.J.1 *In situ*/*in vivo* transduction of murine endothelium

Due to the low thickness and good accessibility of the murine mesenteric artery branches (*Arteria mesenterica*), easy vessel isolation and direct visualisation of stained murine mesenteric artery endothelial cells (MMAEC) by fluorescence microscopy is possible. This is advantageous, since chemical or cryo-fixation of tissue usually needed for immunohistochemic (IHC) analysis can be avoided, leaving the physiological structure of endothelium unaltered. Healthy female NMRI mice were sacrificed and secondary branch artery pieces of ~5 mm length were excised (Chapter II.F.7.1). Exposure to leading vector AAV9-SLRSPPS or mock occurred immediately upon removal from mice in a myograph device by *in situ* perfusion of vessel pieces with 2.3E+9 gc/µl vector solution followed by a 48 h exposure. A detachment of endothelial tissue was observed from vector incubations that exceeded 48 h, determining the maximum possible maintenance time of endothelium in physiological condition *ex vivo*. After TRITC-labelled lectin counter-staining of MMAEC, transduction by vector was monitored using a fluorescence microscope. The presence of an endothelial layer within the blood vessel pieces was confirmed after 48 h treatment with vector or mock (Figure III.J.1, TRITC-lectin). However, no EGFP-fluorescence above background (mock, EGFP) could be detected in AAV9-SLRSPPS treated arteries (48 h, EGFP).

Assuming a successful transduction, 48 h exposure of endothelium to the vector may be sufficient for a proper uptake of vectors into the cells *in situ* but unfolding of EGFP expression strongly depends on rate-limiting post-entry processes like endosomal release, nuclear import and uncoating of the transgene and may require a prolonged time.

Since *ex vivo*-maintenance of endothelium for more than 48 h was not possible, mice were *in vivo*-exposed to mock or 4.6E+11 vector gc/animal AAV9-SLRSPPS vector by tail vein injection. Two weeks later the animals were sacrificed and transduction of mesenteric artery endothelium was analysed as shown above. Again, endothelium presence but no EGFP fluorescence could be detected in vessel pieces from mice treated with vector (results not shown). Although a low efficiency of the CMV promoter in quiescent ECs cannot be ruled out, this outcome, together with the poor transduction of H5V *in vitro* (Chapter III.E.2) points rather towards a low efficiency of AAV9-SLRSPPS in murine endothelium rather than to an inadequate dose or evaluation technique.

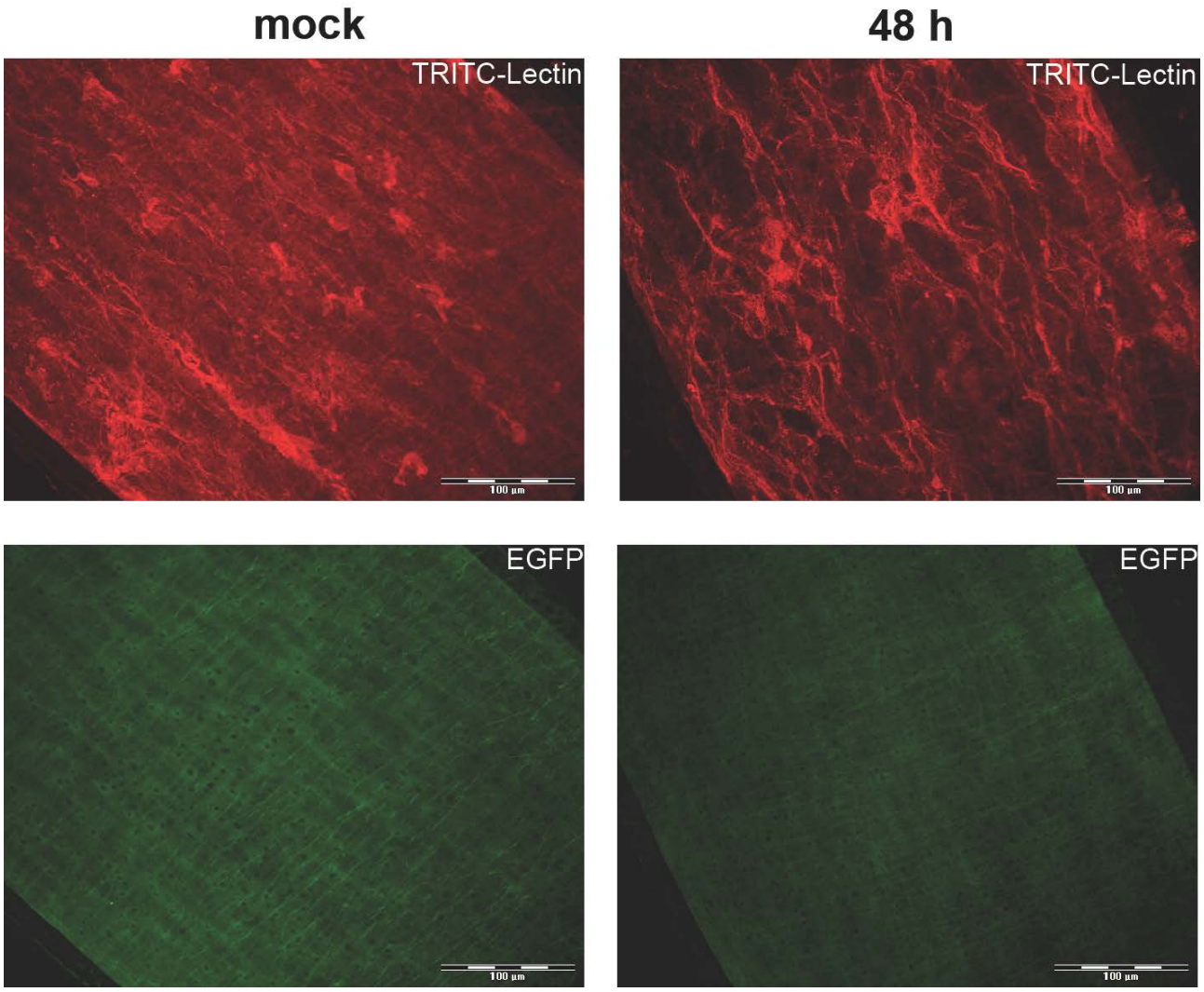

Figure III.J.1: *In situ* visualisation of murine mesenteric artery fragments treated with an AAV vector. Vessel pieces (~5 mm) were isolated from sacrificed female NMRI mice and were perfused with HCAEC medium containing 2.3E+9 gc/µl of a scAAV-CMV-EGFP vector displaying SLRSPPS or medium only (mock). After an exposure of 48 h, fragments were rinsed with 1x PBS and endothelium-counterstaining with TRITC-labelled lectin was performed. Red (TRITC) and green (EGFP) fluorescence were separately monitored with a fluorescence microscope at 20x magnification. The vessel margins can be recognized in the lower left and upper right corners of the images.

III.J.2 *In situ* transduction of human endothelium

The AAV9-SLRSPPS mutant vector developed in this study was efficient for *in vitro* transduction of human ECs but failed to transduce murine ECs *in vitro* (H5V) and *in situ* (MMAEC). The AAV9 library was selected on ECs of human origin and a specificity of vectors towards species is imaginable. Therefore, a new model based on the human umbilical vein (*Vena umbilica*) endothelium was assayed. Direct evaluation of longitudinal vein stretches by fluorescence microscopy as performed in the case of murine mesenteric arteries, however, was not possible due to the opaqueness and size of the umbilical vein. Thus, evaluation of transduction occurred by cryo-fixation and cross-sectioning of treated veins (Chapter II.F.7.2). Preliminary attempts reduced the *ex vivo* maintenance time to 24 h as longer incubations lead to a detachment and loss of endothelium. Endothelial tissue was exposed for 24 h to 4.3E+8 gc/cm vein AAV9-SLRSPPS bearing a CMV-EGFP expression cassette without separation of veins from cords, thus maintaining the natural environment of human umbilical vein endothelial cells (HUVEC) and avoiding endothelial damage. The endothelium was detectable after 24 h via TRITC-lectin counter-staining of cross-sectioned veins but no EGFP fluorescence was present (data not shown). *In vitro* transduction of human umbilical vein ECs (HUVEC) by AAV9-SLRSPPS was confirmed in a separate attempt (Figure III.J.2). Analogously to transduction of murine mesenteric artery endothelium it was assumed that unfolding of EGFP-expression may require more than 24 h. In a new attempt to detect *in situ*-transduction of HUVEC, umbilical veins were exposed only 2 h to wild type or mutant AAV9 vectors displaying SLRSPPS. After exposure, HUVEC were isolated from veins by dispase treatment and propagated *in vitro* for 4 d (Chapter II.F.7.2). The advantage of *in vitro* cultivation was a removal of non-adherent cells and an increase of available cell numbers for transduction analysis by flow cytometry, the method applied to analyse transduction of HUVEC.

First, the endothelial character of vector-untreated cells was confimred after isolation and *in vitro*-cultivation by flow cytometry using a FITC-conjugated PECAM-1 (CD31) antibody. CD31 is an endothelial marker also expressed on several other cell types like platelets, macrophages, granulocytes, lymphocytes, megakaryocytes, killer cells and neutrophils but not on other cell types of the vascular wall (vascular smooth muscle cells, pericytes). Over 99% of cultivated cells were $CD31^+$ (Figure III.J.2. **A**, green dots) proving their endothelial character. Moreover, no detectable contamination with $CD31^-$ mural cells was present in the analysed population.

To detect transduction by AAV9 vectors, *in situ*-exposure was performed as described above. After 4 d of *in vitro* propagation, isolated HUVEC (further referred to as *in situ*-exposed HUVEC) showed a high transduction efficiency of 80.3+11.9% from AAV9-SLRSPPS, in contrast to wtAAV9 which had an efficiency of below 1% (Figure III.J.2 **B**, grey bars). Due to an unknown amount of cells lining the umbilical veins, calculation of MOI was not possible but a high MOI can be expected at 4.3E+8 vector gc/cm vein.

A parallel *in vitro* transduction assay was performed by exposing HUVEC to AAV9-SLRSPPS at four different MOIs (further referred to as *in vitro*-exposed HUVEC; see Chapter II.F.2, code 9). Here, a correlation of applied MOI and increment of transduction efficiency was observed, that peaked at MOI 5E+4 gc/cell (Figure III.J.2 **B**, white bars). At this MOI, transduction of *in vitro* and *in situ*-exposed HUVEC were comparable.

To rule out *in vitro* transduction by vector contamination carry-overs into cell culture and to further strengthen the proof for *in situ* transduction, the presence of vector genomes in HUVEC isolated immediately after exposure to AAV9-SLRSPPS (as before) was attempted. The number of isolated cells was determined (see Chapter II.F.7.2) and vector genome copies from purified total DNA were quantified by qRT-PCR yielding a total of 148.7±45.8 gc/cell (Figure III.J.2 **B**, black dot within grey bar). Similarly, presence of vector genome copies/cell was analysed in *in vitro*-exposed HUVEC at different MOIs, resulting in detection of more copies/cell from higher MOIs (Figure III.J.2 **B**, black dots within white bars). A direct comparison of vector genome presence and transduction efficiency between *in vitro* and *in situ*-exposed HUVEC however can not be made, since in case of *in vitro*-exposed HUVEC the data was obtained from the same cell sample, while independent samples were used in case of *in situ*-exposed HUVEC.

The experiments within this chapter revealed that *in situ*-exposure to AAV9-SLRSPPS but not to wtAAV9 lead to transduction of HUVEC embedded in their natural context of a blood vessel. This experimental setup represents therefore a good approximation of what the vector would enable in an *in vivo* attempt. However, EGFP-expression from *in situ*-exposed HUVEC was observed only after isolation and *in vitro* propagation of cells but not within vasculature-embedded cells.

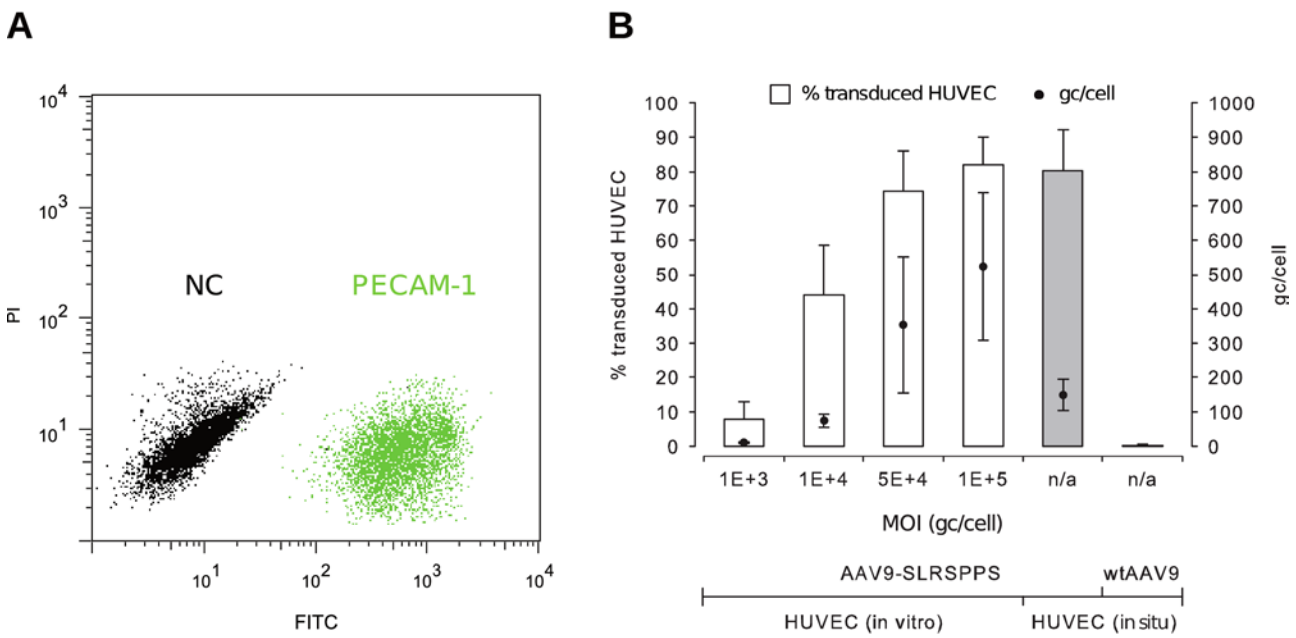

Figure III.J.2: *In situ* and *in vitro* transduction of human umbilical vein endothelial cells (HUVEC). (**A**) HUVEC were isolated by dispase treatment from umbilical veins and were propagated *in vitro* for 4 d. Endothelial character was confirmed by flow cytometric analysis of >10.000 cells treated with a FITC-conjugated human PECAM-1 antibody (n = 3). The representative PI-versus-FITC dot plot shows an overlay of treated (green dots) versus non-treated cells (black dots). A subset of antibody-treated $CD31^{-}$ cells would appear as green dots among the subset of black dots. Only live cells gathered at 10^1 RFI in the PI-channel were analysed for CD31-presence. (**B**) *In situ*-exposure of HUVEC to wtAAV9 or mutant AAV9 vectors displaying peptide SLRSPPS behind VP1 residue 589 occurred for 2 h at 4.3E+8 gc/cm umbilical vein. Both vectors packaged a CMV-EGFP expression cassette. After enzymatic isolation, cells were further propagated *in vitro* for 4 d. In another attempt, HUVEC were *in vitro*-exposed to AAV9-SLRSPPS only at various MOIs (X-axis) for 2 h and were further incubated in presence of fresh medium *ad* 48 h to allow unfolding of EGFP-expression. In either case, transduction was monitored by FACS analysis and efficiencies are given in % EGFP-positive cells as means + SD (grey bars for *in situ*, white bars for *in vitro*, n = 3 each). To determine the intracelular presence of vector genomes, HUVEC exposed to AAV9-SLRSPPS *in situ* or *in vitro* were counted, total DNA was isolated and vector genomes were quantified by qRT-PCR. The amount of genome copies/cell is presented as means± SD (black dots, n = 3, right Y-axis).

III.K Supplementary material

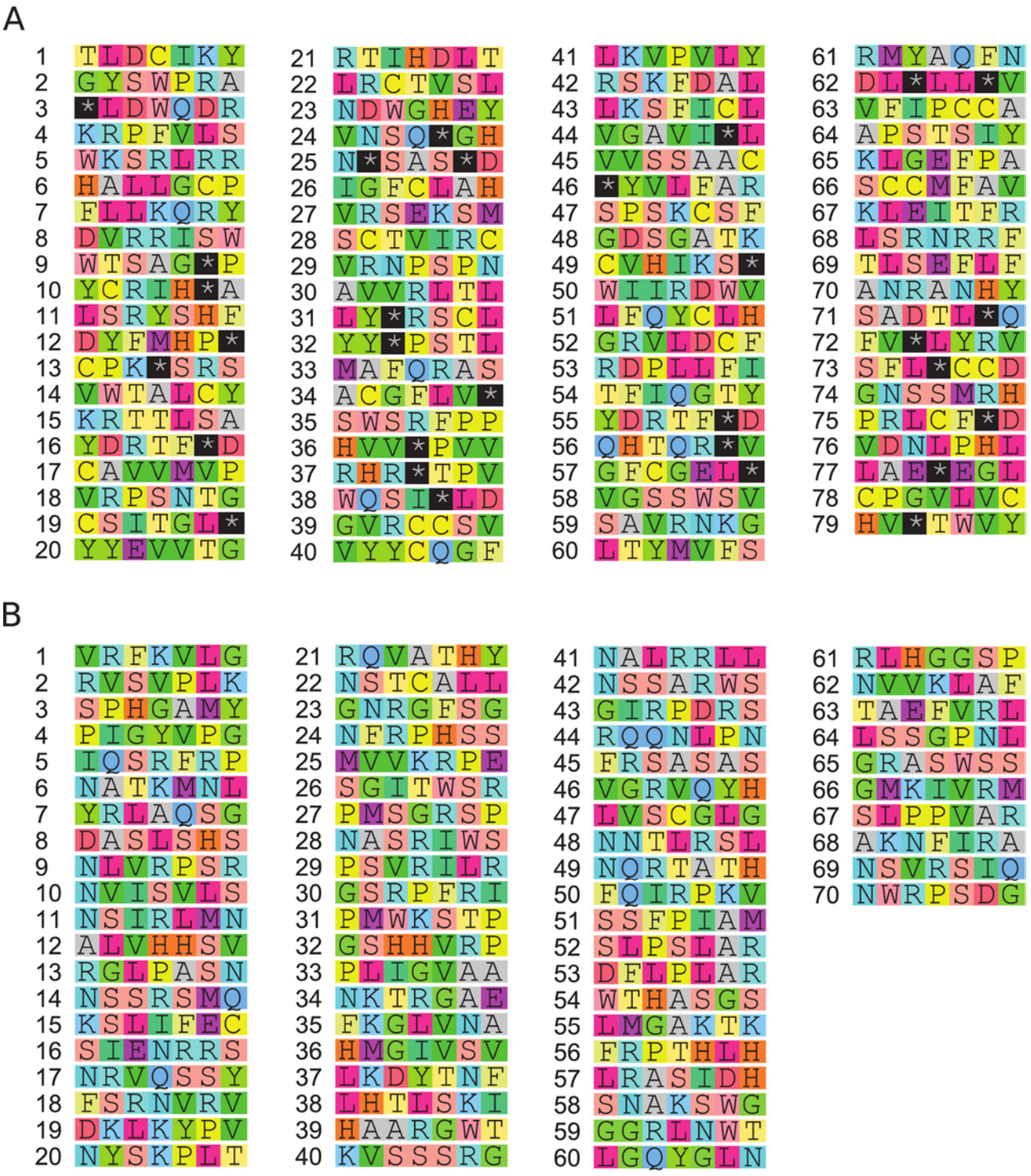

Figure S1: Peptide sequences obtained from sequencing of library clones. A total of 79 library plasmid clones (**A**) or 70 unselected virus library clones (**B**) were sequenced to reveal the amino acid composition of the heptamers. Nucleotide sequences were translated into protein sequences using Geneious software and amino acids were highlighted in unique colours. Stop codons in (**A**) are represented by stars on black background. Within the plasmid library clones 30 stop codons were identified rendering 27/79 sequences unfeasible for AAV capsid formation.

Table S1: Occurrence of amino acids within 79 plasmid library (white background) or 70 virus library (grey background) heptamers

AA[1]	Counts/amino acid position														% occurrence																	
	I		II		III		IV		V		VI		VII		I		II		III		IV		V		VI		VII		M[2]		TM[3]
A	4	2	6	6	1	4	6	6	2	4	6	8	5	3	5.1	2.9	7.6	8.6	1.3	5.7	7.6	8.6	2.5	5.7	7.6	11.4	6.3	4.3	**5.4**	**6.7**	**6.3**
C	5	0	4	0	3	0	5	2	5	0	7	0	3	1	6.3	0.0	5.1	0.0	3.8	0.0	6.3	2.9	6.3	0.0	8.9	0.0	3.8	1.4	**5.8**	**0.6**	**3.1**
D	3	3	6	0	3	1	0	0	4	1	1	2	5	0	3.8	4.3	7.6	0.0	3.8	1.4	0.0	0.0	5.1	1.4	1.3	2.9	6.3	0.0	**4.0**	**1.4**	**3.1**
E	0	0	0	0	3	2	3	0	2	0	1	1	0	2	0.0	0.0	0.0	0.0	3.8	2.9	3.8	0.0	2.5	0.0	1.3	1.4	0.0	0.0	**1.6**	**1.0**	**3.1**
F	2	5	5	2	3	2	4	2	9	4	4	0	6	3	2.5	7.1	6.3	2.9	3.8	2.9	5.1	2.9	11.4	5.7	5.1	0.0	7.6	2.9	**6.0**	**3.5**	**3.1**
G	6	7	3	5	3	4	3	6	4	5	3	1	3	8	7.6	10.0	3.8	7.1	3.8	5.7	3.8	8.6	5.1	7.1	3.8	1.4	3.8	11.4	**4.5**	**7.3**	**6.3**
H	3	2	2	1	1	4	1	2	3	3	3	2	4	4	3.8	2.9	2.5	1.4	1.3	5.7	1.3	2.9	3.8	4.3	3.8	2.9	5.1	5.7	**3.1**	**3.7**	**3.1**
I	1	1	1	3	5	5	4	3	5	5	1	1	1	2	1.3	1.4	1.3	4.3	6.3	7.1	5.1	4.3	6.3	7.1	1.3	1.4	1.3	2.9	**3.3**	**4.1**	**3.1**
K	4	2	3	5	2	1	2	9	2	1	2	2	1	2	5.1	2.9	3.8	7.1	2.5	1.4	2.5	12.9	2.5	1.4	2.5	2.9	1.3	2.9	**2.9**	**4.5**	**3.1**
L	9	7	6	6	4	5	7	4	10	5	8	10	9	6	11.4	10.0	7.6	8.6	5.1	7.1	8.9	5.7	12.7	7.1	10.1	14.3	11.4	8.6	**9.6**	**8.8**	**9.4**
M	1	1	1	5	0	0	3	0	3	1	0	3	1	2	1.3	1.4	1.3	7.1	0.0	0.0	3.8	0.0	3.8	1.4	0.0	4.3	1.3	2.9	**1.6**	**2.4**	**3.1**
N	2	18	3	3	2	1	1	3	3	1	0	4	2	4	2.5	25.7	3.8	4.3	2.5	1.4	1.3	4.2	3.8	1.4	0.0	5.7	2.5	5.7	**2.4**	**6.9**	**3.1**
P	1	5	4	1	3	3	4	8	3	5	5	4	4	5	1.3	7.1	5.1	1.4	3.8	4.3	5.1	11.4	3.8	7.1	6.3	5.7	5.1	7.3	**4.3**	**6.1**	**6.3**
Q	1	0	1	5	1	2	4	1	4	2	0	0	1	2	1.3	0.0	1.3	7.1	1.3	2.9	5.1	1.4	5.1	2.9	0.0	0.0	1.3	2.9	**2.2**	**2.4**	**3.1**
R	5	5	8	7	9	9	7	10	3	6	8	9	4	6	6.3	7.1	10.1	10.0	11.4	12.9	8.9	14.3	3.8	8.6	10.1	12.9	5.1	8.6	**8.0**	**10.6**	**9.4**
S	7	7	4	13	16	11	4	5	7	11	8	13	4	10	8.9	10.0	5.1	18.6	20.3	15.7	5.1	7.1	8.9	15.7	10.1	18.6	5.1	14.3	**9.0**	**14.3**	**9.4**
T	3	1	3	1	4	5	8	3	2	2	6	3	1	3	3.8	1.4	3.8	1.4	5.1	7.1	10.1	4.3	2.5	2.9	7.6	4.3	1.3	4.3	**4.9**	**3.7**	**6.3**
V	11	2	8	5	7	9	5	3	4	10	5	0	9	5	13.9	2.9	10.1	7.1	8.9	12.9	6.3	4.3	5.1	14.3	6.3	0.0	11.4	7.1	**8.9**	**6.9**	**6.3**
W	4	1	3	1	1	1	2	0	2	2	1	5	1	0	5.1	1.4	3.8	1.4	1.3	1.4	2.5	0.0	2.5	2.9	1.3	7.1	1.3	0.0	**2.5**	**2.0**	**3.1**
Y	5	1	7	1	3	0	2	2	1	2	0	1	9	3	6.3	1.4	8.9	1.4	3.8	0.0	2.5	2.9	1.3	2.9	0.0	1.4	11.4	4.3	**4.9**	**2.0**	**3.1**
Stop[4]	2		1		5		5		2		9		5		2.5		1.3		6.3		6.3		2.5		11.4		6.3		**5.2**		**3.1**

[1]amino acid (one letter code), [2]mean, [3]theoretical mean, [4]stop codon (amber)

Table S2: Codon table for amino acids

	T			C			A			G			
T	TTT	Phe	F	TCT	Ser	S	TAT	Tyr	Y	TGT	Cys	C	T
	TTC	Phe	F	TCC	Ser	S	TAC	Tyr	Y	TGC	Cys	C	C
	TTA	Leu	L	TCA	Ser	S	TAA	Ochre	Stop	TGA	Opal	Stop	A
	TTG	Leu	L	TCG	Ser	S	TAG	Amber	Stop	TGG	Trp	W	G
C	CTT	Leu	L	CCT	Pro	P	CAT	His	H	CGT	Arg	R	T
	CTC	Leu	L	CCC	Pro	P	CAC	His	H	CGC	Arg	R	C
	CTA	Leu	L	CCA	Pro	P	CAA	Gln	Q	CGA	Arg	R	A
	CTG	Leu	L	CCG	Pro	P	CAG	Gln	Q	CGG	Arg	R	G
A	ATT	Ile	I	ACT	Thr	T	AAT	Asn	N	AGT	Ser	S	T
	ATC	Ile	I	ACC	Thr	T	AAC	Asn	N	AGC	Ser	S	C
	ATA	Ile	I	ACA	Thr	T	AAA	Lys	K	AGA	Arg	R	A
	ATG	Met	M	ACG	Thr	T	AAG	Lys	K	AGG	Arg	R	G
G	GTT	Val	V	GCT	Ala	A	GAT	Asp	D	GGT	Gly	G	T
	GTC	Val	V	GCC	Ala	A	GAC	Asp	D	GGC	Gly	G	C
	GTA	Val	V	GCA	Ala	A	GAA	Glu	E	GGA	Gly	G	A
	GTG	Val	V	GCG	Ala	A	GAG	Glu	E	GGG	Gly	G	G

acidic | polar (uncharged) | non-polar | basic

IV. DISCUSSION

IV.A Overview

One of the major challenges in gene therapy is posed by the poor efficiency of gene transfer vectors. A good vector unifies tissue specificity, efficient transduction of targeted cells and low adverse immune effects. Recombinant Adeno-associated virus (AAV) vectors have become popular as gene therapy vectors due to their ability to deliver stable and efficient gene expression together with a good biological safety profile. Vectors based on AAV serotype 2 (AAV2), the most extensively investigated serotype, are to date the most widely used vectors due to their non-existent pathogenicity, replication deficiency and low rate of integration into the host genome. However, a main drawback of AAV vectors is represented by their poor specificity, since a wide variety of cells and tissue are equally well transduced. This issue has been addressed by many studies that attempted to improve targeting by using alternative AAV serotypes or capsid modification. The most recent approaches involved insertion of receptor-targeting ligands or selection of capsid libraries and yielded targeting and transduction-optimized AAV vectors. Approaches employing directed evolution by error-prone PCR or DNA shuffling by fragmentation and re-assembly of AAV *cap* genes from different serotypes may complement the combinatoric peptide display system at exposed capsid sites involved in receptor binding and transduction. Each technique has advantages and disadvantages and the application decides which method will be preferred to select for targeted vectors.

The potential of random peptide libraries displayed on AAV2 to select for AAV2 vectors with improved efficiency for endothelium-directed gene transfer has been demonstrated. However, AAV2 serotype vectors may not be ideal as backbones since there is a high prevalence of IgG against AAV2 in human serum. In contrast, AAV9 serotype vectors might represent a more suitable basis due to a lower susceptibility by neutralizing antibodies and a more efficient gene transfer after intravenous vector administration. Thus, the main focus of the present study was (I) to identify a suitable insertion site for targeting peptides within the AAV9 capsid surface, (II) to generate a random AAV9 peptide display library for selection of an AAV9-based targeting vector on endothelial cells, and (III) to compare vectors selected from AAV9 libraries with those from previous AAV2 libraries.

IV.B The display of foreign peptides on AAV9 capsids

Insertion of foreign peptides on AAV capsids must be approached with caution. Disruption of functional capsid domains can impair host recognition, intracellular processing or in the worst case capsid assembly. The VP proteins of AAV1-9 share highly conserved regions as well as variable regions (VR I-VIII)[100], which probably contribute to the different tropism of different AAV serotypes. Although the yet unknown AAV9 capsid structure disallows precise mutation design, modification of the variable regions, especially VR VIII that is a part of the 3-fold protrusion and harbours A589, should similarly to R588 of AAV2 exercise an influence on tropism. As a basis, it was assumed that display of foreign peptides behind AAV9 VP1 residue A589, analogously to peptide display behind R588 in AAV2, would yield similar targeting possibilities. Comparison of vectors displaying endothelium-targeted control peptide NDVRAVS behind R588 of AAV2 or A589 of AAV9 confirmed this assumption as the AAV9 mutant was able to transduce wtAAV-refractory HCAEC with significant higher efficiency than both wild type AAV2 or AAV9 (Chapter III.B.2.2).

IV.C The AAV9 random peptide display library

In order to develop an endothelial targeting vector with a peptide optimally displayed within the context of the AAV9 capsid, the evolutionary approach based on selection of a AAV9 random peptide display library was used. The AAV9 library was generated according to a multi-step procedure which has successfully been applied for generation of AAV2-based[201,195] or capsid shuffled libraries[213] and was characterized according to complexity, amino acid usage, functionality of virus particles and wtAAV9 contamination.

IV.C.1 The library complexity

The creation of a randomized peptide library demands an exhaustive complexity, i.e. an abundance of different peptide sequences matching theoretical expectations, that raises the probability of identifying a variant most adapted to the needs. The first attempt to estimate the complexity of the NNK-based peptide heptamer library was done after plasmid library synthesis by counting of bacterial colonies grown from a transformed aliquot. The quality of information obtained from the transformation efficiency is however poor, since calculation of transformation efficiency implements several dilution steps and therefore leaves room for statistical deviations. Additionally, it was assumed that the counted clones were unique and did not contain sequence repetitions. Therefore, the complexity of 6.02E+8 clones represents a maximal value which is further lowered by presence of stop codons within the peptide (discussed below) to a functional complexity of 3.89E+8 clones (Chapter III.C.1.2). Nevertheless, the complexity can be regarded as sufficient when compared to theoretical 1.28E+9 and equals previously published AAV2 counterparts ranging from 1.2E+7 to 1.7E+8 clones[201,213,207,202].

Complexity is further reduced due to losses during TSL production and purification as well as by intolerance of certain peptide motives that reduce the fitness of library variants. Both transfer shuttle libraries (TSL) using AAV2 or AAV9 helper plasmids (2-TSL, 9-TSL) yielded absolute infectious titres of 5E+7 IU at the same time representing the maximal complexity (Chapter III.C.3.1). Thus, the main limiting factor that defines the final virus library complexity is the replicative titre of TSL particles.

IV.C.2 Amino acid usage of the library

For a closer characterization, 79 or 70 independently assigned clones from plasmid and final virus library were sequenced, respectively. The aim was to reveal deviations from theoretical amino acid distribution (biases), since randomness is a central point of the library approach. The appearance of more than expected stop codons within the NNK-designed plasmid library (37.9% instead theoretical 35.4%, Supplementary Figure 1 **A**) could be explained by the low amount of sequenced clones. Analysis of additional clones would yield a more representative result, but as the functional complexity (Chapter III.C.1.2) was higher than the TSL complexity (Chapter III.C.3.1), no complications were expected from this point of view.

Deviations of mean amino acid occurrences from theoretical values were judged without performing statistical calculations according to Figure III.C.1.3 and Supplementary Table 1. Basically, the presence of amino acids was regarded as above (over-represented), below (under-represented) or similar to theoretical calculations. The plasmid library seemed to over-represent amino acids C, F, W and Y, but as no selective pressure acted upon its synthesis, it is difficult to estimate the importance of this finding. Increasing the amount of analysed clones probably would yield more representative results. In contrast, during the synthesis of the virus library a selective pressure potentially acts on the amino acid distribution, shifting their occurrence. Indeed, a noticeably decreased (C, D, E, T) or increased (N, S) mean occurrence of amino acids was seen within analysed clones from the virus library. A comparison to the plasmid library revealed that under-representation in case of E can be explained by a lowered presence in the plasmid library, but not in case of N, S and C (see Chapter III.C.3.2). Particularly N and S differences were detected in a residue-specific manner at positions 1 (N), 2 and 5-7 (all S). This outcome points indeed towards a selective allocation which may be explained by a varying tolerance of the capsid for certain amino acids at distinct residues. Similar observations were made for other AAV2 libraries[234,235,236,237], although other amino acids (and another serotype) were involved. Another plausible theory for this bias will be discussed in Chapters IV.C.3 and IV.D. Taken together, the concept of random peptide display developed for AAV2 by has also proven efficient for AAV9.

IV.C.3 The functional characterisation of library particles

Insertion of foreign peptides on AAV capsid may have severe impacts on packaging, intracellular trafficking or uncoating of the genetic load. A low virus stability will not only reduce the final yield but also the complexity of the library particles. In this study, production of the AAV9 library from two different TSL sources was attempted (Chapter III.C.2). The mosaic TSL capsids consist of wild type and mutant VP monomers encoded by a wtAAV helper plasmid and several mutant *cap* genes from the plasmid library, respectively. In case of AAV2, a helper plasmid providing wtAAV2 VPs was used providing efficient and approximately equal re-infection efficiency to all library variants. Since on the one hand wtAAV9 does not transduce HEK293T very well and on the other hand efficient transcapsidation of AAV9 and AAV2 was not shown yet, both possibilities were considered for the production of the AAV9 TSL.

Comparable genomic titres between 2-TSL and 9-TSL particles (Chapters III.C.2 and III.C.3.1) proved an efficient transcapsidation of AAV2 and AAV9. Interestingly, although not expected, the replicative titre of both TSLs was the same (5E+7 IU). Obviously, the 9-TSL did not suffer disadvantages to the 2-TSL although wtAAV2 infects HEK 293T much more efficient than wtAAV9. Due to the equal efficiency of both TSLs, comparable test-productions of final libraries were possible yielding absolute titres of 3E+9 gc. The factor that compensated helper VP-related differences of TSL particles may have acted during uptake and could be represented by the mutant VPs present in the TSL shells. Synergistic effects between mutant and wtAAV VPs are not inconceivable and offer an explanation for the bias of some amino acids within distinct residues of the library peptides (see also IV.C.2). This and a potentially improved intracellular processing of some TSL variants may have lead to a slight pre-selection of the library on HEK 293T. The final AAV9 library was produced using 2-TSL and yielded a genomic titre of 4.6E+11 gc translating into 4.6E+3 gc/cell. This efficiency is comparable to AAV2 or AAV9 vector productions (Chapter III.E.1) and proves that insertion of peptides at capsid site A589 does not hamper genome packaging or capsid assembly.

IV.C.4 Wild type contamination of the library

A major challenge in generation of capsid libraries is given by the need to package the virus library genomes into corresponding capsids. A direct transfection of plasmid library into producer cells would provide many library plasmids per cell and create mosaic capsids as in the case of Perabo *et al*.[194]. To avoid this, the present AAV9 library was synthesized in a three-step procedure that employs intermediate-step transfer shuttle library (TSL) particles (see also Chapter I.C.3.1). The chimerical TSL shells enable an equal re-infection of producer cells via their wtAAV capsid domains but do not transfer wild type *cap* sequences upon re-infection of cells, since wtAAV helper plasmids used for TSL synthesis lack ITRs and can not be packaged. Thus, wild type-free final virus library particles with genomes corresponding to the capsids can be produced.

A library contamination with wild type viruses can only occur if the initial plasmid library contains wtAAV-encoding genomes or by a recombination effect between plasmid library and wtAAV helper plasmid sequences taking place during TSL production. Waterkamp *et al*.[201], developed a codon-modified wtAAV2 helper plasmid that impeded recombination events with library plasmids and generated a wild type-free library.

The use of this modified wtAAV2 helper plasmid proved also efficient for the AAV9 library production but still wtAAV9 contaminations were detectable in library test-productions made from 2-TSL or 9-TSL. A recursive PCR analysis revealed a wtAAV9 contamination within the plasmid library stock that persisted during virus library test-productions (Chapter III.C.2). Notably, the contamination of the 9-TSL was slightly higher than that of the 2-TSL. Consequently, the advanced contamination of 9-TSL lead to a stronger amplification of contaminating wtAAV9 viruses during production of the final virus library. It cannot be ruled out that a recombination event that took place between wtAAV9 but not wtAAV2 helper and library plasmid during TSL production creating an additional wtAAV9 contamination has added to the already present contamination from the library plasmid.

Wild type-contaminations pose a potential drawback and could severely hamper the library selection process on cells that are wtAAV permissive. It is well imaginable that in contrast to wtAAV, a potentially efficient library clone does not efficiently enrich due to its considerably lower copy number. As well, the presence of ITR-positive wild type and library genomes in a cell during the first library selection round leads to the formation of chimerical capsids comparable to the TSL. While the lowered selection pressure on library clones in context of the TSL application is desired, wild type-contaminations led to a delayed selection of specific library variants during subsequent selection rounds. These difficulties are negligible in case wtAAV-refractory cells are used for selection as done in the case of this study (HCAEC). An *in vivo* selection of a wild type-contaminated library however would re-initiate the synthesis of chimerical capsids from tissue that can be infected by both, wild type and library viruses. Due to the broad wtAAV9 tropism, subsequent application of the library in a new selection round would redirect library genome variants encapsidated in chimerical capsids to tissues prone to wtAAV9 infection, resulting in low specificity and a mislead readout. Therefore, considering the increased complexity level of an *in vivo*-selection attempt, only wild type-free AAV peptide libraries should be employed to facilitate evaluation of potential interesting library clones.

IV.D The library selection on HCAEC

The *in vitro* selection represents a strongly accelerated capsid evolution resulting in variants better adapted to the host. The process affects the entire infection pathway of a virus comprising receptor-binding, endocytosis, intracellular processing and replication. Consecutive re-application of pre-selected libraries will further discriminate between leading mutants, finally establishing the most efficient of them. Selection of the AAV9 library on HCAEC led to a strong enrichment of distinct peptides after three or four rounds (Chapter III.D-2). Three different MOIs of 10, 100 and 1000 gc/cell were applied each round to analyse the effect of an increased stringency. The amount of different peptides isolated from the MOI 10 approach was lower and more specific in comparison to other approaches with higher MOIs, although a comparable number of clones was analysed. Still, peptide RGDLRVS represented the most prominent peptide. This outcome would profit from analysis of more clones and/or widening the difference between applied MOIs but it still indicates that raising the stringency of the selection process by lowering the MOI (and therefore the complexity) of the library may lead to propagation of „positive“ mutants (i.e. mutants truly enhancing transduction efficiency) at the same time depleting „false positive“ mutants that are internalized and processed at low rates and thus only simulate high efficiency. Some of the selected peptides shared certain motifs (RGD, $^{S}/_{T}{}^{L}/_{I}R^{S}/_{A}PP^{S}/_{A}$) and nearly all peptides show biased incorporations of certain amino acids. Amino acids P, R and L had a similar presence in both, unselected peptide and plasmid library. Their elevated presence within the selected peptides at certain residues can be ascribed to the selection process, as their presence conferred to AAV9 a selectional advantage. Amino acids N and S were distributed as expected within the plasmid library but had an elevated occurrence in the unselected peptide library as well as in selected clones. Remarkably, the residues occupied by these amino acids (1st for N, 2nd and 7th for S) were comparable to those from unselected peptide libraries (1st for N, 2nd and 5-7th for S) although also adjacent residues were affected (4th for S). In fact, their presence may arise from selection of the library on HCAEC but could also represent a pre-selection artefact of library production (see also IV.C.3).

The tripeptide RGD as a cell binding mediator was initially shown for fibronectin[238] with its receptor described as a 140kDa cell surface glycoprotein[239] that later was named integrin[240]. Since peptides RGDLRVS and RGDFRVG both contain RGD, a retargeting of AAV9 towards integrins receptors is imaginable (see also Chapter IV.G).

Several enriched peptides contained basic arginine (R) residues at any but the second position within the heptamer. Arginine has the highest pKa (12.48, followed by K with 10.53 and H with 6.0) and has therefore the highest electrostatic interaction potential. In case of AAV2, capsid binding to heparin/HSPG was shown to be driven by electrostatic forces[90], and it is imaginable that the elevated presence of arginine in peptides selected in this, as well as other AAV2 studies[195,207,201,203] are required for a certain net charge of the binding domain to allow AAV capsid/receptor interactions.

An interesting finding was that selected peptides descended from the same DNA clone, independent of MOI or selection round. Peptide heptamers based on a NNK architecture can be encoded by 32 different oligonucleotide sequences. Most probably, not all of them will be represented in the initial construct, the oligonucleotide library. The entire library production process comprises many steps and leads to a secondary loss of complexity. Since enriched peptides were not detected in the unselected virus library, no obvious restriction of library complexity can be stated. Furthermore, the analysis of enriched peptides covers only a tiny part of the range of clones and is therefore not necessarily comprehensive. It is probable that analysis of more clones could reveal more than one DNA sequence encoding the same enriched peptide. Additionally, a preference of certain codon variants encoding a peptide is imaginable and thus a selective force would be applied also on the DNA sequence leading to the enrichment of distinct DNA sequences for a peptide.

PCR-analysis for wtAAV9 contaminations within the selected library confirmed the assumption that wtAAV9-refractory HCAEC would “remove” the contamination (Chapter III.C.4). After selection round one, faint wild type DNA-bands were detectable which disappeared after round four. In addition, no wild type sequences were found within the 70 analysed virus library clones. This outcome is conform with the finding of Waterkamp *et al*.[201] who showed a persistence of wtAAV2 contaminations during selection of an AAV2 library only from cells that were wtAAV2-permissive.

IV.E The efficiency of mutant AAV9 vectors

IV.E.1 Production titres

A trivial way of enhancing transgene expression to detectable (reporter genes) or biologically significant (therapeutic genes) levels *in vitro* or *in vivo* is posed by increasing the applied AAV vector dose. Easy-to-produce dose ranges of 1E+10 to 1E+12 gc used for *in vivo*-treatment of mice or rats yield sufficient levels of transgene expression[50,241,242]. While such low doses allow systemic application, *in vivo* exposure of larger animals or even humans via this route would require doses that exceed economical or technical prospects. More restricted intra-muscular, retinal or intracranial vector administrations performed in several human trials allowed lower doses ranging from 1E+11 to 6E+13 gc (reviewed by[14]).

The administration of elevated doses involves an efficient production of particles, which in case of AAV vector mutants that affect the packaging efficiency may be problematic. The titres obtained from novel AAV9 mutant vectors engineered in this study compared very well and in some cases even exceeded those of mutant AAV2 vectors (Chapter III.E.1) proving efficient packaging and the feasibility of the peptide insertion concept for AAV9. Of note, vectors displaying unselected (TEWDQPF) or scrambled (PSLPSRS from SLRSPPS) peptides yielded titres comparable to selected counterparts. Although the library selection process supports the notion of a synergistic effect of peptides and capsid apart from mere receptor targeting, production efficiencies of vectors displaying unselected peptides that parallel those of vectors displaying selected peptides may be coincidence. Indeed, another scrambled peptide, SDLRRGV (from RGDLRVS) yielded a vector titre one log step lower, supporting the synergistic effect of selection.

IV.E.2 *In vitro* and *in situ* transduction of AAV9 vectors displaying selected peptides

IV.E.2.1 In vitro transduction

The selection of the AAV9 library on HCAEC yielded peptide SLRSPPS that outperformed transduction of HCAEC over wtAAV9 and, more important, AAV9-NDVRAVS at a low dose of 1E+3 gc/cell (Chapter III.E.2), posing an improvement over the tenfold higher MOI previously applied to enable efficient transduction of endothelial cells (ECs)[195,201]. Such high efficiency with a low vector dose could also be advantageous for a future clinical use since a lower vector exposure might provoke a reduced immune response[243] that complements the ability of this vector to escape neutralizing antibodies (Chapter III.H). Improvement of transduction does not arise from the mere insertion of a foreign peptide into an infection-relevant capsid site but is peptide sequence specific, since unselected control-peptide TEWDQPF abolished HCAEC transduction completely. Interestingly, the most abundant selected peptide RGDLRVS yielded a slightly lower transduction of HCAEC in contrast the less represented SLRSPPS. This was also observed for NDVRAVS selected in the context of an AAV2 library that outperformed most abundant NSSRDLG and NSVSSAS[195] and can be explained by differential uptake and intracellular processing of the vectors. Enrichment of a peptide requires an efficient uptake leading to many genome copies/cell while vector transduction depends additionally on efficient downstream processing. SLRSPPS may have a more reduced uptake rate than RGDLRVS but its intracellular processing might be more efficient, leading to a (slightly) improved transduction of HCAEC. Obviously, there is no correlation between abundance of peptides and their efficiency and therefore criteria for the choice of peptides for further analyses should be rather their sequence than their abundance.

A key finding of this study is the fact that not only the peptide, but also the serotype backbone it is embedded in seems to influence the transduction efficiency. Clones derived from AAV2 libraries conferred lower efficiencies to AAV9 vectors than AAV9-derived peptides (Chapter III.G). This result underlines the need of a selection process in the context of the capsid on which the peptide is considered to be expressed and further confirms the assumption that peptide sequences selected from an library displayed on one serotype not necessarily work in the context of another serotype. Thus, it cannot be generalized from the performance of a peptide sequence from one serotype to another, justifying generation of an AAV9 library.

So far, *in vitro* proof-of-concept for selection of targeted vectors from AAV peptide libraries has been shown for AAV2 and AAV9 random peptide libraries. However, the specificity towards the targeted cells still remains a matter of concern that must be solved in order to develop attractive vectors for gene transfer applications. The specificity of this study's most abundant peptide RGDLRVS and most potent peptide SLRSPPS was tested *in vitro* on primary (HCAEC, HCASMC) or immortalized cells (HeLa, 293T, 911, HepG2). At a low MOI of 2.5E+3 gc/cell AAV9-SLRSPPS was more specific than RGDLRVS although transduction of cells other than HCAEC was not completely abolished (Chapter III.F.1). The targeting of receptors commonly expressed by these cell types seems probable, explaining the general difficulty of increasing vector specificity by this method alone. The targeted receptor(s) must be likewise involved in uptake and it is less likely that each cell type has developed unique receptor sets that control the endocytosis process. Therefore, specific EC transgene expression was attempted in several studies by augmenting transductional with transcriptional targeting using human and murine endothelium specific promoters. Gory *et al*.[233] successfully restricted transgene expression to bovine aortic ECs using the 313 bp fragment from murine VE-cadherin promoter. In the present study the combination of most potent vector AAV9-SLRSPPS and the 163/313 bp fragments from this promoter improved transcriptional targeting only moderately over the previously used CMV promoter (Chapter III.F.2). The CMV enhancer element was not removed before insertion of the VE-cadherin promoter and it is therefore likely that its influence has affected the EC-specificity. In combination with the efficient vector AAV9-SLRSPPS, however, a potent transgene delivery and expression system for *in vitro* studies involving human ECs could be created, since the advantageous size of the 163 bp fragment outperforms that of CMV (635 bp) enabling insertion of larger transgenes.

IV.E.2.2 In situ transduction

Efficient *in vitro* transduction from *in vitro*-selected vectors is not necessarily transferable to tissue that is embedded in its natural context *in vivo*. To assess the potential of this study's leading vector AAV9-SLRSPPS to transduce endothelium present in the context of blood vessels, gene transfer efficiency in murine mesenteric arteries and human umbilical veins was analysed.

Previously, transduction of H5V, a murine malignant hemangiosarcoma cell line derived from heart capillaries, using targeted AAV9 vectors (same vector stocks) was very low, probably due to a defective targeted receptor profile or a inefficient intracellular processing of vectors. A 48 h *in situ* or a 14 d *in vivo* exposure of mesenteric artery endothelium in mice to this vector at sufficiently high doses similarly did not lead to transduction (Chapter III.J.1). This surprising result opens several scenarios: (I) transduction of murine ECs does not occur due to the vector's specificity to ECs of human origin, (II) transduction takes place and missing EGFP-expression is explained by a very low intracellular processing rate of vector particles (e.g. due to the non-dividing state of ECs), (III) mesenteric endothelium was successfully transduced and missing EGFP fluorescence is due to a CMV promoter downregulation and (IV) the mesenteric artery ECs do not express the targeted receptor(s) at all. The data obtained so far does not allow a discrimination between these scenarios. The onset of transgene expression in mice from AAV mediated gene transfer is delayed[244] but a 2 week exposure should be sufficient for detectable levels of transgene expression by fluorescence microscopy. Similarly, AAV is able to transduce dividing and non-dividing cells *in vitro* [245] and *in vivo* in a variety of tissues[246,247,248,249,250,251,252]. Targeting the vascular endothelium with peptides selected *in vitro* implicit reliance on target receptor expression *in vivo*. Endothelial cells, however differ strongly in receptor profiles *in vitro*[253] and *in vivo*[254,255,256,257]. Furthermore, the existence of complex endothelial zip codes *in vivo* render it heterogeneous. Thus, the AAV9-SLRSPPS vector may have been selected for receptors that redirect it to a certain type of endothelium which is not of mesenteric artery origin.

Data obtained from successful and efficient *in situ* transduction of umbilical vein endothelium by AAV9-SLRSPPS but not by wtAAV9 (Chapter III.J.2) does not clarify the situation, as well. Quantification of genome copies from HUVEC exposed to AAV9-SLRSPPS *in situ* was performed to analyse whether vector uptake would occur during exposure or by contamination carry-overs *in vitro.* A substantial amount of vector genomes was found in HUVEC lysates that were prepared immediately after exposure and isolation. However, the experiment does not distinguish between endocytosed vectors or vectors that only have bound to receptors but were not internalized. The receptor(s) targeted by AAV9-SLRSPPS are unknown and it is unclear whether HUVEC isolation via dispase, a bacterial protease that cleaves leucine-phenylalanine bonds and digests fibronectin, collagen IV, and to a lesser extent collagen I, would also remove the targeted receptor(s) allowing only detection of intracellularly accumulated vector genomes. HUVEC exposed to the vector *in vitro* were collected with trypsin, a serine protease, which in fact removes HSPG[258] but may as well not be able to remove the targeted receptor, leading to detection of bound but not internalized vectors. Therefore, none of the above mentioned scenarios (I)-(IV) can be excluded. Assuming an *in situ*-uptake of vectors and absence of technical limitations, the missing EGFP expression in cross-sectioned veins could be ascribed to a low intracellular processing of the vector from quiescent cells (scenario (II)).

Since intracellular vector processing varies between different vectors the testing of more enriched peptides using the umbilical vein model could yield vectors with an improved processing efficiency. The employment of EC-specific promoters may represent an alternative option to improve transgene expression in quiescent ECs.

IV.F Escape from neutralization by pre-existing AAV antibodies

Along with a good transduction efficiency and target specificity, the ability of a vector to evade neutralisation by pre-existing host antibodies determines the quality of a gene transfer vector. The selection of novel AAV vectors from combinatorial peptide libraries shared besides improvement of transduction efficiency another strategy: removal of antigenic epitopes from surface-exposed capsid domains. Neutralizing antibodies in general bind to capsid epitopes, thus preventing interaction of AAV with cellular surface receptor(s)[172]. For AAV2, several epitopes have been mapped within the loops of the threefold spike, the most prominent domain of the capsid[173]. Huttner *et al*.[174] reported two AAV2 mutants carrying peptide insertions I-534 and I-573 with a reduced affinity for AAV antibodies in the majority of the analysed serum samples. These two insertions, especially I-573, are located in close proximity to R588, probably pointing to a relationship between capsid domains involved in tropism and domains serving as epitopes. This relationship is further sustained by the results obtained from the *in vitro* neutralization attempt in this study (Chapter III.H). The attempt analysed the ability of the novel AAV9 vector mutants displaying RGDLRVS and SLRSPPS to evade neutralization by IVIG, a pool of human antisera applicable for *in vitro* neutralization studies of AAV[213,109] and ADK9, a monoclonal antibody raised in mice against wtAAV9 capsids. AAV9 mutants RGDLRVS and SLRSPPS improved *in vitro* escape from IVIG neutralization over wtAAV2, wtAAV9 and AAV2-NDVRAVS, underlining the suitability of AAV9 rather than AAV2 as a backbone for targeted peptide display. Still, IVIG dilutions below 1:160 completely neutralized transduction of the AAV9 mutants. However, the improved evasion (and the lowered MOI required for efficient transduction) lowers the vector dose required for gene transfer thereby reducing the dose-dependent immune response to vectors in treated subjects[243]. In contrast to an efficient recognition and neutralization by IVIG, ADK9-neutralization occurred only in case of wtAAV9. The epitope of monoclonal ADK9 seems to have been disrupted completely by insertion of peptides behind VP1 589, while the epitopes recognized by the pool of polyclonal AAV9 capsid antibodies present in IVIG were less affected. This outcome indicates that the capsid domain displaying peptides embraces a significant role in targeting and antibody recognition supporting the notion that epitope formation is more likely to occur at exposed capsid domains with good accessibility to the immune system (i.e. the threefold spikes).

IV.G Secondary characterisation of endothelium-targeted peptides

Binding of AAV2 to HSPG receptors depends mainly on a subset of basic arginines (particularly R585/R588) that are absent in the corresponding region of AAV9. According to the heparin competition results, wtAAV2 vectors efficiently transduced HSPG-positive HepG2 cells in a heparin-dependent manner (Chapter III.I.2). Since augmentation of missing arginines can be achieved by displaying enriched heptamers like SLRSPPS and especially RGDLRVS, the effect of heparin on transduction efficiencies of AAV9 vectors displaying these peptides was analysed. For RGDLRVS, relevant (HCAEC) and notable (HepG2) transduction efficiencies were attained, which were slightly modulated by heparin. In case of SLRSPPS, only HCAEC was transduced at noteworthy levels and presence of heparin did not alter the transduction. Due to the minimal (unspecific) inhibitory effect heparin carries on RGDLRVS and the missing effect on SLRSPPS, a transduction that has been accidentally redirected to HSPG receptors can be excluded.

The capsid competition experiments suggest that both peptides are capable of competing each other but not if the competing peptide is displayed in a scrambled manner (Chapter III.I.1). This indicates that (I) the peptides specifically modulate transduction patterns and (II) partly use a common transduction pathway. Since both vectors cannot be completely inhibited by each others (dose response experiments revealed that the inhibitory effect can be saturated), additional alternative receptors/post entry mechanisms might exist which also could explain different transduction patterns of cell lines and primary cells (Chapter III.F.1). It is known, that AAV2 utilizes co-receptors that enable endocytosis into the cell and that these receptors interact with different capsid sites. This could also be the case for AAV9 and the mutants. Both vectors might target the same primary receptor which explains the mutual competition, but different secondary receptors specifically targeted by each mutant may modulate transduction of different cell types and could impede a complete competitor-mediated inhibition of transduction. A vague indication is given by the motif RGD that is included in RGDLRVS but not SLRSPPS. The trimer is known to promote binding to a multitude of receptors from the integrin family (reviewed by[259]) and it has been demonstrated that integrins play an essential role as cellular entry receptors for AAV2[19] and AAV9[125]. Perabo *et al*.[194] showed that the expression of RGD at position 587 enables AAV2 to efficiently infect cells via an integrin subtype and, importantly, those RGD-expressing vectors lacked cellular specificity which the authors ascribed to the wide-ranged expression profile of integrins on different tissues.

V. REFERENCES

[1] Shen YM *et al.,* Gene transfer: DNA microinjection compared with DNA transfection with a very high efficiency. *Mol Cell Biol* 1982, **2** (9)**:** 1145-54, PMID: 6294505.

[2] Fromm ME *et al.,* Stable transformation of maize after gene transfer by electroporation. *Nature* 1986, **319** (6056)**:** 791-3, PMID: 3005872.

[3] Wagner E *et al.,* Transferrin-polycation conjugates as carriers for DNA uptake into cells. *Proc Natl Acad Sci USA* 1990, **87** (9)**:** 3410-4, PMID: 2333290.

[4] Boussif O *et al.,* A versatile vector for gene and oligonucleotide transfer into cells in culture and in vivo: polyethylenimine. *Proc Natl Acad Sci USA* 1995, **92** (16)**:** 7297-301, PMID: 7638184.

[5] Friend DS *et al.,* Endocytosis and intracellular processing accompanying transfection mediated by cationic liposomes. *Biochim Biophys Acta* 1996, **1278** (1)**:** 41-50, PMID: 8611605.

[6] Schaffer DV *et al.,* Molecular engineering of viral gene delivery vehicles. *Annu Rev Biomed Eng* 2008, **10:** 169-94, PMID: 18647114.

[7] Verma IM, Weitzman MD Gene therapy: twenty-first century medicine. *Annu Rev Biochem* 2005, **74:** 711-38, PMID: 15952901.

[8] Pfeifer A, Verma IM Gene therapy: promises and problems. *Annu Rev Genomics Hum Genet* 2001, **2:** 177-211, PMID: 11701648.

[9] Boyce N Trial halted after gene shows up in semen. *Nature* 2001, **414** (6865)**:** 677, PMID: 11742355.

[10] Anderson WF Excitement in gene therapy! *Hum Gene Ther* 2001, **12** (12)**:** 1483-4, PMID: 11506691.

[11] Marshall E Clinical research. Gene therapy a suspect in leukemia-like disease. *Science* 2002, **298** (5591)**:** 34-5, PMID: 12364755.

[12] Trepel M *et al.,* Exploring vascular heterogeneity for gene therapy targeting. *Gene Ther* 2000, **7** (24)**:** 2059-60, PMID: 11223985.

[13] Verma IM, Somia N Gene therapy -- promises, problems and prospects. *Nature* 1997, **389** (6648)**:** 239-42, PMID: 9305836.

[14] Mueller C, Flotte TR Clinical gene therapy using recombinant adeno-associated virus vectors. *Gene Ther* 2008, **15** (11)**:** 858-63, PMID: 18418415.

[15] Daya S, Berns KI Gene therapy using adeno-associated virus vectors. *Clin Microbiol Rev* 2008, **21** (4)**:** 583-93, PMID: 18854481.

[16] Flotte T *et al.,* A phase I study of an adeno-associated virus-CFTR gene vector in adult CF patients with mild lung disease. *Hum Gene Ther* 1996, **7** (9)**:** 1145-59, PMID: 8773517.

[17] Kay MA *et al.,* Evidence for gene transfer and expression of factor IX in haemophilia B patients treated with an AAV vector. *Nat Genet* 2000, **24** (3)**:** 257-61, PMID: 10700178.

[18] Manno CS *et al.,* AAV-mediated factor IX gene transfer to skeletal muscle in patients with severe hemophilia B. *Blood* 2003, **101** (8)**:** 2963-72, PMID: 12515715.

[19] Jessup M *et al.,* Calcium Upregulation by Percutaneous Administration of Gene Therapy in Cardiac Disease (CUPID): A Phase 2 Trial of Intracoronary Gene Therapy of Sarcoplasmic Reticulum Ca2+-ATPase in Patients With Advanced Heart Failure. *Circulation* 2011, **124** (3)**:** 304-313, PMID: 21709064.

[20] Brantly ML *et al.,* Phase I trial of intramuscular injection of a recombinant adeno-associated virus serotype 2 alphal-antitrypsin (AAT) vector in AAT-deficient adults. *Hum Gene Ther* 2006, **17** (12)**:** 1177-86, PMID: 17115945.

[21] Feigin A *et al.,* Modulation of metabolic brain networks after subthalamic gene therapy for Parkinson's disease. *Proc Natl Acad Sci USA* 2007, **104** (49)**:** 19559-64, PMID: 18042721.

[22] Kaplitt MG *et al.,* Safety and tolerability of gene therapy with an adeno-associated virus (AAV) borne GAD gene for Parkinson's disease: an open label, phase I trial. *Lancet* 2007, **369** (9579)**:** 2097-105, PMID: 17586305.

[23] Jacobson SG *et al.,* Safety of recombinant adeno-associated virus type 2-RPE65 vector delivered by ocular subretinal injection. *Mol Ther* 2006, **13** (6)**:** 1074-84, PMID: 16644289.

[24] Li C *et al.,* Adeno-associated virus vectors: potential applications for cancer gene therapy. *Cancer Gene Ther* 2005, **12** (12)**:** 913-25, PMID: 15962012.

[25] Carter BJ Adeno-associated virus vectors in clinical trials. *Hum Gene Ther* 2005, **16** (5)**:** 541-50, PMID: 15916479.

[26] Atchison RW *et al.,* Adenovirus-Associated Defective Virus Particles. *Science* 1965, **149:** 754-6, PMID: 14325163.

[27] Hoggan MD *et al.,* Studies of small DNA viruses found in various adenovirus preparations: physical, biological, and immunological characteristics. *Proc Natl Acad Sci USA* 1966, **55** (6)**:** 1467-74, PMID: 5227666.

[28] Siegl G *et al.,* Characteristics and taxonomy of Parvoviridae. *Intervirology* 1985, **23** (2)**:** 61-73, PMID: 3980186.

[29] Muzyczka N and Berns KI. Parvoviridae: the viruses and their replication, *Fields Virology*, Vol. 1, Knipe DM and Howley PM (eds), New York, N.Y., Lippincott, Williams and Wilkins, 2001.

[30] Buller RM *et al.,* Herpes simplex virus types 1 and 2 completely help adenovirus-associated virus replication. *J Virol* 1981, **40** (1)**:** 241-7, PMID: 6270377.

[31] McPherson RA *et al.,* Human cytomegalovirus completely helps adeno-associated virus replication. *Virology* 1985, **147** (1)**:** 217-22, PMID: 2998066.

[32] Schlehofer JR *et al.,* Vaccinia virus, herpes simplex virus, and carcinogens induce DNA amplification in a human cell line and support replication of a helpervirus dependent parvovirus. *Virology* 1986, **152** (1)**:** 110-7, PMID: 3012864.

[33] Meyers C *et al.,* Altered biology of adeno-associated virus type 2 and human papillomavirus during dual infection of natural host tissue. *Virology* 2001, **287** (1)**:** 30-9, PMID: 11504539.

[34] Berns KI *et al.,* Detection of adeno-associated virus (AAV)-specific nucleotide sequences in DNA isolated from latently infected Detroit 6 cells. *Virology* 1975, **68** (2)**:** 556-60, PMID: 1198930.

[35] Kotin RM *et al.,* Site-specific integration by adeno-associated virus. *Proc Natl Acad Sci USA* 1990, **87** (6)**:** 2211-5, PMID: 2156265.

[36] Samulski RJ *et al.,* Targeted integration of adeno-associated virus (AAV) into human chromosome 19. *EMBO J* 1991, **10** (12)**:** 3941-50, PMID: 1657596.

[37] Huser D *et al.,* Integration preferences of wild type AAV-2 for consensus rep-binding sites at numerous loci in the human genome. *PLoS Pathog* 2010, **6** (7)**:** e1000985, PMID: 20628575.

[38] Srivastava A *et al.,* Nucleotide sequence and organization of the adeno-associated virus 2 genome. *J Virol* 1983, **45** (2)**:** 555-64, PMID: 6300419.

[39] Muramatsu S *et al.,* Nucleotide sequencing and generation of an infectious clone of adeno-associated virus 3. *Virology* 1996, **221** (1)**:** 208-17, PMID: 8661429.

[40] Chiorini JA *et al.,* Cloning and characterization of adeno-associated virus type 5. *J Virol* 1999, **73** (2)**:** 1309-19, PMID: 9882336.

[41] Rutledge EA *et al.,* Infectious clones and vectors derived from adeno-associated virus (AAV) serotypes other than AAV type 2. *J Virol* 1998, **72** (1)**:** 309-19, PMID: 9420229.

[42] Gao G *et al.,* Clades of Adeno-associated viruses are widely disseminated in human tissues. *J Virol* 2004, **78** (12)**:** 6381-8, PMID: 15163731.

[43] Xiao W *et al.,* Gene therapy vectors based on adeno-associated virus type 1. *J Virol* 1999, **73** (5)**:** 3994-4003, PMID: 10196295.

[44] Chiorini JA *et al.,* Cloning of adeno-associated virus type 4 (AAV4) and generation of recombinant AAV4 particles. *J Virol* 1997, **71** (9)**:** 6823-33, PMID: 9261407.

[45] Gao GP *et al.,* Novel adeno-associated viruses from rhesus monkeys as vectors for human gene therapy. *Proc Natl Acad Sci USA* 2002, **99** (18)**:** 11854-9, PMID: 12192090.

[46] Mori S *et al.,* Two novel adeno-associated viruses from cynomolgus monkey: pseudotyping characterization of capsid protein. *Virology* 2004, **330** (2)**:** 375-83, PMID: 15567432.

[47] Schmidt M *et al.,* Adeno-associated virus type 12 (AAV12): a novel AAV serotype with sialic acid- and heparan sulfate proteoglycan-independent transduction activity. *J Virol* 2008, **82** (3)**:** 1399-406, PMID: 18045941.

[48] Forsayeth JR, Bankiewicz KS AAV9: Over the Fence and Into the Woods. *Mol Ther* 2011, **19** (6)**:** 1006-7, PMID: 21629257.

[49] Pacak CA *et al.,* Recombinant adeno-associated virus serotype 9 leads to preferential cardiac transduction in vivo. *Circ Res* 2006, **99** (4)**:** e3-9, PMID: 16873720.

[50] Inagaki K *et al.,* Robust systemic transduction with AAV9 vectors in mice: efficient global cardiac gene transfer superior to that of AAV8. *Mol Ther* 2006, **14** (1)**:** 45-53, PMID: 16713360.

[51] Qi Y *et al.,* Selective tropism of the recombinant adeno-associated virus 9 serotype for rat cardiac tissue. *J Gene Med* 2010, **12** (1)**:** 22-34, PMID: 19830780.

[52] Mayor HD *et al.,* Plus and minus single-stranded DNA separately encapsidated in adeno-associated satellite virions. *Science* 1969, **166** (910)**:** 1280-2, PMID: 5350322.

[53] Hermonat PL *et al.,* Genetics of adeno-associated virus: isolation and preliminary characterization of adeno-associated virus type 2 mutants. *J Virol* 1984, **51** (2)**:** 329-39, PMID: 6086948.

[54] Johnson FB *et al.,* Structural proteins of adenovirus-associated virus type 3. *J Virol* 1971, **8** (6)**:** 860-63, PMID: 5172922.

[55] Rose JA *et al.,* Structural proteins of adenovirus-associated viruses. *J Virol* 1971, **8** (5)**:** 766-70, PMID: 5132697.

[56] Sonntag F *et al.,* A viral assembly factor promotes AAV2 capsid formation in the nucleolus. *Proc Natl Acad Sci USA* 2010, **107** (22)**:** 10220-5, PMID: 20479244.

[57] Lusby E *et al.,* Inverted terminal repetition in adeno-associated virus DNA: independence of the orientation at either end of the genome. *J Virol* 1981, **37** (3)**:** 1083-6, PMID: 6262528.

[58] McLaughlin SK *et al.,* Adeno-associated virus general transduction vectors: analysis of proviral structures. *J Virol* 1988, **62** (6)**:** 1963-73, PMID: 2835501.

[59] Samulski RJ *et al.,* Helper-free stocks of recombinant adeno-associated viruses: normal integration does not require viral gene expression. *J Virol* 1989, **63** (9)**:** 3822-8, PMID: 2547998.

[60] Goncalves MA Adeno-associated virus: from defective virus to effective vector. *Virol J* 2005, **2:** 43, PMID: 15877812.

[61] Balague C *et al.,* Adeno-associated virus Rep78 protein and terminal repeats enhance integration of DNA sequences into the cellular genome. *J Virol* 1997, **71** (4)**:** 3299-306, PMID: 9060699.

[62] Im DS, Muzyczka N The AAV origin binding protein Rep68 is an ATP-dependent site-specific endonuclease with DNA helicase activity. *Cell* 1990, **61** (3)**:** 447-57, PMID: 2159383.

[63] Snyder RO *et al.,* Evidence for covalent attachment of the adeno-associated virus (AAV) rep protein to the ends of the AAV genome. *J Virol* 1990, **64** (12)**:** 6204-13, PMID: 2173787.

[64] Ryan JH *et al.,* Sequence requirements for binding of Rep68 to the adeno-associated virus terminal repeats. *J Virol* 1996, **70** (3)**:** 1542-53, PMID: 8627673.

[65] Wang XS *et al.,* Rescue and replication signals of the adeno-associated virus 2 genome. *J Mol Biol* 1995, **250** (5)**:** 573-80, PMID: 7623375.

[66] Wang XS *et al.,* Adeno-associated virus type 2 DNA replication in vivo: mutation analyses of the D sequence in viral inverted terminal repeats. *J Virol* 1997, **71** (4)**:** 3077-82, PMID: 9060669.

[67] Wang XS *et al.,* Rescue and replication of adeno-associated virus type 2 as well as vector DNA sequences from recombinant plasmids containing deletions in the viral inverted terminal repeats: selective encapsidation of viral genomes in progeny virions. *J Virol* 1996, **70** (3)**:** 1668-77, PMID: 8627687.

[68] Di Pasquale G, Chiorini JA PKA/PrKX activity is a modulator of AAV/adenovirus interaction. *EMBO J* 2003, **22** (7)**:** 1716-24, PMID: 12660177.

[69] Di Pasquale G, Stacey SN Adeno-associated virus Rep78 protein interacts with protein kinase A and its homolog PRKX and inhibits CREB-dependent transcriptional activation. *J Virol* 1998, **72** (10)**:** 7916-25, PMID: 9733829.

[70] Han SI *et al.,* Rep68 protein of adeno-associated virus type 2 interacts with 14-3-3 proteins depending on phosphorylation at serine 535. *Virology* 2004, **320** (1)**:** 144-55, PMID: 15003870.

[71] Tratschin JD *et al.,* Genetic analysis of adeno-associated virus: properties of deletion mutants constructed in vitro and evidence for an adeno-associated virus replication function. *J Virol* 1984, **51** (3)**:** 611-9, PMID: 6088786.

[72] Chejanovsky N, Carter BJ Mutagenesis of an AUG codon in the adeno-associated virus rep gene: effects on viral DNA replication. *Virology* 1989, **173** (1)**:** 120-8, PMID: 2554565.

[73] Im DS, Muzyczka N Partial purification of adeno-associated virus Rep78, Rep52, and Rep40 and their biochemical characterization. *J Virol* 1992, **66** (2)**:** 1119-28, PMID: 1309894.

[74] Chiorini JA *et al.,* The roles of AAV Rep proteins in gene expression and targeted integration. *Curr Top Microbiol Immunol* 1996, **218:** 25-33, PMID: 8794243.

[75] Zhou X *et al.,* Biochemical characterization of adeno-associated virus rep68 DNA helicase and ATPase activities. *J Virol* 1999, **73** (2)**:** 1580-90, PMID: 9882364.

[76] King JA *et al.,* DNA helicase-mediated packaging of adeno-associated virus type 2 genomes into preformed capsids. *EMBO J* 2001, **20** (12)**:** 3282-91, PMID: 11406604.

[77] Nash K *et al.,* Identification of cellular proteins that interact with the adeno-associated virus rep protein. *J Virol* 2009, **83** (1)**:** 454-69, PMID: 18971280.

[78] Kyostio SR *et al.,* Analysis of adeno-associated virus (AAV) wild-type and mutant Rep proteins for their abilities to negatively regulate AAV p5 and p19 mRNA levels. *J Virol* 1994, **68** (5)**:** 2947-57, PMID: 8151765.

[79] Horer M *et al.,* Mutational analysis of adeno-associated virus Rep protein-mediated inhibition of heterologous and homologous promoters. *J Virol* 1995, **69** (9)**:** 5485-96, PMID: 7636994.

[80] Laughlin CA *et al.,* Spliced adenovirus-associated virus RNA. *Proc Natl Acad Sci USA* 1979, **76** (11)**:** 5567-71, PMID: 230481.

[81] Cassinotti P *et al.,* Organization of the adeno-associated virus (AAV) capsid gene: mapping of a minor spliced mRNA coding for virus capsid protein. *Virology* 1988, **167** (1)**:** 176-84, PMID: 18644583.

[82] Trempe JP, Carter BJ Alternate mRNA splicing is required for synthesis of adeno-associated virus VP1 capsid protein. *J Virol* 1988, **62** (9)**:** 3356-63, PMID: 2841488.

[83] Bleker S *et al.,* Mutational analysis of narrow pores at the fivefold symmetry axes of adeno-associated virus type 2 capsids reveals a dual role in genome packaging and activation of phospholipase A2 activity. *J Virol* 2005, **79** (4)**:** 2528-40, PMID: 15681453.

[84] Girod A *et al.,* The VP1 capsid protein of adeno-associated virus type 2 is carrying a phospholipase A2 domain required for virus infectivity. *J Gen Virol* 2002, **83** (Pt 5)**:** 973-8, PMID: 11961250.

[85] Zadori Z *et al.,* A viral phospholipase A2 is required for parvovirus infectivity. *Dev Cell* 2001, **1** (2)**:** 291-302, PMID: 11702787.

[86] Sonntag F *et al.,* Adeno-associated virus type 2 capsids with externalized VP1/VP2 trafficking domains are generated prior to passage through the cytoplasm and are maintained until uncoating occurs in the nucleus. *J Virol* 2006, **80** (22)**:** 11040-54, PMID: 16956943.

[87] Grieger JC *et al.,* Separate basic region motifs within the adeno-associated virus capsid proteins are essential for infectivity and assembly. *J Virol* 2006, **80** (11)**:** 5199-210, PMID: 16699000.

[88] Grieger JC *et al.,* Surface-exposed adeno-associated virus Vp1-NLS capsid fusion protein rescues infectivity of noninfectious wild-type Vp2/Vp3 and Vp3-only capsids but not that of fivefold pore mutant virions. *J Virol* 2007, **81** (15)**:** 7833-43, PMID: 17507473.

[89] Hoque M *et al.,* Nuclear transport of the major capsid protein is essential for adeno-associated virus capsid formation. *J Virol* 1999, **73** (9)**:** 7912-5, PMID: 10438891.

[90] Kern A *et al.,* Identification of a heparin-binding motif on adeno-associated virus type 2 capsids. *J Virol* 2003, **77** (20)**:** 11072-81, PMID: 14512555.

[91] Opie SR *et al.,* Identification of amino acid residues in the capsid proteins of adeno-associated virus type 2 that contribute to heparan sulfate proteoglycan binding. *J Virol* 2003, **77** (12)**:** 6995-7006, PMID: 12768018.

[92] Summerford C, Samulski RJ Membrane-associated heparan sulfate proteoglycan is a receptor for adeno-associated virus type 2 virions. *J Virol* 1998, **72** (2)**:** 1438-45, PMID: 9445046.

[93] Caspar DL, Klug A Physical principles in the construction of regular viruses. *Cold Spring Harb Symp Quant Biol* 1962, **27:** 1-24, PMID: 14019094.

[94] Xie Q *et al.,* The atomic structure of adeno-associated virus (AAV-2), a vector for human gene therapy. *Proc Natl Acad Sci USA* 2002, **99** (16)**:** 10405-10, PMID: 12136130.

[95] Lerch TF *et al.,* Twinned crystals of adeno-associated virus serotype 3b prove suitable for structural studies. *Acta Crystallogr Sect F Struct Biol Cryst Commun* 2009, **65** (Pt 2)**:** 177-83, PMID: 19194015.

[96] Govindasamy L *et al.,* Structurally mapping the diverse phenotype of adeno-associated virus serotype 4. *J Virol* 2006, **80** (23)**:** 11556-70, PMID: 16971437.

[97] Ng R *et al.,* Structural characterization of the dual glycan binding adeno-associated virus serotype 6. *J Virol* 2010, **84** (24)**:** 12945-57, PMID: 20861247.

[98] Nam HJ *et al.,* Structure of adeno-associated virus serotype 8, a gene therapy vector. *J Virol* 2007, **81** (22)**:** 12260-71, PMID: 17728238.

[99] Kronenberg S *et al.,* Electron cryo-microscopy and image reconstruction of adeno-associated virus type 2 empty capsids. *EMBO Rep* 2001, **2** (11)**:** 997-1002, PMID: 11713191.

[100] Padron E *et al.,* Structure of adeno-associated virus type 4. *J Virol* 2005, **79** (8)**:** 5047-58, PMID: 15795290.

[101] Walters RW *et al.,* Structure of adeno-associated virus serotype 5. *J Virol* 2004, **78** (7)**:** 3361-71, PMID: 15016858.

[102] Miller EB *et al.,* Production, purification and preliminary X-ray crystallographic studies of adeno-associated virus serotype 1. *Acta Crystallogr Sect F Struct Biol Cryst Commun* 2006, **62** (Pt 12)**:** 1271-4, PMID: 17142915.

[103] Quesada O *et al.,* Production, purification and preliminary X-ray crystallographic studies of adeno-associated virus serotype 7. *Acta Crystallogr Sect F Struct Biol Cryst Commun* 2007, **63** (Pt 12)**:** 1073-6, PMID: 18084098.

[104] Mitchell M *et al.,* Production, purification and preliminary X-ray crystallographic studies of adeno-associated virus serotype 9. *Acta Crystallogr Sect F Struct Biol Cryst Commun* 2009, **65** (Pt 7)**:** 715-8, PMID: 19574648.

[105] Tsao J *et al.,* The three-dimensional structure of canine parvovirus and its functional implications. *Science* 1991, **251** (5000)**:** 1456-64, PMID: 2006420.

[106] Agbandje M *et al.,* Structure determination of feline panleukopenia virus empty particles. *Proteins* 1993, **16** (2)**:** 155-71, PMID: 8392729.

[107] Agbandje-McKenna M *et al.,* Functional implications of the structure of the murine parvovirus, minute virus of mice. *Structure* 1998, **6** (11)**:** 1369-81, PMID: 9817841.

[108] Agbandje M *et al.,* The structure of human parvovirus B19 at 8 A resolution. *Virology* 1994, **203** (1)**:** 106-15, PMID: 8030266.

[109] Lochrie MA *et al.,* Mutations on the external surfaces of adeno-associated virus type 2 capsids that affect transduction and neutralization. *J Virol* 2006, **80** (2)**:** 821-34, PMID: 16378984.

[110] Chapman MS, Rossmann MG Structure, sequence, and function correlations among parvoviruses. *Virology* 1993, **194** (2)**:** 491-508, PMID: 8503170.

[111] Shen X *et al.,* Characterization of the relationship of AAV capsid domain swapping to liver transduction efficiency. *Mol Ther* 2007, **15** (11)**:** 1955-62, PMID: 17726459.

[112] DiPrimio N *et al.,* Surface loop dynamics in adeno-associated virus capsid assembly. *J Virol* 2008, **82** (11)**:** 5178-89, PMID: 18367523.

[113] Ling C *et al.,* Human hepatocyte growth factor receptor is a cellular coreceptor for adeno-associated virus serotype 3. *Hum Gene Ther* 2010, **21** (12)**:** 1741-7, PMID: 20545554.

[114] Kaludov N *et al.,* Adeno-associated virus serotype 4 (AAV4) and AAV5 both require sialic acid binding for hemagglutination and efficient transduction but differ in sialic acid linkage specificity. *J Virol* 2001, **75** (15)**:** 6884-93, PMID: 11435568.

[115] Seiler MP *et al.,* Adeno-associated virus types 5 and 6 use distinct receptors for cell entry. *Hum Gene Ther* 2006, **17** (1)**:** 10-9, PMID: 16409121.

[116] Wu Z *et al.,* Alpha2,3 and alpha2,6 N-linked sialic acids facilitate efficient binding and transduction by adeno-associated virus types 1 and 6. *J Virol* 2006, **80** (18)**:** 9093-103, PMID: 16940521.

[117] Bell CL *et al.,* The AAV9 receptor and its modification to improve in vivo lung gene transfer in mice. *J Clin Invest* 2011, **121** (6)**:** 2427-35, PMID: 21576824.

[118] Boyle MP *et al.,* Membrane-associated heparan sulfate is not required for rAAV-2 infection of human respiratory epithelia. *Virol J* 2006, **3:** 29, PMID: 16630361.

[119] Handa A *et al.,* Adeno-associated virus (AAV)-3-based vectors transduce haematopoietic cells not susceptible to transduction with AAV-2-based vectors. *J Gen Virol* 2000, **81** (Pt 8)**:** 2077-84, PMID: 10900047.

[120] Summerford C *et al.,* AlphaVbeta5 integrin: a co-receptor for adeno-associated virus type 2 infection. *Nat Med* 1999, **5** (1)**:** 78-82, PMID: 9883843.

[121] Kashiwakura Y *et al.,* Hepatocyte growth factor receptor is a coreceptor for adeno-associated virus type 2 infection. *J Virol* 2005, **79** (1)**:** 609-14, PMID: 15596854.

[122] Kurzeder C *et al.,* CD9 promotes adeno-associated virus type 2 infection of mammary carcinoma cells with low cell surface expression of heparan sulphate proteoglycans. *Int J Mol Med* 2007, **19** (2)**:** 325-33, PMID: 17203208.

[123] Qing K *et al.,* Human fibroblast growth factor receptor 1 is a co-receptor for infection by adeno-associated virus 2. *Nat Med* 1999, **5** (1)**:** 71-7, PMID: 9883842.

[124] Blackburn SD *et al.,* Attachment of adeno-associated virus type 3H to fibroblast growth factor receptor 1. *Arch Virol* 2006, **151** (3)**:** 617-23, PMID: 16195782.

[125] Akache B *et al.,* The 37/67-kilodalton laminin receptor is a receptor for adeno-associated virus serotypes 8, 2, 3, and 9. *J Virol* 2006, **80** (19)**:** 9831-6, PMID: 16973587.

[126] Di Pasquale G *et al.,* Identification of PDGFR as a receptor for AAV-5 transduction. *Nat Med* 2003, **9** (10)**:** 1306-12, PMID: 14502277.

[127] O'Donnell J *et al.,* Adeno-associated virus-2 and its primary cellular receptor--Cryo-EM structure of a heparin complex. *Virology* 2009, **385** (2)**:** 434-43, PMID: 19144372.

[128] Bartlett JS *et al.,* Infectious entry pathway of adeno-associated virus and adeno-associated virus vectors. *J Virol* 2000, **74** (6)**:** 2777-85, PMID: 10684294.

[129] Duan D *et al.,* Dynamin is required for recombinant adeno-associated virus type 2 infection. *J Virol* 1999, **73** (12)**:** 10371-6, PMID: 10559355.

[130] Bantel-Schaal U *et al.,* Adeno-associated virus type 5 exploits two different entry pathways in human embryo fibroblasts. *J Gen Virol* 2009, **90** (Pt 2)**:** 317-22, PMID: 19141440.

[131] Seisenberger G *et al.,* Real-time single-molecule imaging of the infection pathway of an adeno-associated virus. *Science* 2001, **294** (5548)**:** 1929-32, PMID: 11729319.

[132] Sanlioglu S *et al.,* Endocytosis and nuclear trafficking of adeno-associated virus type 2 are controlled by rac1 and phosphatidylinositol-3 kinase activation. *J Virol* 2000, **74** (19)**:** 9184-96, PMID: 10982365.

[133] Duan D *et al.,* Endosomal processing limits gene transfer to polarized airway epithelia by adeno-associated virus. *J Clin Invest* 2000, **105** (11)**:** 1573-87, PMID: 10841516.

[134] Hansen J *et al.,* Impaired intracellular trafficking of adeno-associated virus type 2 vectors limits efficient transduction of murine fibroblasts. *J Virol* 2000, **74** (2)**:** 992-6, PMID: 10623762.

[135] Hansen J *et al.,* Adeno-associated virus type 2-mediated gene transfer: altered endocytic processing enhances transduction efficiency in murine fibroblasts. *J Virol* 2001, **75** (9)**:** 4080-90, PMID: 11287557.

[136] Hauck B *et al.,* Intracellular viral processing, not single-stranded DNA accumulation, is crucial for recombinant adeno-associated virus transduction. *J Virol* 2004, **78** (24)**:** 13678-86, PMID: 15564477.

[137] Xiao W *et al.,* Adenovirus-facilitated nuclear translocation of adeno-associated virus type 2. *J Virol* 2002, **76** (22)**:** 11505-17, PMID: 12388712.

[138] Douar AM *et al.,* Intracellular trafficking of adeno-associated virus vectors: routing to the late endosomal compartment and proteasome degradation. *J Virol* 2001, **75** (4)**:** 1824-33, PMID: 11160681.

[139] Yan Z *et al.,* Distinct classes of proteasome-modulating agents cooperatively augment recombinant adeno-associated virus type 2 and type 5-mediated transduction from the apical surfaces of human airway epithelia. *J Virol* 2004, **78** (6)**:** 2863-74, PMID: 14990705.

[140] Ding W *et al.,* Intracellular trafficking of adeno-associated viral vectors. *Gene Ther* 2005, **12** (11)**:** 873-80, PMID: 15829993.

[141] Pajusola K *et al.,* Cell-type-specific characteristics modulate the transduction efficiency of adeno-associated virus type 2 and restrain infection of endothelial cells. *J Virol* 2002, **76** (22)**:** 11530-40, PMID: 12388714.

[142] Ding W *et al.,* rAAV2 traffics through both the late and the recycling endosomes in a dose-dependent fashion. *Mol Ther* 2006, **13** (4)**:** 671-82, PMID: 16442847.

[143] Stahnke S *et al.,* Intrinsic phospholipase A2 activity of adeno-associated virus is involved in endosomal escape of incoming particles. *Virology* 2011, **409** (1)**:** 77-83, PMID: 20974479.

[144] Farr GA *et al.,* Parvoviral virions deploy a capsid-tethered lipolytic enzyme to breach the endosomal membrane during cell entry. *Proc Natl Acad Sci USA* 2005, **102** (47)**:** 17148-53, PMID: 16284249.

[145] Akache B *et al.,* A two-hybrid screen identifies cathepsins B and L as uncoating factors for adeno-associated virus 2 and 8. *Mol Ther* 2007, **15** (2)**:** 330-9, PMID: 17235311.

[146] Yan Z *et al.,* Ubiquitination of both adeno-associated virus type 2 and 5 capsid proteins affects the transduction efficiency of recombinant vectors. *J Virol* 2002, **76** (5)**:** 2043-53, PMID: 11836382.

[147] Zhong L *et al.,* Tyrosine-phosphorylation of AAV2 vectors and its consequences on viral intracellular trafficking and transgene expression. *Virology* 2008, **381** (2)**:** 194-202, PMID: 18834608.

[148] Kelkar S *et al.,* A common mechanism for cytoplasmic dynein-dependent microtubule binding shared among adeno-associated virus and adenovirus serotypes. *J Virol* 2006, **80** (15)**:** 7781-5, PMID: 16840360.

[149] Ferrari FK *et al.,* Second-strand synthesis is a rate-limiting step for efficient transduction by recombinant adeno-associated virus vectors. *J Virol* 1996, **70** (5)**:** 3227-34, PMID: 8627803.

[150] Fisher KJ *et al.,* Transduction with recombinant adeno-associated virus for gene therapy is limited by leading-strand synthesis. *J Virol* 1996, **70** (1)**:** 520-32, PMID: 8523565.

[151] Johnson JS, Samulski RJ Enhancement of adeno-associated virus infection by mobilizing capsids into and out of the nucleolus. *J Virol* 2009, **83** (6)**:** 2632-44, PMID: 19109385.

[152] Cervelli T *et al.,* Processing of recombinant AAV genomes occurs in specific nuclear structures that overlap with foci of DNA-damage-response proteins. *J Cell Sci* 2008, **121** (Pt 3)**:** 349-57, PMID: 18216333.

[153] Schnepp BC *et al.,* Characterization of adeno-associated virus genomes isolated from human tissues. *J Virol* 2005, **79** (23)**:** 14793-803, PMID: 16282479.

[154] Wistuba A *et al.,* Subcellular compartmentalization of adeno-associated virus type 2 assembly. *J Virol* 1997, **71** (2)**:** 1341-52, PMID: 8995658.

[155] Qiu J, Brown KE A 110-kDa nuclear shuttle protein, nucleolin, specifically binds to adeno-associated virus type 2 (AAV-2) capsid. *Virology* 1999, **257** (2)**:** 373-82, PMID: 10329548.

[156] Bevington JM *et al.,* Adeno-associated virus interactions with B23/Nucleophosmin: identification of sub-nucleolar virion regions. *Virology* 2007, **357** (1)**:** 102-13, PMID: 16959286.

[157] Prasad KM, Trempe JP The adeno-associated virus Rep78 protein is covalently linked to viral DNA in a preformed virion. *Virology* 1995, **214** (2)**:** 360-70, PMID: 8553536.

[158] Wistuba A *et al.,* Intermediates of adeno-associated virus type 2 assembly: identification of soluble complexes containing Rep and Cap proteins. *J Virol* 1995, **69** (9)**:** 5311-9, PMID: 7636974.

[159] Dubielzig R *et al.,* Adeno-associated virus type 2 protein interactions: formation of pre-encapsidation complexes. *J Virol* 1999, **73** (11)**:** 8989-98, PMID: 10516005.

[160] Bleker S. Funktionelle Analyse der Kanäle an dem 5-fachen Symmetrieachsen von Kapsiden des Adeno-assoziierten Virus des Typ 2. Ruprecht-Karls Universität, Heidelberg, 2006.

[161] Boutin S *et al.,* Prevalence of serum IgG and neutralizing factors against adeno-associated virus (AAV) types 1, 2, 5, 6, 8, and 9 in the healthy population: implications for gene therapy using AAV vectors. *Hum Gene Ther* 2010, **21** (6)**:** 704-12, PMID: 20095819.

[162] Calcedo R *et al.,* Worldwide epidemiology of neutralizing antibodies to adeno-associated viruses. *J Infect Dis* 2009, **199** (3)**:** 381-90, PMID: 19133809.

[163] Zaiss AK, Muruve DA Immunity to adeno-associated virus vectors in animals and humans: a continued challenge. *Gene Ther* 2008, **15** (11)**:** 808-16, PMID: 18385765.

[164] Nayak S, Herzog RW Progress and prospects: immune responses to viral vectors. *Gene Ther* 2010, **17** (3)**:** 295-304, PMID: 19907498.

[165] Zaiss AK *et al.,* Differential activation of innate immune responses by adenovirus and adeno-associated virus vectors. *J Virol* 2002, **76** (9)**:** 4580-90, PMID: 11932423.

[166] McCaffrey AP *et al.,* The host response to adenovirus, helper-dependent adenovirus, and adeno-associated virus in mouse liver. *Mol Ther* 2008, **16** (5)**:** 931-41, PMID: 18388926.

[167] Zhu J *et al.,* The TLR9-MyD88 pathway is critical for adaptive immune responses to adeno-associated virus gene therapy vectors in mice. *J Clin Invest* 2009, **119** (8)**:** 2388-98, PMID: 19587448.

[168] Madsen D *et al.,* Adeno-associated virus serotype 2 induces cell-mediated immune responses directed against multiple epitopes of the capsid protein VP1. *J Gen Virol* 2009, **90** (Pt 11)**:** 2622-33, PMID: 19641045.

[169] Zaiss AK, Muruve DA Immune responses to adeno-associated virus vectors. *Curr Gene Ther* 2005, **5** (3)**:** 323-31, PMID: 15975009.

[170] Murphy SL *et al.,* Diverse IgG subclass responses to adeno-associated virus infection and vector administration. *J Med Virol* 2009, **81** (1)**:** 65-74, PMID: 19031458.

[171] Mingozzi F *et al.,* CD8(+) T-cell responses to adeno-associated virus capsid in humans. *Nat Med* 2007, **13** (4)**:** 419-22, PMID: 17369837.

[172] Moskalenko M *et al.,* Epitope mapping of human anti-adeno-associated virus type 2 neutralizing antibodies: implications for gene therapy and virus structure. *J Virol* 2000, **74** (4)**:** 1761-6, PMID: 10644347.

[173] Wobus CE *et al.,* Monoclonal antibodies against the adeno-associated virus type 2 (AAV-2) capsid: epitope mapping and identification of capsid domains involved in AAV-2-cell interaction and neutralization of AAV-2 infection. *J Virol* 2000, **74** (19)**:** 9281-93, PMID: 10982375.

[174] Huttner NA *et al.,* Genetic modifications of the adeno-associated virus type 2 capsid reduce the affinity and the neutralizing effects of human serum antibodies. *Gene Ther* 2003, **10** (26)**:** 2139-47, PMID: 14625569.

[175] Manno CS *et al.,* Successful transduction of liver in hemophilia by AAV-Factor IX and limitations imposed by the host immune response. *Nat Med* 2006, **12** (3)**:** 342-7, PMID: 16474400.

[176] Grimm D *et al.,* Novel tools for production and purification of recombinant adenoassociated virus vectors. *Hum Gene Ther* 1998, **9** (18)**:** 2745-60, PMID: 9874273.

[177] Xiao X *et al.,* Production of high-titer recombinant adeno-associated virus vectors in the absence of helper adenovirus. *J Virol* 1998, **72** (3)**:** 2224-32, PMID: 9499080.

[178] Grimm D *et al.,* Helper virus-free, optically controllable, and two-plasmid-based production of adeno-associated virus vectors of serotypes 1 to 6. *Mol Ther* 2003, **7** (6)**:** 839-50, PMID: 12788658.

[179] Wu J *et al.,* Self-complementary recombinant adeno-associated viral vectors: packaging capacity and the role of rep proteins in vector purity. *Hum Gene Ther* 2007, **18** (2)**:** 171-82, PMID: 17328683.

[180] McCarty DM *et al.,* Self-complementary recombinant adeno-associated virus (scAAV) vectors promote efficient transduction independently of DNA synthesis. *Gene Ther* 2001, **8** (16)**:** 1248-54, PMID: 11509958.

[181] McCarty DM Self-complementary AAV vectors; advances and applications. *Mol Ther* 2008, **16** (10)**:** 1648-56, PMID: 18682697.

[182] Michelfelder S, Trepel M Adeno-associated viral vectors and their redirection to cell-type specific receptors. *Adv Genet* 2009, **67:** 29-60, PMID: 19914449.

[183] Kwon I, Schaffer DV Designer gene delivery vectors: molecular engineering and evolution of adeno-associated viral vectors for enhanced gene transfer. *Pharm Res* 2008, **25** (3)**:** 489-99, PMID: 17763830.

[184] Vandenberghe LH *et al.,* Tailoring the AAV vector capsid for gene therapy. *Gene Ther* 2009, **16** (3)**:** 311-9, PMID: 19052631.

[185] Davidson BL *et al.,* Recombinant adeno-associated virus type 2, 4, and 5 vectors: transduction of variant cell types and regions in the mammalian central nervous system. *Proc Natl Acad Sci USA* 2000, **97** (7)**:** 3428-32, PMID: 10688913.

[186] Hauck B *et al.,* Generation and characterization of chimeric recombinant AAV vectors. *Mol Ther* 2003, **7** (3)**:** 419-25, PMID: 12668138.

[187] Rabinowitz JE *et al.,* Cross-dressing the virion: the transcapsidation of adeno-associated virus serotypes functionally defines subgroups. *J Virol* 2004, **78** (9)**:** 4421-32, PMID: 15078923.

[188] Bartlett JS *et al.,* Targeted adeno-associated virus vector transduction of nonpermissive cells mediated by a bispecific F(ab'gamma)2 antibody. *Nat Biotechnol* 1999, **17** (2)**:** 181-6, PMID: 10052356.

[189] Ponnazhagan S *et al.,* Conjugate-based targeting of recombinant adeno-associated virus type 2 vectors by using avidin-linked ligands. *J Virol* 2002, **76** (24)**:** 12900-7, PMID: 12438615.

[190] Yang Q *et al.,* Development of novel cell surface CD34-targeted recombinant adeno-associated virus vectors for gene therapy. *Hum Gene Ther* 1998, **9** (13)**:** 1929-37, PMID: 9741431.

[191] Wu P *et al.,* Mutational analysis of the adeno-associated virus type 2 (AAV2) capsid gene and construction of AAV2 vectors with altered tropism. *J Virol* 2000, **74** (18)**:** 8635-47, PMID: 10954565.

[192] Loiler SA *et al.,* Targeting recombinant adeno-associated virus vectors to enhance gene transfer to pancreatic islets and liver. *Gene Ther* 2003, **10** (18)**:** 1551-8, PMID: 12907946.

[193] Girod A *et al.,* Genetic capsid modifications allow efficient re-targeting of adeno-associated virus type 2. *Nat Med* 1999, **5** (12)**:** 1438, PMID: 10581091.

[194] Perabo L *et al.,* In vitro selection of viral vectors with modified tropism: the adeno-associated virus display. *Mol Ther* 2003, **8** (1)**:** 151-7, PMID: 12842438.

[195] Muller OJ *et al.,* Random peptide libraries displayed on adeno-associated virus to select for targeted gene therapy vectors. *Nat Biotechnol* 2003, **21** (9)**:** 1040-6, PMID: 12897791.

[196] Michelfelder S *et al.,* Successful expansion but not complete restriction of tropism of adeno-associated virus by in vivo biopanning of random virus display peptide libraries. *PLoS One* 2009, **4** (4)**:** e5122, PMID: 19357785.

[197] Buning H *et al.,* Receptor targeting of adeno-associated virus vectors. *Gene Ther* 2003, **10** (14)**:** 1142-51, PMID: 12833123.

[198] Pasqualini R, Ruoslahti E Organ targeting in vivo using phage display peptide libraries. *Nature* 1996, **380** (6572)**:** 364-6, PMID: 8598934.

[199] Grifman M *et al.,* Incorporation of tumor-targeting peptides into recombinant adeno-associated virus capsids. *Mol Ther* 2001, **3** (6)**:** 964-75, PMID: 11407911.

[200] Nicklin SA *et al.,* Efficient and selective AAV2-mediated gene transfer directed to human vascular endothelial cells. *Mol Ther* 2001, **4** (3)**:** 174-81, PMID: 11545607.

[201] Waterkamp DA *et al.,* Isolation of targeted AAV2 vectors from novel virus display libraries. *J Gene Med* 2006, **8** (11)**:** 1307-19, PMID: 16955542.

[202] Michelfelder S *et al.,* Vectors selected from adeno-associated viral display peptide libraries for leukemia cell-targeted cytotoxic gene therapy. *Exp Hematol* 2007, **35** (12)**:** 1766-76, PMID: 17920758.

[203] Ying Y *et al.,* Heart-targeted adeno-associated viral vectors selected by in vivo biopanning of a random viral display peptide library. *Gene Ther* 2010, **17** (8)**:** 980-90, PMID: 20393510.

[204] Rothe A *et al.,* In vitro display technologies reveal novel biopharmaceutics. *FASEB J* 2006, **20** (10)**:** 1599-610, PMID: 16873883.

[205] Hoogenboom HR Selecting and screening recombinant antibody libraries. *Nat Biotechnol* 2005, **23** (9)**:** 1105-16, PMID: 16151404.

[206] Bupp K *et al.,* Selection of feline leukemia virus envelope proteins from a library by functional association with a murine leukemia virus envelope. *Virology* 2006, **351** (2)**:** 340-8, PMID: 16678875.

[207] Perabo L *et al.,* Combinatorial engineering of a gene therapy vector: directed evolution of adeno-associated virus. *J Gene Med* 2006, **8** (2)**:** 155-62, PMID: 16285001.

[208] Maheshri N *et al.,* Directed evolution of adeno-associated virus yields enhanced gene delivery vectors. *Nat Biotechnol* 2006, **24** (2)**:** 198-204, PMID: 16429148.

[209] Zhao H *et al.,* Molecular evolution by staggered extension process (StEP) in vitro recombination. *Nat Biotechnol* 1998, **16** (3)**:** 258-61, PMID: 9528005.

[210] Stemmer WP DNA shuffling by random fragmentation and reassembly: in vitro recombination for molecular evolution. *Proc Natl Acad Sci USA* 1994, **91** (22)**:** 10747-51, PMID: 7938023.

[211] Soong NW *et al.,* Molecular breeding of viruses. *Nat Genet* 2000, **25** (4)**:** 436-9, PMID: 10932190.

[212] Koerber JT *et al.,* DNA shuffling of adeno-associated virus yields functionally diverse viral progeny. *Mol Ther* 2008, **16** (10)**:** 1703-9, PMID: 18728640.

[213] Grimm D *et al.,* In vitro and in vivo gene therapy vector evolution via multispecies interbreeding and retargeting of adeno-associated viruses. *J Virol* 2008, **82** (12)**:** 5887-911, PMID: 18400866.

[214] Yang L *et al.,* A myocardium tropic adeno-associated virus (AAV) evolved by DNA shuffling and in vivo selection. *Proc Natl Acad Sci USA* 2009, **106** (10)**:** 3946-51, PMID: 19234115.

[215] Gray SJ *et al.,* Directed evolution of a novel adeno-associated virus (AAV) vector that crosses the seizure-compromised blood-brain barrier (BBB). *Mol Ther* 2010, **18** (3)**:** 570-8, PMID: 20040913.

[216] Jang JH *et al.,* An evolved adeno-associated viral variant enhances gene delivery and gene targeting in neural stem cells. *Mol Ther* 2011, **19** (4)**:** 667-75, PMID: 21224831.

[217] Deanfield J *et al.,* Endothelial function and dysfunction. Part I: Methodological issues for assessment in the different vascular beds: a statement by the Working Group on Endothelin and Endothelial Factors of the European Society of Hypertension. *J Hypertens* 2005, **23** (1)**:** 7-17, PMID: 15643116.

[218] Gruchala M *et al.,* Gene transfer into rabbit arteries with adeno-associated virus and adenovirus vectors. *J Gene Med* 2004, **6** (5)**:** 545-54, PMID: 15133765.

[219] Sen S *et al.,* Gene delivery to the vasculature mediated by low-titre adeno-associated virus serotypes 1 and 5. *J Gene Med* 2008, **10** (2)**:** 143-51, PMID: 18067196.

[220] Denby L *et al.,* Adeno-associated virus (AAV)-7 and -8 poorly transduce vascular endothelial cells and are sensitive to proteasomal degradation. *Gene Ther* 2005, **12** (20)**:** 1534-8, PMID: 15944729.

[221] Nicklin SA *et al.,* Selective targeting of gene transfer to vascular endothelial cells by use of peptides isolated by phage display. *Circulation* 2000, **102** (2)**:** 231-7, PMID: 10889136.

[222] White SJ *et al.,* Targeted gene delivery to vascular tissue in vivo by tropism-modified adeno-associated virus vectors. *Circulation* 2004, **109** (4)**:** 513-9, PMID: 14732747.

[223] Work LM *et al.,* Vascular bed-targeted in vivo gene delivery using tropism-modified adeno-associated viruses. *Mol Ther* 2006, **13** (4)**:** 683-93, PMID: 16387552.

[224] Goehringer C *et al.,* Prevention of cardiomyopathy in delta-sarcoglycan knockout mice after systemic transfer of targeted adeno-associated viral vectors. *Cardiovasc Res* 2009, **82** (3)**:** 404-10, PMID: 19218289.

[225] Zincarelli C *et al.,* Analysis of AAV serotypes 1-9 mediated gene expression and tropism in mice after systemic injection. *Mol Ther* 2008, **16** (6)**:** 1073-80, PMID: 18414476.

[226] Fallaux FJ *et al.,* Characterization of 911: a new helper cell line for the titration and propagation of early region 1-deleted adenoviral vectors. *Hum Gene Ther* 1996, **7** (2)**:** 215-22, PMID: 8788172.

[227] DuBridge RB *et al.,* Analysis of mutation in human cells by using an Epstein-Barr virus shuttle system. *Mol Cell Biol* 1987, **7** (1)**:** 379-87, PMID: 3031469.

[228] Garlanda C *et al.,* Progressive growth in immunodeficient mice and host cell recruitment by mouse endothelial cells transformed by polyoma middle-sized T antigen: implications for the pathogenesis of opportunistic vascular tumors. *Proc Natl Acad Sci USA* 1994, **91** (15)**:** 7291-5, PMID: 8041783.

[229] Boecker W *et al.,* Cardiac-specific gene expression facilitated by an enhanced myosin light chain promoter. *Mol Imaging* 2004, **3** (2)**:** 69-75, PMID: 15296671.

[230] Samulski RJ *et al.,* A recombinant plasmid from which an infectious adeno-associated virus genome can be excised in vitro and its use to study viral replication. *J Virol* 1987, **61** (10)**:** 3096-101, PMID: 3041032.

[231] Reed SE *et al.,* Transfection of mammalian cells using linear polyethylenimine is a simple and effective means of producing recombinant adeno-associated virus vectors. *J Virol Methods* 2006, **138** (1-2)**:** 85-98, PMID: 16950522.

[232] Bazan-Peregrino M *et al.,* Gene therapy targeting to tumor endothelium. *Cancer Gene Ther* 2007, **14** (2)**:** 117-27, PMID: 17096029.

[233] Gory S *et al.,* The vascular endothelial-cadherin promoter directs endothelial-specific expression in transgenic mice. *Blood* 1999, **93** (1)**:** 184-92, PMID: 9864160.

[234] Naumer M. Implications of capsid modifications by selected peptide ligands on rAAV-mediated gene transduction. Ruprecht-Karls Universität, Heidelberg, 2011.

[235] Waterkamp D. Optimierung und Anwendung einer randomisierten auf Adeno-assoziierten Viren exprimierten Peptidbank. Ruprecht-Karls Universität, Heidelberg, 2005.

[236] Ying Y. Improvement and application of random adeno-associated virus type 2 (AAV2) display peptide libraries for selection of targeted gene transfer AAV2 vectors. Ruprecht-Karls Universität, Heidelberg, 2008.

[237] Perabo L. Adeno-associated virus display: *in vitro* evolution of AAV retargeted vectors. Ruprecht-Karls Universität, Heidelberg, 2003.

[238] Pierschbacher MD, Ruoslahti E Cell attachment activity of fibronectin can be duplicated by small synthetic fragments of the molecule. *Nature* 1984, **309** (5963)**:** 30-3, PMID: 6325925.

[239] Pytela R *et al.,* Identification and isolation of a 140 kd cell surface glycoprotein with properties expected of a fibronectin receptor. *Cell* 1985, **40** (1)**:** 191-8, PMID: 3155652.

[240] Tamkun JW *et al.,* Structure of integrin, a glycoprotein involved in the transmembrane linkage between fibronectin and actin. *Cell* 1986, **46** (2)**:** 271-82, PMID: 3487386.

[241] Conlon TJ *et al.,* Efficient hepatic delivery and expression from a recombinant adeno-associated virus 8 pseudotyped alpha1-antitrypsin vector. *Mol Ther* 2005, **12** (5)**:** 867-75, PMID: 16085464.

[242] Graham T *et al.,* Performance of AAV8 vectors expressing human factor IX from a hepatic-selective promoter following intravenous injection into rats. *Genet Vaccines Ther* 2008, **6:** 9, PMID: 18312698.

[243] Bessis N *et al.,* Immune responses to gene therapy vectors: influence on vector function and effector mechanisms. *Gene Ther* 2004, **11 Suppl 1:** S10-7, PMID: 15454952.

[244] Snyder RO *et al.,* Persistent and therapeutic concentrations of human factor IX in mice after hepatic gene transfer of recombinant AAV vectors. *Nat Genet* 1997, **16** (3)**:** 270-6, PMID: 9207793.

[245] Muzyczka N Use of adeno-associated virus as a general transduction vector for mammalian cells. *Curr Top Microbiol Immunol* 1992, **158:** 97-129, PMID: 1316261.

[246] Xiao X *et al.,* Efficient long-term gene transfer into muscle tissue of immunocompetent mice by adeno-associated virus vector. *J Virol* 1996, **70** (11)**:** 8098-108, PMID: 8892935.

[247] McCown TJ *et al.,* Differential and persistent expression patterns of CNS gene transfer by an adeno-associated virus (AAV) vector. *Brain Res* 1996, **713** (1-2)**:** 99-107, PMID: 8724980.

[248] Kaplitt MG *et al.,* Long-term gene expression and phenotypic correction using adeno-associated virus vectors in the mammalian brain. *Nat Genet* 1994, **8** (2)**:** 148-54, PMID: 7842013.

[249] Kaplitt MG *et al.,* Long-term gene transfer in porcine myocardium after coronary infusion of an adeno-associated virus vector. *Ann Thorac Surg* 1996, **62** (6)**:** 1669-76, PMID: 8957370.

[250] Lalwani AK *et al.,* Development of in vivo gene therapy for hearing disorders: introduction of adeno-associated virus into the cochlea of the guinea pig. *Gene Ther* 1996, **3** (7)**:** 588-92, PMID: 8818645.

[251] Flotte TR *et al.,* Stable in vivo expression of the cystic fibrosis transmembrane conductance regulator with an adeno-associated virus vector. *Proc Natl Acad Sci USA* 1993, **90** (22)**:** 10613-7, PMID: 7504271.

[252] Afione SA *et al.,* In vivo model of adeno-associated virus vector persistence and rescue. *J Virol* 1996, **70** (5)**:** 3235-41, PMID: 8627804.

[253] Arap W *et al.,* Steps toward mapping the human vasculature by phage display. *Nat Med* 2002, **8** (2)**:** 121-7, PMID: 11821895.

[254] Rajotte D *et al.,* Molecular heterogeneity of the vascular endothelium revealed by in vivo phage display. *J Clin Invest* 1998, **102** (2)**:** 430-7, PMID: 9664085.

[255] Zhang L *et al.,* Molecular profiling of heart endothelial cells. *Circulation* 2005, **112** (11)**:** 1601-11, PMID: 16144998.

[256] Arap W *et al.,* Cancer treatment by targeted drug delivery to tumor vasculature in a mouse model. *Science* 1998, **279** (5349)**:** 377-80, PMID: 9430587.

[257] Arap W *et al.,* Targeting the prostate for destruction through a vascular address. *Proc Natl Acad Sci USA* 2002, **99** (3)**:** 1527-31, PMID: 11830668.

[258] Tuve S *et al.,* Role of cellular heparan sulfate proteoglycans in infection of human adenovirus serotype 3 and 35. *PLoS Pathog* 2008, **4** (10)**:** e1000189, PMID: 18974862.

[259] Ruoslahti E RGD and other recognition sequences for integrins. *Annu Rev Cell Dev Biol* 1996, **12:** 697-715, PMID: 8970741.

VI. ACKNOWLEDGEMENTS

I would like to express my gratitude towards all the people who supported me and my thesis during the last five years.

My gratitude goes to my supervisors Prof. Dr. **Jürgen Kleinschmidt** for many helpful scientific discussions and PD Dr. **Oliver Müller** for giving me the opportunity to work in this very interesting field of science and for the financial support over all these years.

Next, I want to thank all the people from my own or neighbouring labs for science-related support, especially:
Barbara Leuchs and her team @ DKFZ/VP & DU for excellent support with AAV production
Petra Zeisberger and **Kristin Schmidt** (Kleinschmidt Lab) for their excellent technical assistance
Elias Loos @ DKFZ/Augustin for his efforts in a promising *in vivo* attempt that unfortunately failed
Dr. Stefan Michelfelder @ University Hospital Hamburg – Eppendorf for fruitful cooperation
Ender Serbest and **Anja Feldner** @ Physiology, University of Heidelberg for their help with *in situ* endothelial transduction analysis

I would also like to thank people less involved in my own research but who made my day in and outside the lab, including all past and present combatants from Jürgen's and Oliver's lab, followed by Anne Fassl, Sabine "Frau" Häcker and Katrin Faber.

Last but not least I want to express my gratitude towards my parents, Irina and Karl Varadi, who have never ceased to support me in situations that exceed mere financial assistance by far.